DOT/FAA/AR-95/21

Office of Aviation Research
Washington, D.C. 20591

Flight Loads Data for a Boeing 737-400 in Commercial Operation

April 1996

Final Report

This document is available to the U.S. public through the National Technical Information Service, Springfield, Virginia 22161.
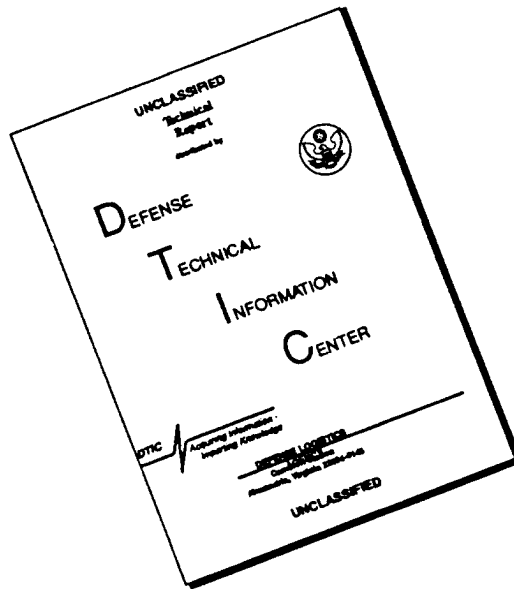
19960708 013

U.S. Department of Transportation
Federal Aviation Administration

DISCLAIMER NOTICE

THIS DOCUMENT IS BEST QUALITY AVAILABLE. THE COPY FURNISHED TO DTIC CONTAINED A SIGNIFICANT NUMBER OF PAGES WHICH DO NOT REPRODUCE LEGIBLY.

NOTICE

This document is disseminated under the sponsorship of the U.S. Department of Transportation in the interest of information exchange. The United States Government assumes no liability for the contents or use thereof. The United States Government does not endorse products or manufacturers. Trade or manufacturer's names appear herein solely because they are considered essential to the objective of this report.

1. Report No. DOT/FAA/AR-95/21	2. Government Accession No.	3. Recipient's Catalog No.

4. Title and Subtitle FLIGHT LOADS DATA FOR A BOEING 737-400 IN COMMERCIAL OPERATION		5. Report Date April 1996
		6. Performing Organization Code

7. Author(s) D. Skinn, P. Miedlar, and L. Kelly		8. Performing Organization Report No. UDR/TR-95-62

9. Performing Organization Name and Address University of Dayton Research Institute Structural integrity Division 300 College Park Dayton, OH 45469-0120		10. Work Unit No. (TRAIS)
		11. Contract or Grant No. 93-G-051

12. Sponsoring Agency Name and Address U.S. Department of Transportation Federal Aviation Administration Office of Aviation Research Washington, D.C. 20591		13. Type of Report and Period Covered Final Report
		14. Sponsoring Agency Code AAR-432

15. Supplementary Notes

FAA Program Monitor: Thomas DeFiore

16. Abstract

This report presents the flight data collected in 1993 from one Boeing 737-400 during routine commercial operation. The data collection program is part of a joint FAA/NASA effort to develop a flight recorder to obtain statistical loads data on commercial transport (FAR Part 25) aircraft during routine operations.

During this prototype data collection program, 593 flights of operational flight loads were collected. Of these, 535 flights representing 817.7 hours, provided usable data. NASA developed the specifications for the recording system, defined the recording format, reduced the data to time histories of engineering units, and tested and evaluated the algorithms for data reduction and statistical reporting. The University of Dayton Research Institute (UDRI) received the flight loads data and data review software from NASA. UDRI developed software to reduce the flight loads data and obtain additional parameters such as derived gust velocity and continuous turbulence gust intensity.

The data reduction includes, but is not limited to, analysis of e.g., accelerations, airspeeds, altitudes, flaps usage, and takeoffs and landings. Data are typically presented in cumulative distribution function or cumulative counts normalized to nautical mile or 1000 hours. Comparisons of typical usage with published FAR's are also presented.

17. Key Words Flight loads, Optical disk recorder, Commercial aircraft, Boeing 737-400, FAR's	18. Distribution Statement This document is available to the public through the National Technical Information Service (NTIS), Springfield, Virginia 22161.

19. Security Classif. (of this report) Unclassified	20. Security Classif. (of this page) Unclassified	21. No. of Pages 86	22. Price

Form DOT F1700.7 (8-72)   Reproduction of completed page authorized

PREFACE

TABLE OF CONTENTS

LIST OF ILLUSTRATIONS

LIST OF TABLES

LIST OF SYMBOLS AND ABBREVIATIONS

$\overline{A}$ aircraft PSD gust response factor

a   speed of sound (ft/sec)

BBS   body balance station

$\overline{c}$ wing mean geometric chord (ft)

$\overline{C}$ aircraft discrete gust response factor

C_{L_α} aircraft lift curve slope per radian

$C_{L_{max}}$ maximum lift coefficient

CAS   calibrated air speed

CDF   cumulative distribution function

c.g.   center of gravity

DFDAU   Digital Flight Data Acquisition Unit

DFDR   Digital Flight Data Recorder

FAA   Federal Aviation Administration

FAR   Federal Aviation Regulation

fpm   feet per minute

F.S.   front spar

F(PSD)   power spectral density function

g   gravity constant, 32.17 ft/sec^2

Hp   pressure altitude, (ft)

K_g discrete gust alleviation factor, $0.88\mu/(5.3 + \mu)$

KCAS   knots calibrated air speed

KEAS   knots equivalent air speed

KIAS   knots indicated air speed

kts   knots

L   turbulence scale length (ft)

MB   megabyte

Mhz   megahertz

n   load factor (g)

N   number of occurrences for U_σ (PSD gust procedure)

NASA   National Aeronautics and Space Administration

nm   nautical mile

n_x longitudinal acceleration (g)

n_y	lateral acceleration (g)
n_z	normal acceleration (g)
N_0	number of zero crossings per kilometer (PSD gust procedure)
POF	phase of flight
POR	Prototype Optical Recorder
PSD	power-spectral-density
q	dynamic pressure (lbs/ft^2)
S	wing area (ft^2)
TAS	true airspeed
TOR	takeoff rotation (deg/sec)
U_{de}	derived gust velocity (ft/sec)
U_σ	continuous turbulence gust velocity (ft/sec)
UDRI	University of Dayton Research Institute
V_B	design speed for maximum gust (kts)
V_C	design cruise speed (kts)
V_D	design dive speed (kts)
V_e	equivalent airspeed (kts)
V_T	true airspeed (kts)
W	gross weight (lbs)
Δm	incremental acceleration due to a turning maneuver
Δn_z	incremental normal acceleration (load factor), $n_z - 1$
$\Delta n_{z_{man}}$	incremental maneuver normal acceleration
$\Delta n_{z_{gust}}$	incremental gust normal acceleration
μ	airplane mass ratio, $\dfrac{2(W/S)}{\rho g \bar{c} C_{L_\alpha}}$
μ_p	statistical mean of p (parameter on plots)
ρ	air density, slugs/ft^3 (at altitude)
ρ_0	standard sea level air density, 0.002377 slugs/ft^3
σ_p	standard deviation of p (parameter on plots)
φ	bank angle (degrees)

EXECUTIVE SUMMARY

The University of Dayton is supporting Federal Aviation Administration (FAA) research on the structural integrity requirements for the US commercial transport airplane fleet. The ultimate objective of this research is to provide information which will enable the FAA to better understand and control those factors that influence the structural integrity of commercial transport aircraft. This activity supports the overall objectives of the FAA transport flight loads data collection program which are (a) to determine whether the loading spectra being used or developed for the design and test of both small and large aircraft are representative of operational usage and (b) to develop structural design criteria for future generations of small and large aircraft. Presented herein are analyses and statistical summaries of data collected from 535 flights representing 817.7 flight hours of typical B737 usage.

1. INTRODUCTION.

The FAA and NASA have initiated a cooperative program to develop a flight recorder system to obtain statistical loads data on Federal Aviation Regulation (FAR), Part 25, Commercial Transport Aircraft During Routine Operations. NASA developed the specifications for the recording system, defined the recording formats, tested and evaluated the algorithms for data reduction and statistical reporting, and provided these findings to the FAA. In 1993, a commercial airline installed an optical disk recorder in a B737-400 airplane and periodically provided FAA/NASA with data on magneto-optical disks for reduction and analysis. NASA carefully reviewed 39 flights for accuracy and suitability for the statistical purposes of this program. NASA then provided the flight time-history files to the University of Dayton Research Institute (UDRI) for processing and reporting. In this program, a total of 593 flights of operational flight loads data were collected from routine operation of the B737-400 aircraft. Of these data, 535 flights, representing 817.7 hours, provided usable data. The time-history data collected under the joint FAA/NASA program were provided to UDRI on high-density magneto-optical disks in binary unit files. Algorithms developed by UDRI transformed these data into the statistical and graphical formats presented in this report.

This report reviews both the data collection program and the data processing procedures and also summarizes the flight recorder data. Reference 1 contains the data development procedures. Section 2 describes the data collection effort, section 3 describes the processing of the time history flight loads data for presentation, and section 4 presents the flight recorder data.

There is similarity in flight loads data requirements for commuter aircraft designed per carrier rules of FAR Part 23, and for large commercial aircraft designed per FAR, Part 25. Since flight loads data are more readily available for the Part 25 aircraft than for the Part 23 aircraft, the research in this report can provide an insight into the Part 23 aircraft operational conditions versus design conditions. Also, the planning and implementation of the commuter aircraft data recording program being developed by UDRI can benefit significantly from knowledge gained from the on-going large transport flight loads monitoring program.

2. DATA COLLECTION PROGRAM.

The flight data summarized in this report were obtained from a Boeing 737-400 commercial transport aircraft during normal operations. The flight data were collected by an on-board recorder, transferred to a ground processing station, and reduced to time-history format. Table 1 lists the parameters that were recorded along with their sampling rates and table names. The significance of table name is discussed in section 2.2.

1

TABLE 1. RECORDED PARAMETERS ON FLIGHT DISK IN TIME HISTORY-FORMAT

Parameter	Sample Rate	Table Name
Normal Acceleration	8 per second	tblm9
Lateral Acceleration	4 per second	tblm10
Longitudinal Acceleration	4 per second	tblm11
Aileron Position	1 per second	tblm12
Elevator Position	1 per second	tblm13
Rudder Position	2 per second	tblm14
Pilot Trim Position	1 per second	tblm15
Flap Detent	1 per second	tblm16
Speed Brake Position	1 per second	tblm17
N_1 Engine - Left	1 per second	tblm18
N_1 Engine - Right	1 per second	tblm19
Throttle #1 Position	1 per second	tblm20
Throttle #2 Position	1 per second	tblm21
Thrust Reverser Position	Discrete	tblm22
Autopilot Status (on or off)	Discrete	tblm23
Squat Switch (main gear)	Discrete	tblm24
Gear Position	Discrete	tblm25
Calibrated Airspeed	1 per second	tblm26
Ground Speed	1 per second	tblm27
Mach Number	1 per 4 seconds	tblm28
Pressure Altitude	1 per second	tblm29
Gross Weight	1 per 64 seconds	tblm31
Bank Angle	2 per second	tblm34
Pitch Angle	4 per second	tblm35

2.1 DESCRIPTION OF AIRCRAFT.

Figure 1 shows front, top, and side views of the Boeing 737-400 aircraft and identifies its major physical dimensions. Table 2 presents certain operational characteristics of the aircraft.

Maximum Taxi Weight	143,000 lbs.
Empty Weight	77,250 lbs.
Maximum Fuel Weight	35,500 lbs. w/o Aux. Tank
2 CFM 56-3 Engines	@ ~22,000 lbs. static thrust, each
Wing Area	980 ft.^{2}
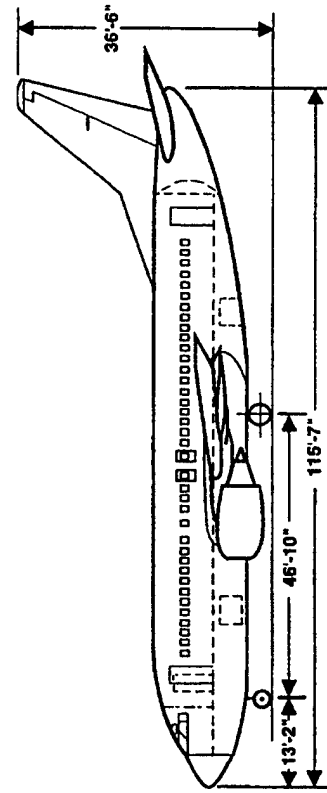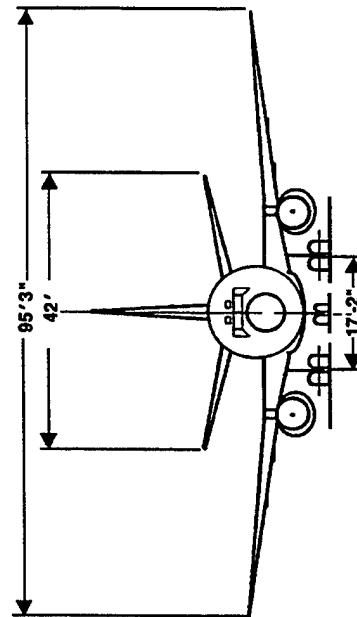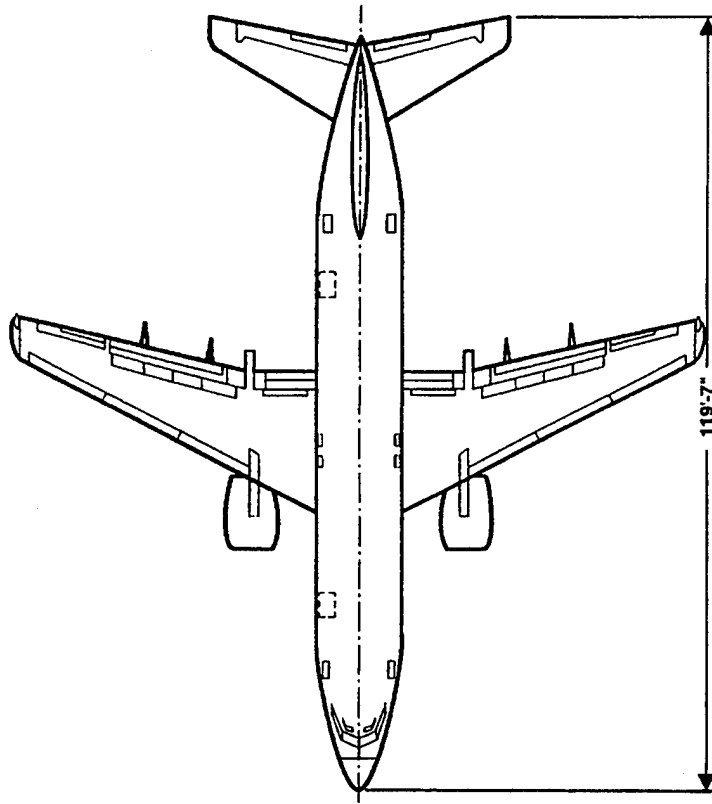
FIGURE 1. BOEING 737-400 AIRCRAFT DESCRIPTION

3

TABLE 2. TYPICAL BOEING 737-400 AIRCRAFT PHYSICAL CHARACTERISTICS [1]

Maximum taxi weight	143,000 lbs
Minimum takeoff weight	84,250 lbs
Maximum landing weight	121,000 lbs
Operational weight empty	77,250 lbs (typical)
Maximum fuel weight	35,500 lbs (w/o auxiliary tanks) 38,800 lbs (with auxiliary tanks)
2 CFM56-3 Engines	@ 22,000 lbs static thrust each
Wing reference area	980 ft^2
Wing mean aerodynamic chord	11 ft 2.46 in
Length	115 ft 7 in (nose to end of fuselage) 119 ft 7 in (nose to tip of horizontal tail)
Wing span	95 ft 3 in
Horizontal tail span	42 ft
Vertical tail span	20 ft 2 in

2.2 DATA COLLECTION AND PROCESSING SYSTEM.

The data processing system consists of two major components: (1) an airborne data collection system and (2) a ground data processing station. The collection and processing system is summarized below. A schematic overview of the system is given in figure 2. A description of the preliminary system design can be found in reference 2.

The airborne data collection system consists of a Digital Flight Data Acquisition Unit (DFDAU), a Digital Flight Data Recorder (DFDR), and a Prototype Optical Recorder (POR). The DFDAU collects sensor signals and sends parallel data signals to both the DFDR and the POR. The POR is programmed to start recording once certain data signals are detected. The POR is equipped with a magneto-optical disk which can store up to 650 hours of flight data, whereas the DFDR uses a 25-hour looptape. When the magneto-optical disk is full, it is removed from the POR and forwarded to the ground processing station.

The ground data processing station consists of an IBM-compatible 486 computer and functions during the process of transferring the raw flight data into DOS file format onto hard disk. Included in these functions are a data integrity check, removal of sensitive parameters, and separation of the data into unique binary files for each flight. Data considered sensitive are those which can be used to readily identify a specific flight.

The collected data are automatically compared against the limits listed in table 3. If a value is outside the limits, the record is flagged and inspected manually to determine the validity of the data point. Each recorded parameter is automatically compared with its appropriate reasonable or maximum value at start up, in flight, and at engine shut down except as noted. Flights having any out-of-tolerance parameters are flagged for manual review.

4

Airborne System (AS):

Prototype Optical
Recorder (POR)

Digital Flight
Data Acquisition Unit
(DFDAU)

permanent on a/c

Ground System (GS):

(Recorded)
Flight Disk

Flight Optical Disk Processor
● Configures Flight Disk
● Reads Flight Disks

power supply

486 Personal Computer

Quick-Look Display Printer

Ground Optical Disk
Storage System
● Processes Data
● Archives Data
● Copy to UDRI

Final Display Printer

FIGURE 2. NASA PROTOTYPE SYSTEM (NPS) – SYSTEM EQUIPMENT REQUIREMENTS

5

TABLE 3. EDIT LIMIT VALUES FOR RECORDED PARAMETERS

Item		Condition	Minimum	Maximum
1.	Gross Weight	at start up	75,000 lbs	150,500 lbs
2.	Pressure Altitude (Hp)	Hp at takeoff and landing	-1000 ft	8000 ft
		Hp_{max} in flight	0	40,000 ft
3.	Calibrated Airspeed	at all times during flight operations	45 kts	420 kts
4.	Normal Acceleration	at start up and shut down	0.95	1.05
		in flight	0	2.0
5.	Lateral Acceleration	at start up and shut down	-0.10	0.10
		ground operations	-0.25	0.25
		in flight	-0.07	0.07
6.	Longitudinal Acceleration	at start up and shut down	-0.1	0.1
		ground operations	-0.5	0.5
		in flight	-0.5	0.5
7.	Flap Handle Position	at start up and shut down	0°	0°
		takeoff	0°	5°
		in flight	0°	40°
8.	Elevator Position	at all times	-25°	25°
9.	Aileron Position	at all times	-25°	25°
10.	Rudder Position	at all times	-30°	30°
11.	Trim Position	at all times	0	17°
12.	Speed Brake Handle Position	at start up and shutdown	0°	0°
		in flight	0°	40°
		landing	0	45°
13.	Throttles 1 and 2	at start up and shutdown	-2°	2°
		takeoff and in flight	0	55°
		landing	0	65°
14.	Thrust Reverser Position	stowed at start up and shutdown	0	1
15.	Autopilot Status	off or on	0	1
16.	Squat Switch (main gear)	closed at start up and shutdown	0	1
17.	Landing Gear Position	down at start up and shutdown up within 10 seconds after takeoff down within 10 minutes before landing	0	1
18.	Pitch Attitude	at start up and shutdown	-5°	3°
		in flight	-10°	22°
19.	Bank Attitude	at start up and shutdown	-5°	5°
		in flight	-45°	45°
20.	Mach Number	at start up	-0.02	+0.02
		at shutdown	-0.02	+0.02
		in flight	+0.15	+0.82
21.	Ground Speed	at start up and shutdown	0	4 kts
		in flight	0	800 kts

The ground processing software converts each binary flight file into a set of time-history files and stores the files for each flight in a "Super Flight File." This file is actually a Microsoft ACCESS database consisting of 27 tables. Each of these tables is a time history of one of the parameters listed in table 1. The table names used in the database are also given in table 1, along with data sampling rates for flight parameters and control surfaces. A copy of the ground processing software and the binary flight files were forwarded to UDRI on magneto-optical disk for the flight data summarization effort.

3. DATA PROCESSING.

UDRI received the FAA/NASA aircraft parameters, ground processing software, and time-history data for the 593 flights of normal service operation of the Boeing 737-400 passenger aircraft from NASA. These data were processed to extract the parameters required for statistical presentation. This section describes the processing of the data and the derivation of required parameters.

3.1 DATA PROCESSING.

The data processing software and airplane in-flight parameter data were provided to UDRI on 127 MB magneto-optical disks. The software was loaded and executed on a 90 MHz Pentium computer. The flight parameter data were provided as binary files. Each file contained the data for one flight. The FAA/NASA software converts a binary file to a Super Flight File to allow the user to view time histories of various flight parameters and control surfaces.

The normal acceleration (n_z) time history was closely examined because n_z is important in determining both the maneuver and gust load experiences. Several flights contained extremely high and/or low n_z readings during the taxi-in phase and/or at the end of the flight. Other parameters were examined for the same time period and were found to deviate greatly from tolerance values. Such readings were assumed to be caused by electrical surges in the onboard computer. These apparently false readings were deleted before processing.

Fifty-eight of the 593 flights were discarded entirely for one of the following three reasons: (1) the aircraft never lifted off (52 flights), (2) the recorded flight data terminated in midair (one flight), or (3) the FAA/NASA software could not reliably rebuild a time history file (five flights).

This report required 16 of the 24 time-history parameters identified in table 1 to provide the summaries and analyses herein. Table 4 lists the parameters used. These parameters exist as time-history tables in the Super Flight File which is a Microsoft ACCESS database. ACCESS was used to convert the time-history tables into files in ASCII form as required by the UDRI summarization software.

7

TABLE 4. RECORDED PARAMETERS ON FLIGHT DISK IN TIME-HISTORY FORMAT

Flight Parameter	Sample Rate	Use
Gross Weight	1 per 64 seconds	plots; calculations
Pressure Altitude	1 per second	plots; calculations
Calibrated Airspeed	1 per second	plots; calculations
Normal Acceleration (n_z)	8 per second	plots; U_{de} and U_σ calculations
Lateral Acceleration (n_y)	4 per second	plots
Longitudinal Acceleration (n_x)	4 per second	plots; determine takeoff roll
Flap Handle Position	1 per second	determine POF; calculations
Speed Brake Handle Position	1 per second	identify when engaged
Thrust Reverser Position	Discrete	determine end of landing roll
Autopilot Status (on or off)	Discrete	determine time engaged
Squat Switch (main gear)	Discrete	indicate liftoff and touchdown
Landing Gear Position	Discrete	identify when gear down
Pitch Angle	4 per second	plots
Bank Angle	2 per second	calculation of maneuver load
Mach Number	1 per 4 seconds	plots; calculations
Ground Speed	1 per second	calculation of climb rate

3.2 PHASES OF FLIGHT.

Each flight was divided into nine flight phases - four on ground phases (taxi-out, takeoff roll, landing roll, taxi-in), and five airborne phases (departure, climb, cruise, descent, approach). Figure 3 defines the nine phases of a typical flight. The phases of flight were not defined within the time histories and therefore had to be derived from the data. Table 5 lists the conditions for determining the starting times for the various phases of flight. It should be noted that the airborne phases can occur several times per flight because they are determined by the rate of climb and the position of the flaps. The UDRI software creates a file which chronologically lists the phases of flight and their corresponding starting times.

3.3 STAGE LENGTH.

A stage is that portion of a flight route from a departure airport to a destination airport. The stage length is determined as the great circle distance in nautical miles between the point of liftoff (departure) and the point of touchdown (destination). Appendix A describes the calculation of great circle distance.
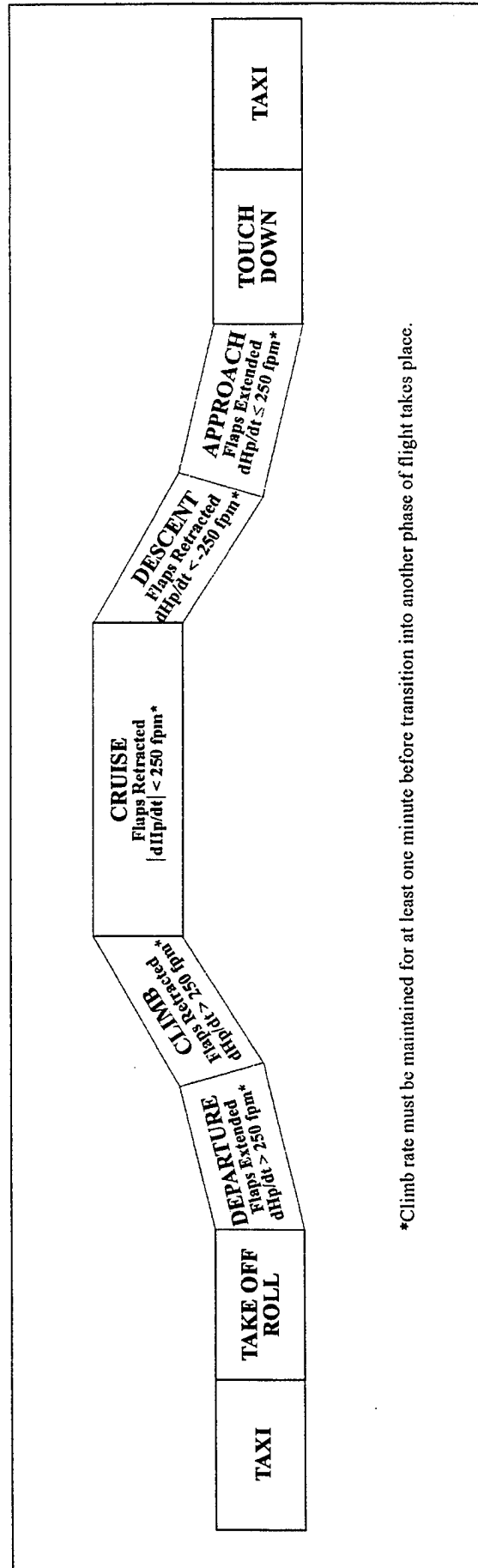
FIGURE 3. DESCRIPTION OF PHASES OF FLIGHT

Flow diagram showing phases of flight (left to right):

TAXI | TAKE OFF ROLL | DEPARTURE — Flaps Extended, dHp/dt > 250 fpm* | CLIMB — Flaps Retracted, dHp/dt > 250 fpm* | CRUISE — Flaps Retracted, |dHp/dt| < 250 fpm* | DESCENT — Flaps Retracted, dHp/dt < -250 fpm* | APPROACH — Flaps Extended, dHp/dt ≤ 250 fpm* | TOUCH DOWN | TAXI

*Climb rate must be maintained for at least one minute before transition into another phase of flight takes place.

9

TABLE 5. PHASE OF FLIGHT STARTING CONDITIONS

Phase of Flight	Conditions at Start of Phase
Taxi-out	initial condition
Takeoff Roll	$n_x \geq 0.15$
Departure	time at liftoff; flaps extended (squat switch off)
Climb	flaps retracted; rate of climb ≥ 250 ft/min for at least one minute
Cruise	flaps retracted; rate of climb < 250 ft/min for at least one minute
Descent	flaps retracted; rate of climb ≤ -250 ft/min for at least one minute
Approach	flaps extended; rate of climb < 250 ft/min for at least one minute
Landing Roll	touchdown; (squat switch on)
Taxi-in	thrust reverser stowed

3.4 ACCELERATION DATA.

Acceleration data are recorded in three directions: normal (z), longitudinal (x), and lateral (y). For the Boeing 737-400, the axis system is shown in figure 4. The positive x direction is aft; the positive y direction is airplane starboard; and the positive z direction is up.

Airplane Axes Definition

x = Body Balance Station (BBS) in inches. The zero BBS is 540 inches forward of the wing front spar (F.S.) on the body. The positive x direction is aft.

y = The airplane centerline is butt line zero. The positive y direction is to the left facing aft.

z = Water line zero is 208.1 inches below the passenger floor. The positive z direction is up.
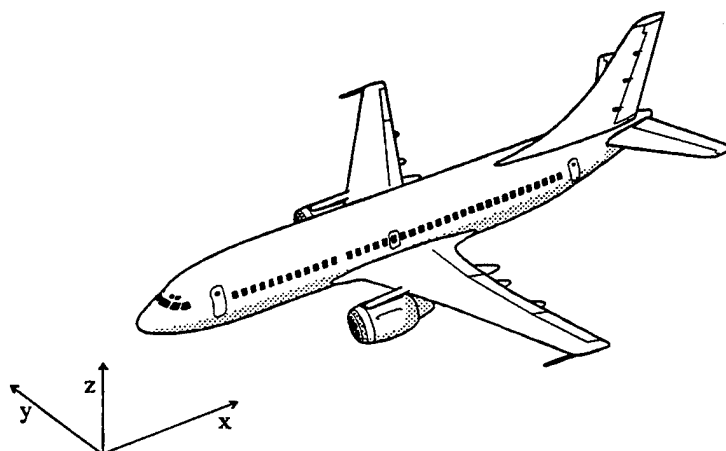
FIGURE 4. AIRPLANE AXES

3.4.1 Normal Acceleration (n_z).

The recorded normal acceleration (n_z) values included the 1 g flight condition. The 1 g condition was removed from each n_z reading which was then recorded as Δn_z. In order to avoid the inclusion of peaks and valleys associated with nonsignificant small load variations, a threshold

zone of $\Delta n_z = \pm 0.05$ g was established. An algorithm was developed to extract the acceleration peaks and valleys from the binary unit files.

For each flight, the maximum and minimum total accelerations were determined from just after liftoff to just before touchdown. For the five in-flight phases, the Δn_z cumulative occurrences were determined as cumulative counts per nautical mile and cumulative counts per 1000 hours using the Peak-Between-Means [3] counting method which is explained in section 3.4.4.

The incremental acceleration measured at the center of gravity (c.g.) of the aircraft may be the result of either maneuvers or gusts or a combination of both. In order to derive gust statistics, the maneuver-induced acceleration is separated from the total acceleration history. Most maneuver-induced loads are associated with turning maneuvers.

The increment due to a turning maneuver (Δm) is determined using the bank angle method [3] to calculate the maneuver acceleration $\Delta n_{z_{man}}$ as follows

$$\Delta n_{z_{man}} = (\sec \varphi - 1) \tag{1}$$

where φ is the bank angle. The remaining peaks and valleys are assumed to be gust induced where gust normal acceleration ($\Delta n_{z_{gust}}$) is calculated as

$$\Delta n_{z_{gust}} = \Delta n_z - \Delta n_{z_{man}} \tag{2}$$

This approach does not separate the pitching maneuvers induced by pilot control inputs. J.B. de Jonge [3] suggests that accelerations resulting from pitch maneuvers induced by pilot input to counteract turbulence can be considered as part of the aircraft system response to the turbulence. Accelerations which are induced by the pitch maneuver at the specific points of rotation and flare during takeoff and climb and approach and touchdown have not been removed during this initial data reduction effort. Since turbulence is a more dominant loading input on commercial aircraft than maneuvers, correcting for pitch maneuvers at a later time will not substantially alter the statistics presented herein.

Once calculated, the measurements of Δn_z, $\Delta n_{z_{gust}}$, and $\Delta n_{z_{man}}$ are maintained as three unique data streams. The $\Delta n_{z_{gust}}$ and $\Delta n_{z_{man}}$ data are plotted as cumulative occurrences of a given acceleration fraction per nautical mile and per 1000 flight hours. Separate plots are provided for each phase of flight and all phases combined. The Δn_z fraction is the recorded incremental normal load factor (airplane limit load factor minus 1.0 g). As a result of the threshold zone, only accelerations greater than ± 0.05 g (measured from a 1.0 g base) are counted for data presentation.

11

3.4.2 Longitudinal Acceleration (n_x).

The longitudinal acceleration data are recorded during all phases of the flight. However, the data that are presented are maximum n_x for the takeoff roll phase and minimum n_x for the landing roll phase. The deadband is 0.005 g with a mean value of zero and a threshold zone of ±0.0025 g.

3.4.3 Lateral Acceleration (n_y).

The lateral acceleration data are presented for all airborne phases of flight. The deadband is 0.01g with a mean value of zero and a threshold zone of ±0.005 g.

3.4.4 Peak-Valley Selection.

The "Peak-Between-Means" method [3] was used to select the peaks and valleys in the acceleration data. This is consistent with past practices and current methods [4] and the method pertains to all accelerations (n_x, n_y, Δn_z, $\Delta n_{z_{man}}$, $\Delta n_{z_{gust}}$). Figure 5 shows the peak-between-mean criterion. This method considers upward displacement as positive and downward displacement as negative. Only one peak or one valley is counted between two successive crossings of the mean. A threshold zone is used in the data reduction to ignore irrelevant loads variations around the mean. For the normal accelerations Δn_z, $\Delta n_{z_{gust}}$, and $\Delta n_{z_{man}}$ the threshold zone is ±0.05 g, for lateral acceleration n_y the threshold zone is ±0.005 g, and for longitudinal accelerations n_x the threshold zone is ±0.0025 g.
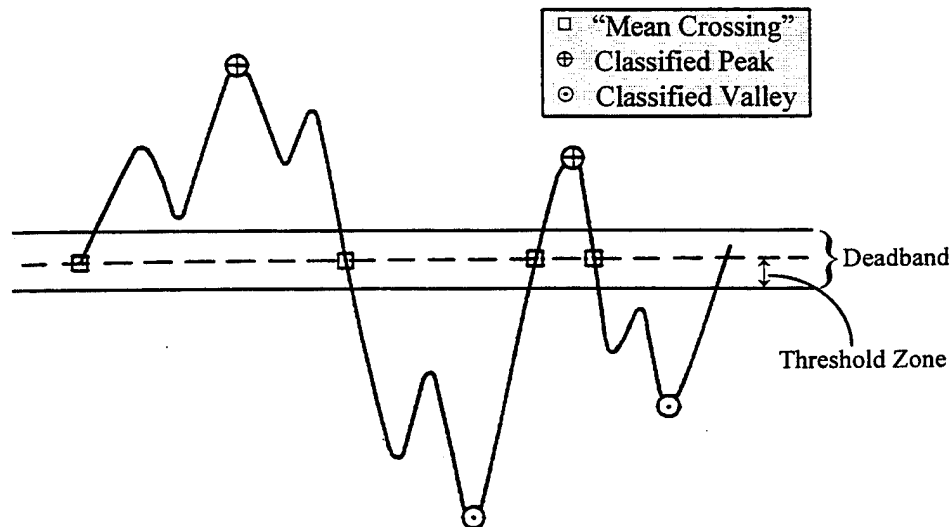

FIGURE 5. THE "PEAK-BETWEEN-MEANS" CLASSIFICATION CRITERIA

A peak is generated only when the acceleration data cross into or through the deadband. Two situations must be considered: the position of the current acceleration value relative to the deadband and the position of the previous acceleration value relative to the deadband. In the peak-between-means counting algorithm, the previous acceleration value is that value in a consecutive set of values all of which lie either above the deadband or below the deadband. The previous value is established as a peak when the current value has crossed into or through the deadband. Italicized text in table 6 summarizes the action(s) taken when the various possibilities occur. Note that when a previous acceleration value is retained as a potential peak, its coincident time is also retained. Figures 6a and 6b demonstrate the concept of current and previous acceleration values. In figure 6a the current acceleration value passes into the deadband, whereas in figure 6b the current value passes through the deadband.

TABLE 6. CRITERIA FOR PEAK CLASSIFICATION

| Previous Acceleration Value Relative to Deadband	Current Acceleration Value Relative to Deadband		
	Below	Within	Above
Above Previous value is potential positive peak	Current acceleration passes through deadband. *Previous value classified as a positive peak. Current value retained as a potential negative peak.*	Current acceleration passes into deadband. *Previous value classified as a positive peak. Acceleration value flagged as being in deadband.*	Current acceleration is on same side of deadband as previous. *If current > previous value, retain current value as potential positive peak and release previous.*
Within At start of processing, or a peak was established but current acceleration value has not since gone outside of deadband	Current acceleration passes downward out of deadband. *Current value is retained as a potential negative peak.*	*No Action Required*	Current acceleration passes upward out of deadband. *Current value retained as potential positive peak.*
Below Previous value is potential negative peak	Current acceleration is on same side of deadband as previous. *If current value < previous value, retain current value as potential negative peak and release previous value.*	Current acceleration passes into deadband. *Previous value is established as a negative peak. Acceleration value flagged as being in deadband.*	Current acceleration passes through deadband. *Previous value is classified as a negative peak. Current value retained as potential positive peak.*

13
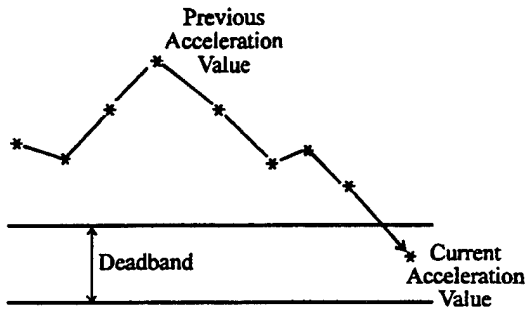
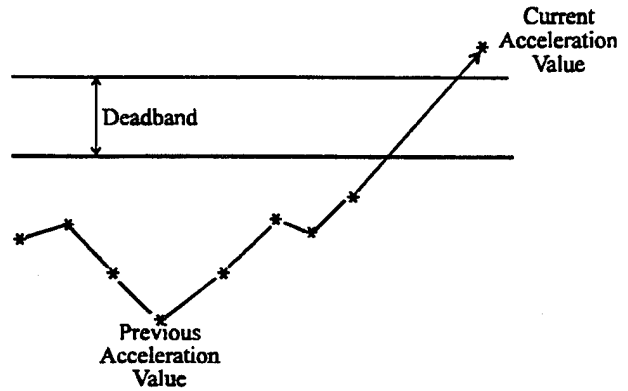FIGURE 6A. CURRENT ACCELERATION
VALUE PASSES *INTO* DEADBAND

FIGURE 6B. CURRENT ACCELERATION
VALUE PASSES *THROUGH* DEADBAND

3.5 DERIVED GUST VELOCITY (U_{de}).

The derived gust velocities, U_{de}, are computed from the peak values of gust normal acceleration as follows:

$$U_{de} = \frac{\Delta n_z}{\overline{C}} \qquad\qquad (3)$$

where Δn_z is gust peak normal acceleration and

$\overline{C}$ is the aircraft response factor considering the plunge-only degree of freedom, and is calculated from

$$\overline{C} = \frac{\rho_0 V_e C_{L_\alpha} S}{2W} K_g \qquad\qquad (4)$$

$\rho_0 = 0.002377$ slugs/ft^3, standard sea level air density

V_e = equivalent airspeed (ft/sec)

C_{L_α} = aircraft lift curve slope per radian

S = wing area (ft^2)

W = gross weight (lbs)

$K_g = \dfrac{0.88\mu}{5.3 + \mu}$ = gust alleviation factor

$\mu = \dfrac{2W}{\rho g \overline{c} C_{L_\alpha} S}$

ρ = air density, slug/ft^3, at pressure altitude (Hp), from standard atmosphere table

g = 32.17 ft/sec^2

$\overline{c}$ = wing mean geometric chord (ft)

14

In this program, the lift-curve slope, C_{L_α}, is the untrimmed flexible lift-curve slope for the entire airplane. For the flaps retracted condition, the lift curve slope is given as a function of Mach number and altitude; for flaps extended, the lift curve slope is a function of flap deflection and calibrated airspeed (KCAS).

3.6 CONTINUOUS GUST INTENSITY (U_σ).

Power Spectral Density (PSD) functions provide a turbulence description in terms of the probability distribution of the root-mean-square gust velocities. The root-mean-square gust velocity, U_σ, is computed from the peak gust value of normal acceleration using the power spectral density technique [2]. The procedure is

$$U_\sigma = \frac{\Delta n_z}{\overline{A}}$$

(5)

where $\quad \Delta n_z =$ gust peak normal acceleration

$$\overline{A} = \text{aircraft PSD gust response factor} = \frac{\rho_0 V_e C_{L_\alpha} S}{2W} \ F(PSD) \ , \frac{1}{ft/\sec}$$

(6)

$\rho_0 = 0.002377$ slugs/ft^3, standard sea level air density
$V_e =$ equivalent airspeed (ft/sec)
$C_{L_\alpha} =$ aircraft lift curve slope per radian
$S =$ wing area (ft^2)
$W =$ gross weight (lbs)

$$F(PSD) = \frac{11.8}{\sqrt{\pi}} \left[\frac{\overline{c}}{2L} \right]^{\frac{1}{3}} \sqrt{\frac{\mu}{110+\mu}}, \ dimensionless$$

(7)

$\overline{c} =$ wing mean geometric chord (ft)
$L =$ turbulence scale length, 2500 ft
$\mu = \dfrac{2W}{\rho g \overline{c} C_{L_\alpha} S}$, dimensionless

(8)

$\rho =$ air density (slugs/ft^3)
$g = 32.17$ ft/sec^2

To determine the number of occurrences (N) for U_σ, calculate

$$N = \frac{N_0(o)_{ref}}{N_0(o)} = \frac{\pi \overline{c}}{203} \left[\frac{\rho}{\rho_0} \mu \right]^{0.46}, \ dimensionless$$

(9)

where $\overline{c}$, ρ, ρ_0, and μ are defined above. Then each U_σ peak is counted as N counts at that U_σ value. This number of counts is used to determine the number of counts per nautical mile (nm),

15

$$\frac{Counts}{nm} = \left(\frac{N}{\text{distance flown in counting interval}} \right) \qquad (10)$$

or

Finally, the number of such counts is summed from the largest plus or minus value toward the smallest to produce the Cumulative Counts per Nautical Mile.

3.7 DYNAMIC PRESSURE (q).

The dynamic pressure (q) is calculated from the air density and velocity

$$q = \frac{1}{2} \rho V^2 \qquad (11)$$

where

ρ = air density at altitude (slugs/ft^3)
V = true air speed (ft/sec)

The true air speed and the air density at altitude are derived from recorded values and are calculated as shown in section 3.9.

3.8 FLAP DETENTS.

When flaps are extended, the flap detent is determined by the flap handle setting as indicated in table 7.

TABLE 7. FLAP DETENT (B737/400)

Flap Detent	Minimum Handle Setting	Maximum Handle Setting	Placard Speed (KIAS)
1	> 0.5	≤ 2.0	250
5	> 2.0	≤ 7.5	250
10	> 7.5	≤ 12.5	218
15	> 12.5	≤ 20.0	213
25	> 20.0	≤ 27.5	206
30	> 27.5	≤ 37.5	199
40	> 37.5	≤ 45.0	162

3.9 CALCULATED VALUES.

To calculate derived gust velocity U_{de}, continuous gust intensity U_σ, and dynamic pressure, air density, equivalent air speed, and lift curve slope C_{L_α} are required. The determination of these values is explained here.

3.9.1 Air Density.

The air density, ρ, is a function of pressure altitude and is calculated as

$$\rho = \rho_o \, (1 - 0.000006879 Hp)^{4.258} \tag{12}$$

where ρ_0 is air density at sea level (0.0023769 slugs/ft^3) and Hp is pressure altitude (ft). Pressure altitude is a recorded parameter. The air density is required in the calculations of equivalent air speed, derived gust velocity, and continuous gust intensity.

3.9.2 Equivalent Air Speed.

Equivalent air speed (V_e) is a function of true air speed (V_T) and the square root of the ratio of air density at altitude (ρ) to air density at sea level (ρ_0)

$$V_e = V_T \sqrt{\frac{\rho}{\rho_0}} = V_T \, (1 - 0.000006879 Hp)^{2.129} \tag{13}$$

True airspeed is derived from Mach number (M) and speed of sound (a). The units of true air speed and speed of sound are ft/sec. The equation for true air speed is

$$V_T = Ma \tag{14}$$

Mach number is a dimensionless, recorded parameter. The speed of sound (a) is a function of pressure altitude (Hp) and, when expressed in ft/sec, is calculated

$$a = 29.02436 \cdot 1.687811 \cdot \sqrt{518.69 - 0.003566 Hp} \tag{15}$$

3.9.3 Lift Curve Slope.

For conditions with flaps retracted, the lift curve slope is a function of Mach number and altitude. For the flaps extended condition, the lift curve slope is a function of flap position and velocity (KCAS). The lift curve slope data were provided to NASA by Boeing [1].

4. STATISTICAL DATA PRESENTATION.

In this section, the statistical data are presented. Table 8 lists the parameters presented in this section and which figures contain the data. The following paragraphs describe the presentation of the data, including descriptions of the different types of plots. Where possible, the FAR design requirements are plotted for comparison.

TABLE 8. SUMMARY OF STATISTICAL DATA PRESENTATION

Flight Parameter	Type of Plot	Data Presented	Figure Number
Thrust Reverser Position	CDF	Time deployed Ground speed	Figure 7 Figure 8
Longitudinal Acceleration	CDF	Positive n_X- before takeoff Negative n_X - after landing	Figure 9 Figure 10
Normal Acceleration	CDF	Δn_z at touchdown	Figure 11
Pitch Angle	CDF	Max at takeoff and landing Maximum takeoff rotation Coincident at landing n_z peak	Figure 12 Figure 13 Figure 14
Calibrated Airspeed	CDF	During takeoff and landing	Figure 15
Gross Weight	Tabular data	Correlation at takeoff and landing	Figure 16
Autopilot Status	CDF	Percent time engaged	Figure 17
Flap Position	Bar chart Bar chart CDF	Detent during departure Detent during approach Calibrated airspeed	Figure 18 Figure 19 Figures 20 - 26
Speed Brake	CDF	Calibrated airspeed	Figure 27
Gear Position	CDF	Time Calibrated airspeed	Figure 28 Figure 29
Normal Acceleration	Occurrences per 1000 hours Occurrences per 1000 hours Occurrences per nautical mile	Δn_z ground loads Δn_z flight loads Δn_z flight loads	Figures 30 - 33 Figures 34 - 39 Figures 40 - 45
Lateral Acceleration	Occurrences per 1000 hours	n_y - all flight phases	Figure 46
Derived Gust Loads	Occurrences per nautical mile	U_{de} by pressure altitude	Figures 47 - 51
Discrete GustLoads	Occurrences per nautical mile	U_{de} - flaps extended U_{de} - flaps retracted	Figure 52 Figure 53
Continuous Gust Loads	Occurrences per nautical mile	U_σ - flaps extended U_σ - flaps retracted	Figure 54 Figure 55
V-n diagrams	Linear	n_z vs. V_e	Figures 56 - 59
Mach Number	Linear	vs. coincident altitude	Figure 60
Velocity, equivalent	Linear	vs. coincident altitude	Figure 61
Maneuvering Load Factor	Range plot	min and max n_z by gross weight range	Figure 62

4.1 PRESENTATION OF THRUST REVERSER DATA.

The cumulative distribution of the length of time (minutes) that the thrust reverser was engaged and the cumulative distribution of ground speed (knots) at deployment are shown in figures 7 and 8, respectively. In figure 7, the mean and standard deviation of length of time are shown on the
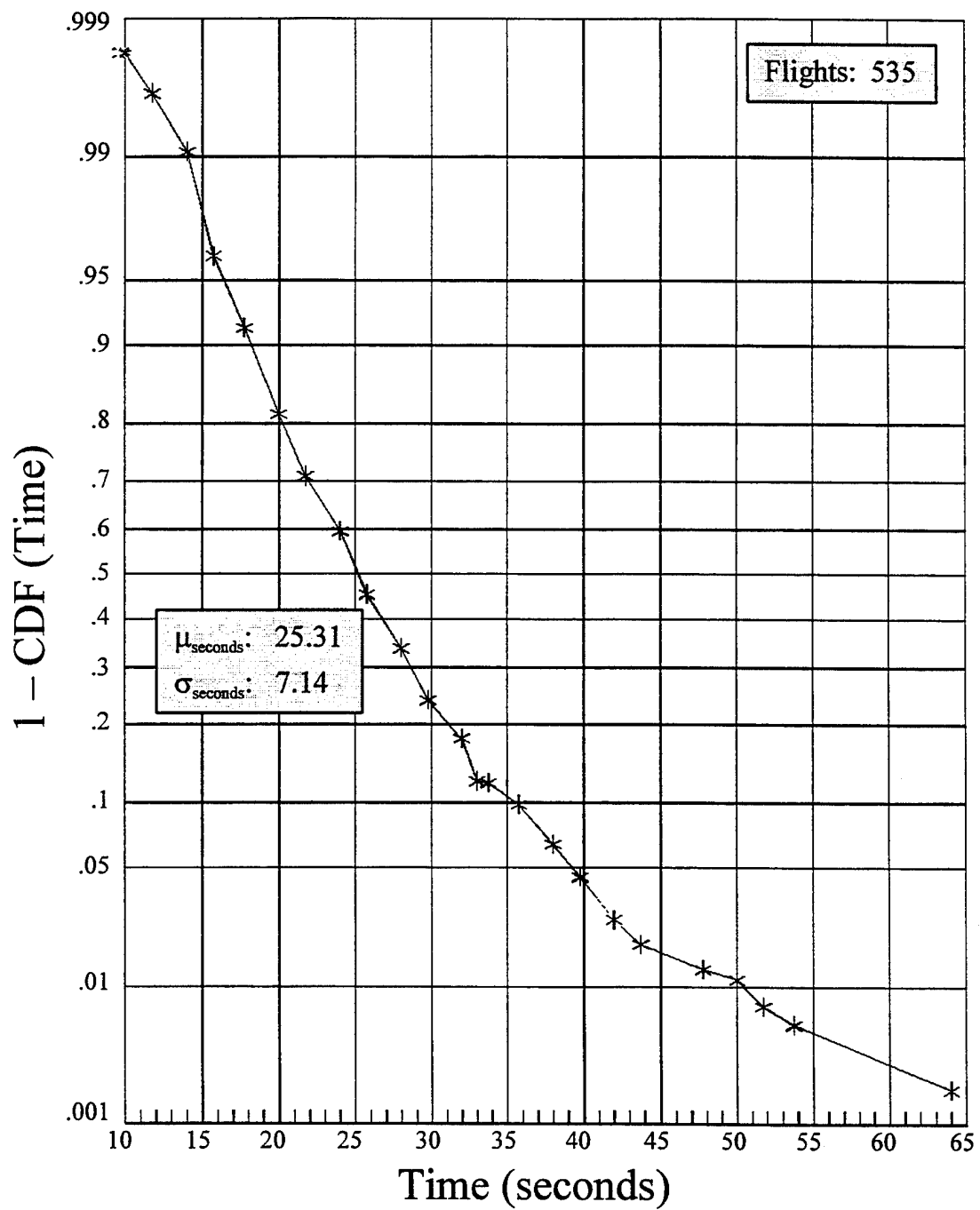
FIGURE 7. CUMULATIVE DISTRIBUTION OF NUMBER OF SECONDS
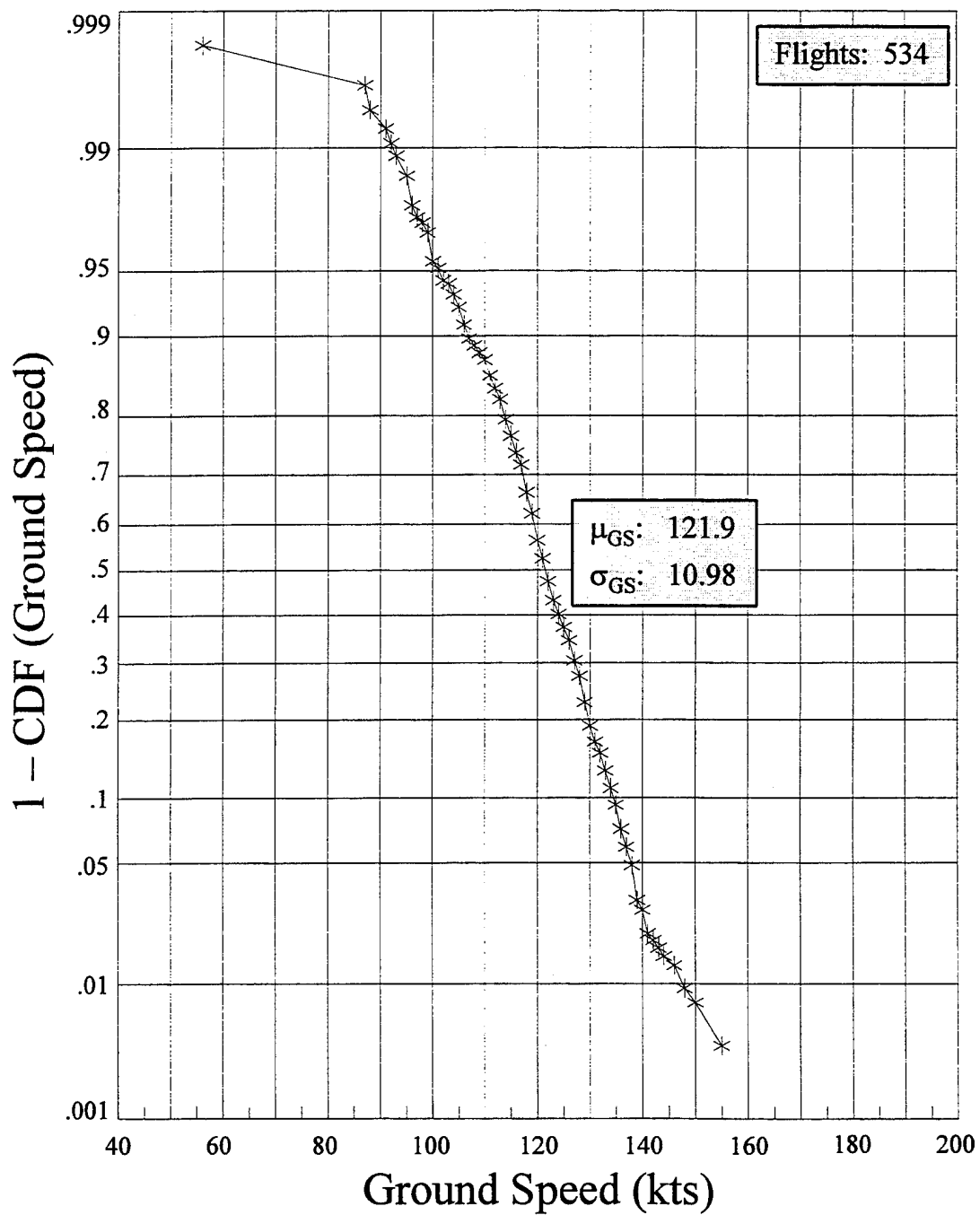WITH THRUST REVERSER DEPLOYED

FIGURE 8. CUMULATIVE DISTRIBUTION OF GROUND SPEED
AT DEPLOYMENT OF THRUST REVERSER

plot. In figure 8, the mean and standard deviation of ground speed are shown. One of the 535 flights is omitted from consideration because there was no indication of thrust reverser deployment.

4.2 PRESENTATION OF TAKEOFF AND LANDING DATA.

Several parameters are of interest during the takeoff and landing phases. These parameters include pitch attitude, pitch rate, airspeed, gross weight at both takeoff and landing, $n_{x_{min}}$ after touchdown, $n_{x_{max}}$ prior to liftoff, and $\Delta n_{z_{min}}$ at touchdown.

Figure 9 shows the cumulative distribution of positive n_x within five seconds prior to liftoff, figure 10 shows the cumulative distribution of negative n_x within five seconds after touchdown, and figure 11 shows the cumulative distribution of Δn_z within five seconds after touchdown.

The cumulative distribution of pitch attitude (degrees) during takeoff and landing is shown by separate curves in figure 12. Distribution of the maximum pitch rate (takeoff rotation) during liftoff is presented in figure 13. The mean and standard deviation for each set of data are shown. Figure 14 also presents cumulative distribution of pitch attitude (degrees) during landing. However, pitch attitude here refers to the pitch angle at the time when the maximum n_z peak occurred during the landing. The mean and standard deviation of pitch angle are also shown.

The cumulative distribution of calibrated airspeed during takeoff and landing is shown by separate curves in figure 15. The mean and standard deviation of calibrated airspeed for each curve are also presented. Takeoff and landing are determined by squat switch setting.

Figure 16 shows the correlation of gross weights at takeoff and touchdown. The data are presented as the number of flights and the percent of total flights in intersecting gross weight bands.

4.3 PRESENTATION OF AUTOPILOT DATA.

The cumulative distribution of the percent of flight time that the autopilot was engaged is shown in figure 17. The mean and standard deviation of percent of time are shown on the plot.

4.4 PRESENTATION OF FLAP USAGE.

Flaps usage during the departure phases and approach phases is summarized in the histograms shown in figures 18 and 19. The data are summarized as a percentage of time spent in each detent, both as a percentage of the total flaps extended time, i.e., departure and approach phases and also as a percent of the total flight time. Figures 20 through 26 present the cumulative distribution of calibrated airspeed during flap extension and retraction for each flap detent. The mean and standard deviation of calibrated airspeed are also presented.
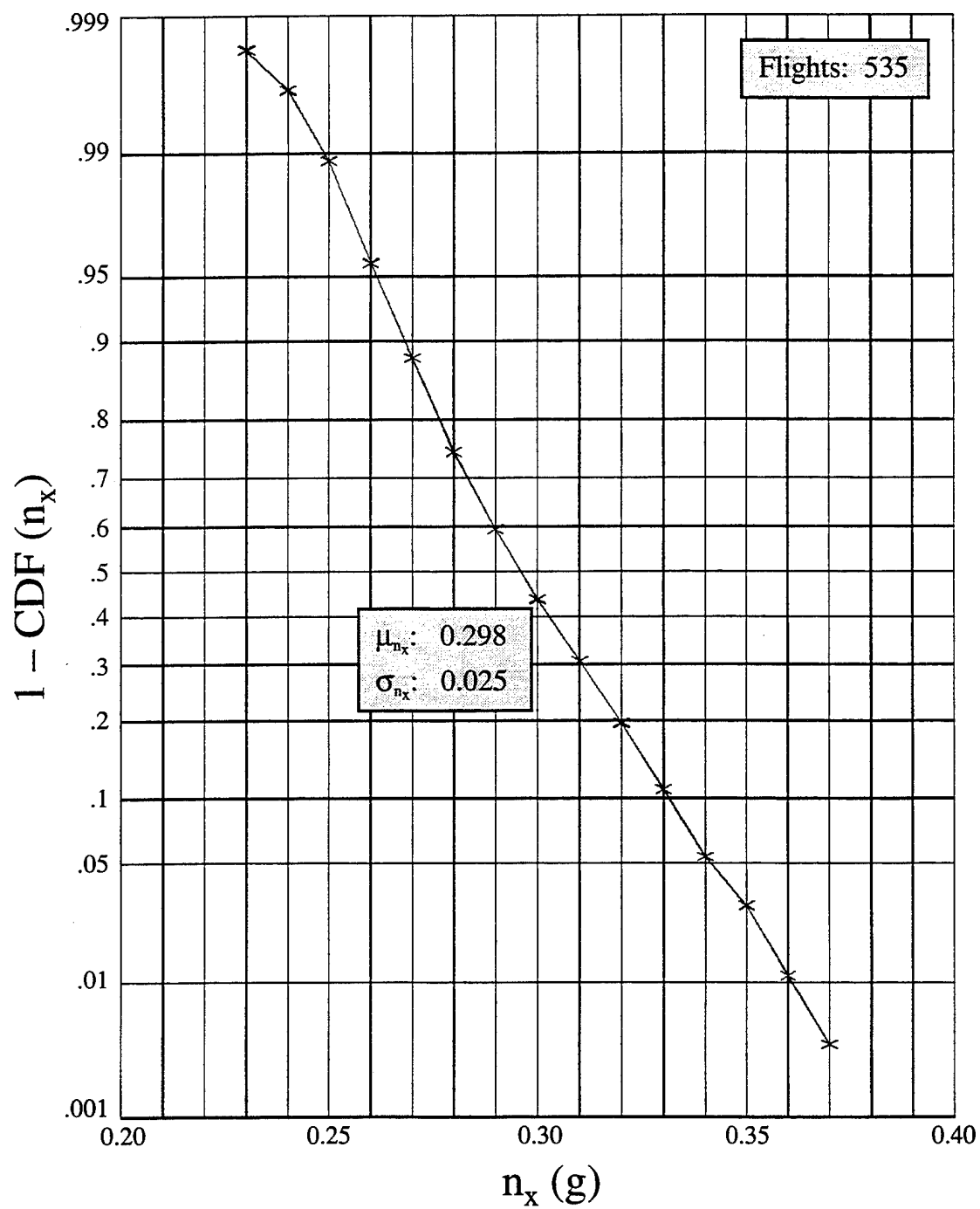
21

FIGURE 9. CUMULATIVE DISTRIBUTION OF MAXIMUM POSITIVE n_x BEFORE TAKEOFF
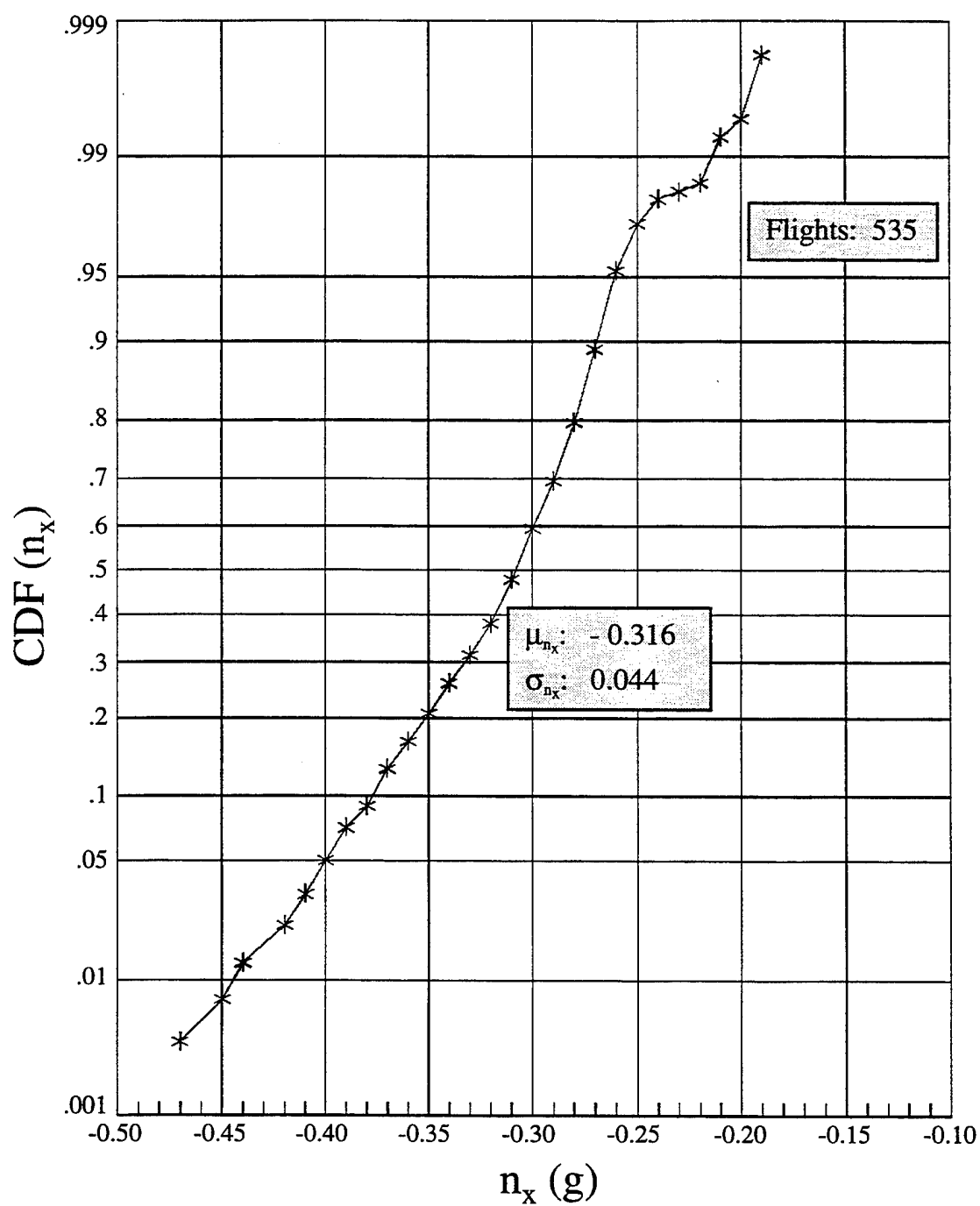
FIGURE 10. CUMULATIVE DISTRIBUTION OF MINIMUM NEGATIVE n_x AFTER LANDING
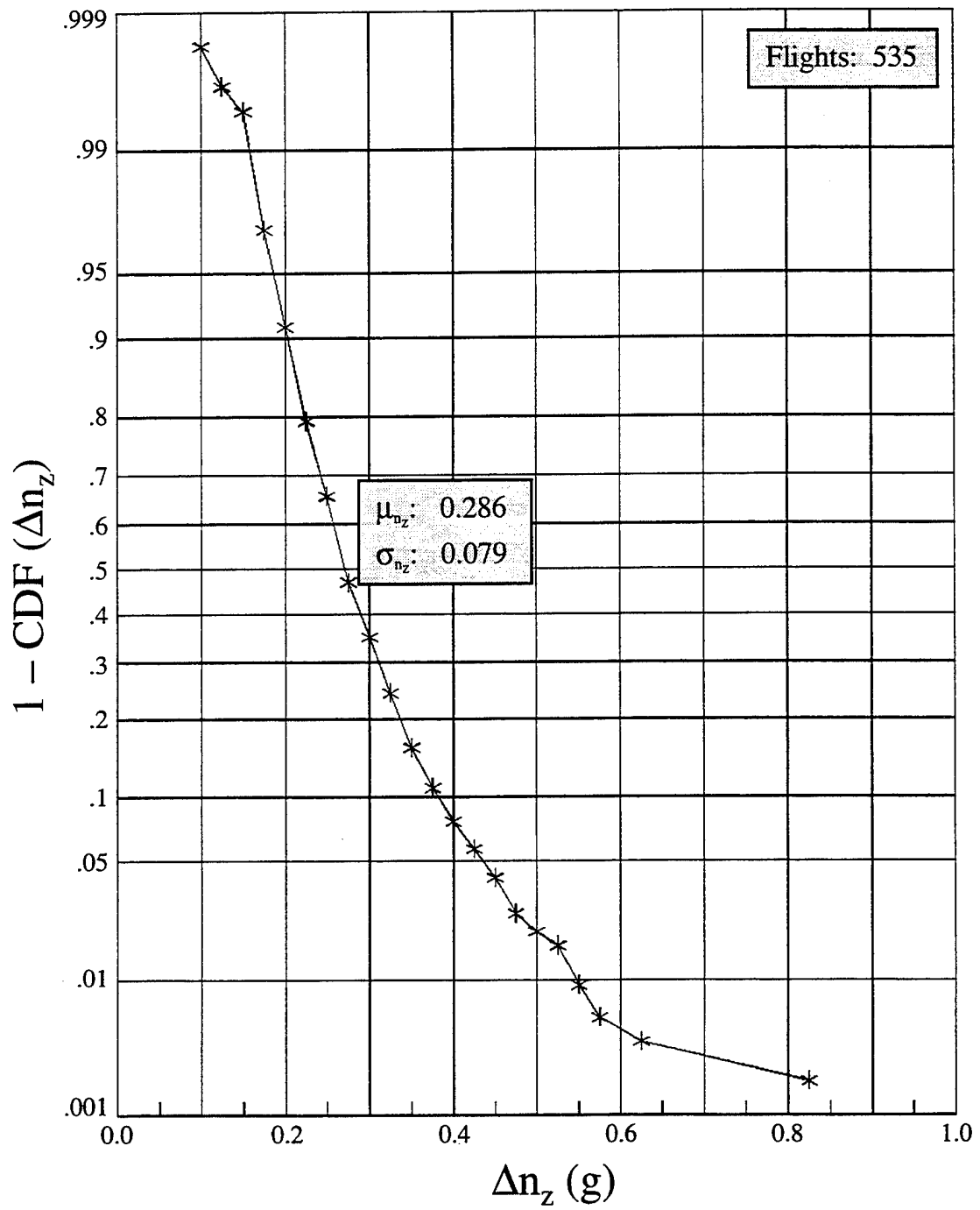
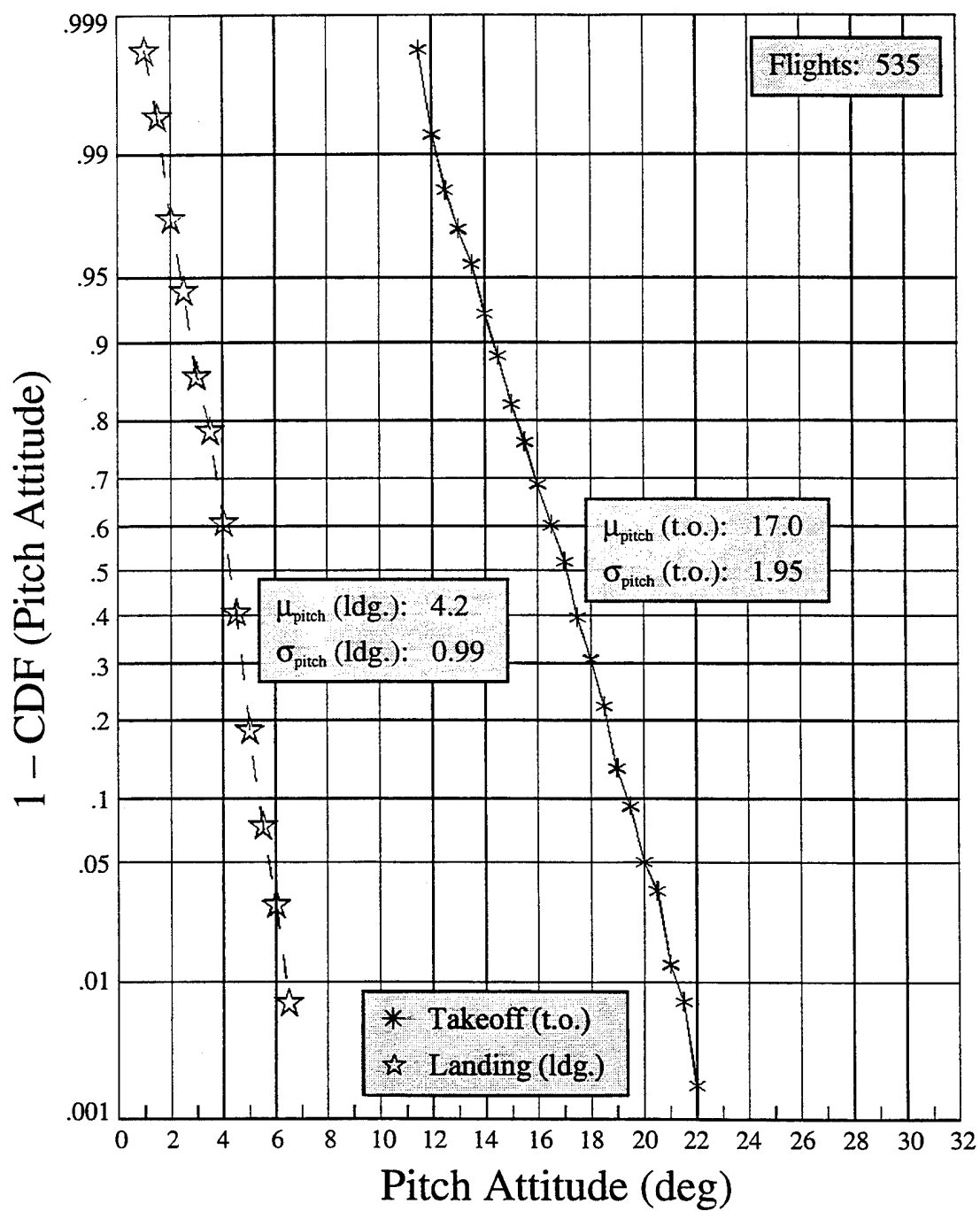FIGURE 11. CUMULATIVE DISTRIBUTION OF MAXIMUM Δn_z AT TOUCHDOWN

FIGURE 12.   CUMULATIVE DISTRIBUTION OF MAXIMUM PITCH ATTITUDE
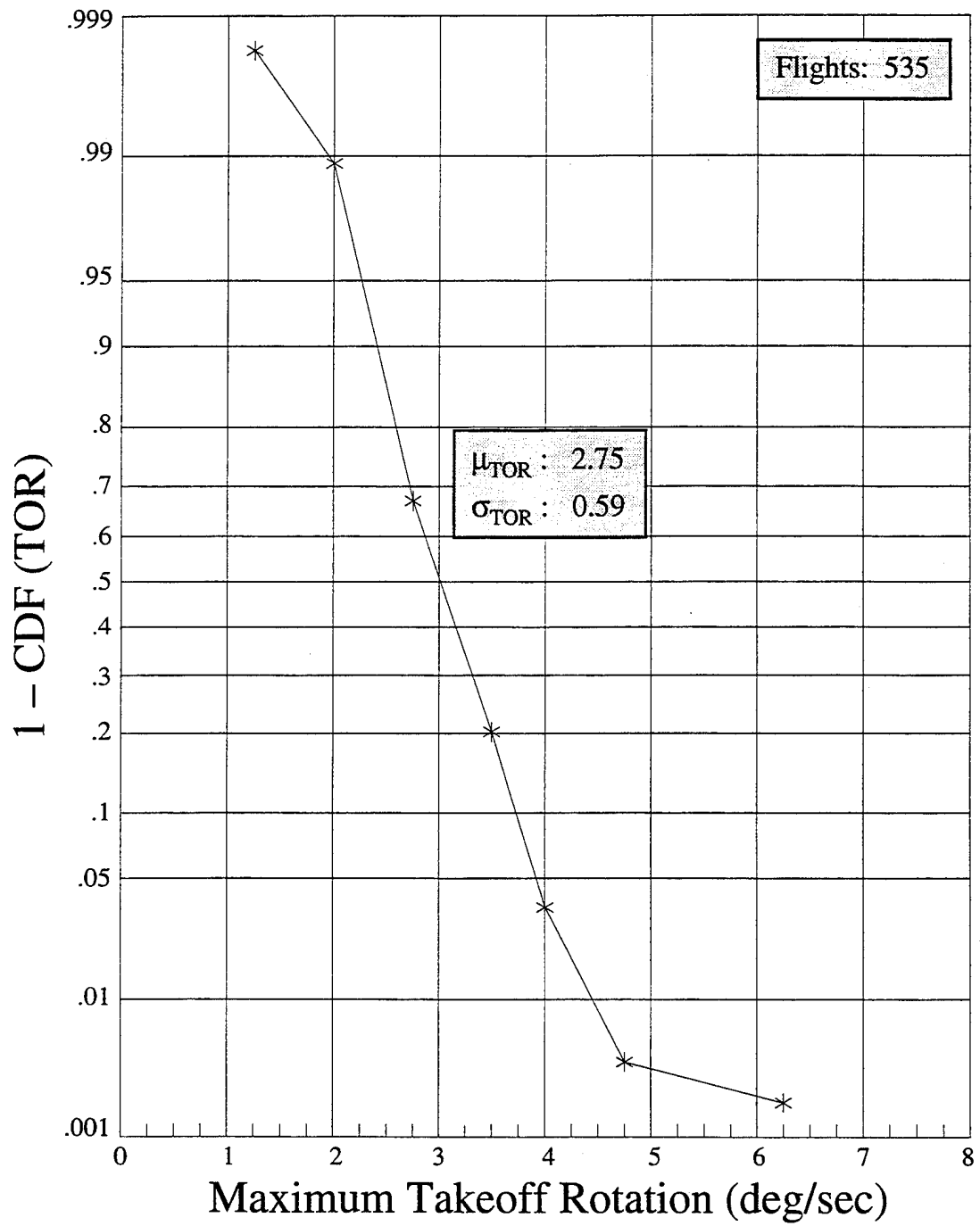   DURING TAKEOFF AND LANDING

25

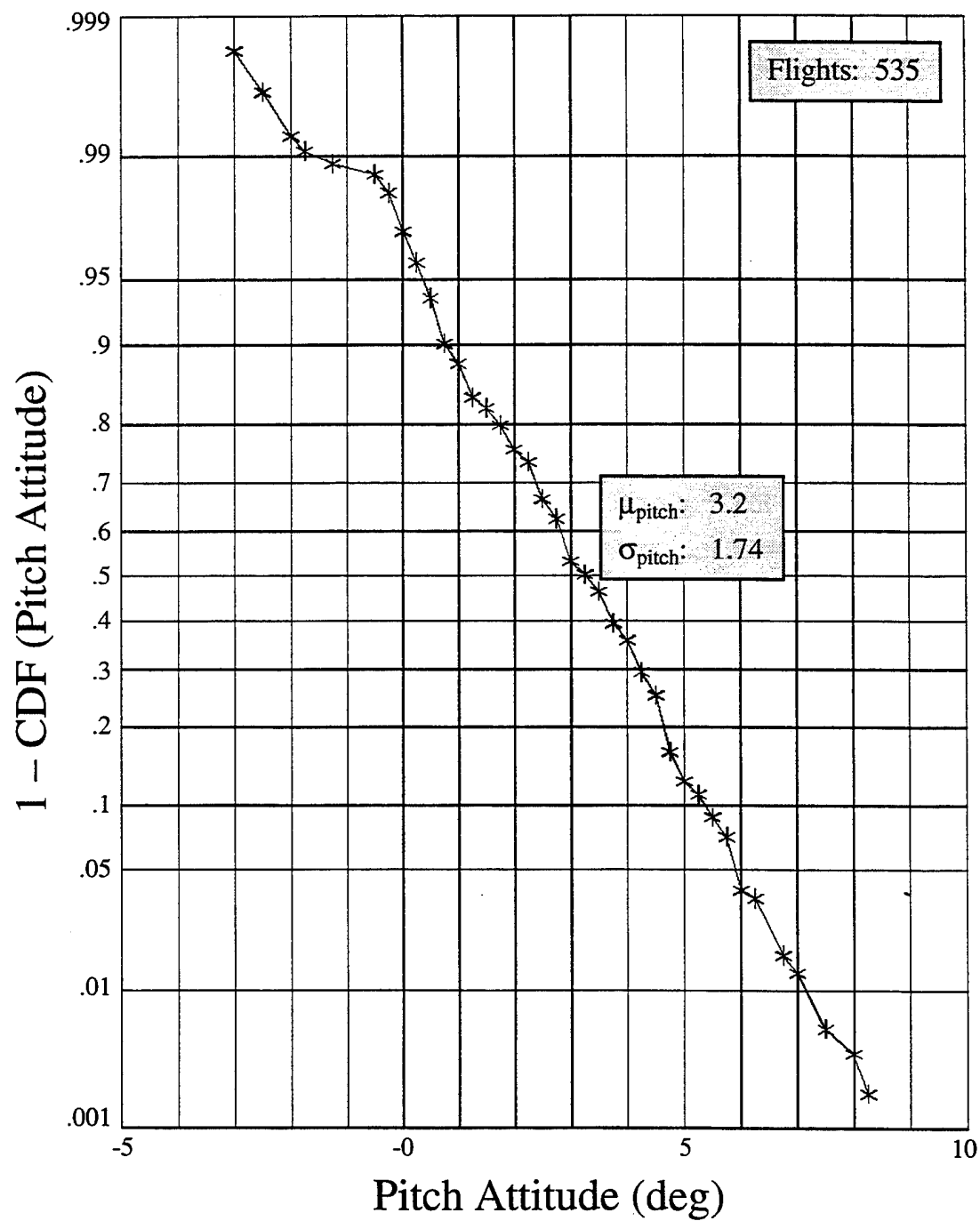FIGURE 13. CUMULATIVE DISTRIBUTION OF MAXIMUM TAKEOFF ROTATION

FIGURE 14. CUMULATIVE DISTRIBUTION OF MAXIMUM PITCH ATTITUDE AT TOUCHDOWN PEAK n_z

27
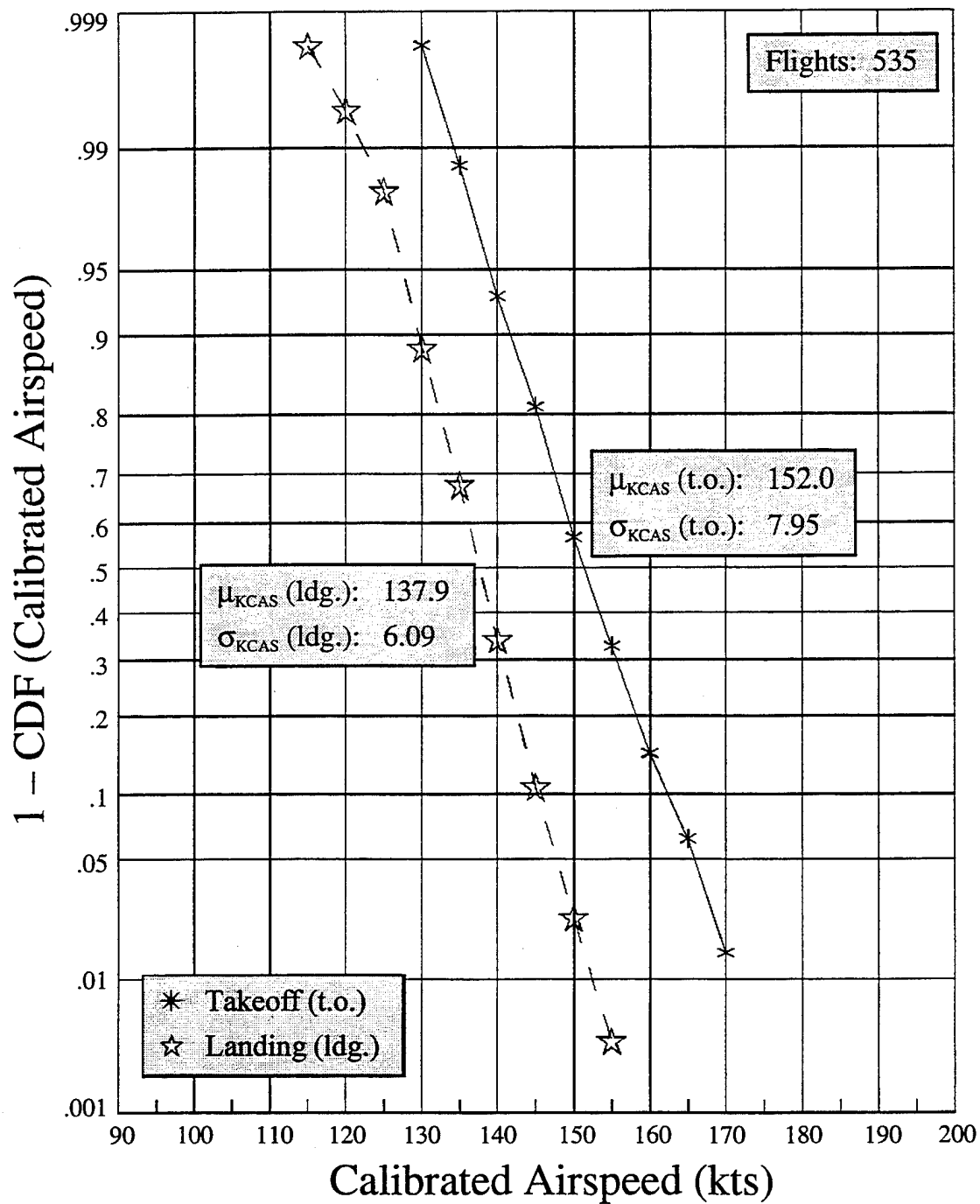
FIGURE 15. CUMULATIVE DISTRIBUTION OF CALIBRATED AIR SPEED
DURING TAKEOFF AND LANDING

Figure 16 — Correlation of Gross Weight at Liftoff and Touchdown (Percent of Flights)

Number of Flights (Percent of Flights)

Gross Weight at Touchdown (1000 lbs.)	Gross Weight at Liftoff (1000 lbs.)							Total
	80–90	90–100	100–110	110–120	120–130	130–140	140–150	
120–130					2 (0.4)			2 (0.4)
110–120				29 (5.4)	71 (13.3)	24 (4.5)		124 (23.2)
100–110			63 (11.8)	111 (20.7)	45 (8.4)	1 (0.2)		220 (41.1)
90–100		52 (9.7)	96 (17.8)	15 (2.8)	1 (0.2)			163 (30.5)
80–90	1 (0.2)	23 (4.3)	1 (0.2)		1 (0.2)			26 (4.9)
Total	1 (0.2)	75 (14.0)	159 (29.7)	155 (29.0)	120 (22.4)	25 (4.7)		535 (100)

FIGURE 16. CORRELATION OF GROSS WEIGHT AT LIFTOFF
AND TOUCHDOWN (PERCENT OF FLIGHTS)

FIGURE 17. CUMULATIVE DISTRIBUTION OF PERCENT OF
FLIGHT TIME ON AUTOPILOT

Flap Detent Usage (Departure)

Flights: 535
Total Flight Hours: 817.7
Hours in Departure: 8.8

■ % of Departure Time
□ % of Total Flight Time

Percent Detent Usage

100%
90%
80%
70%
60%
50%
40%
30%
20%
10%
0%

Detent 1
Detent 5
Detent 10
Detent 15
Detent 25
Detent 30
Detent 40

2.848 hours
5.896 hours
0.002 hours
0.013 hours
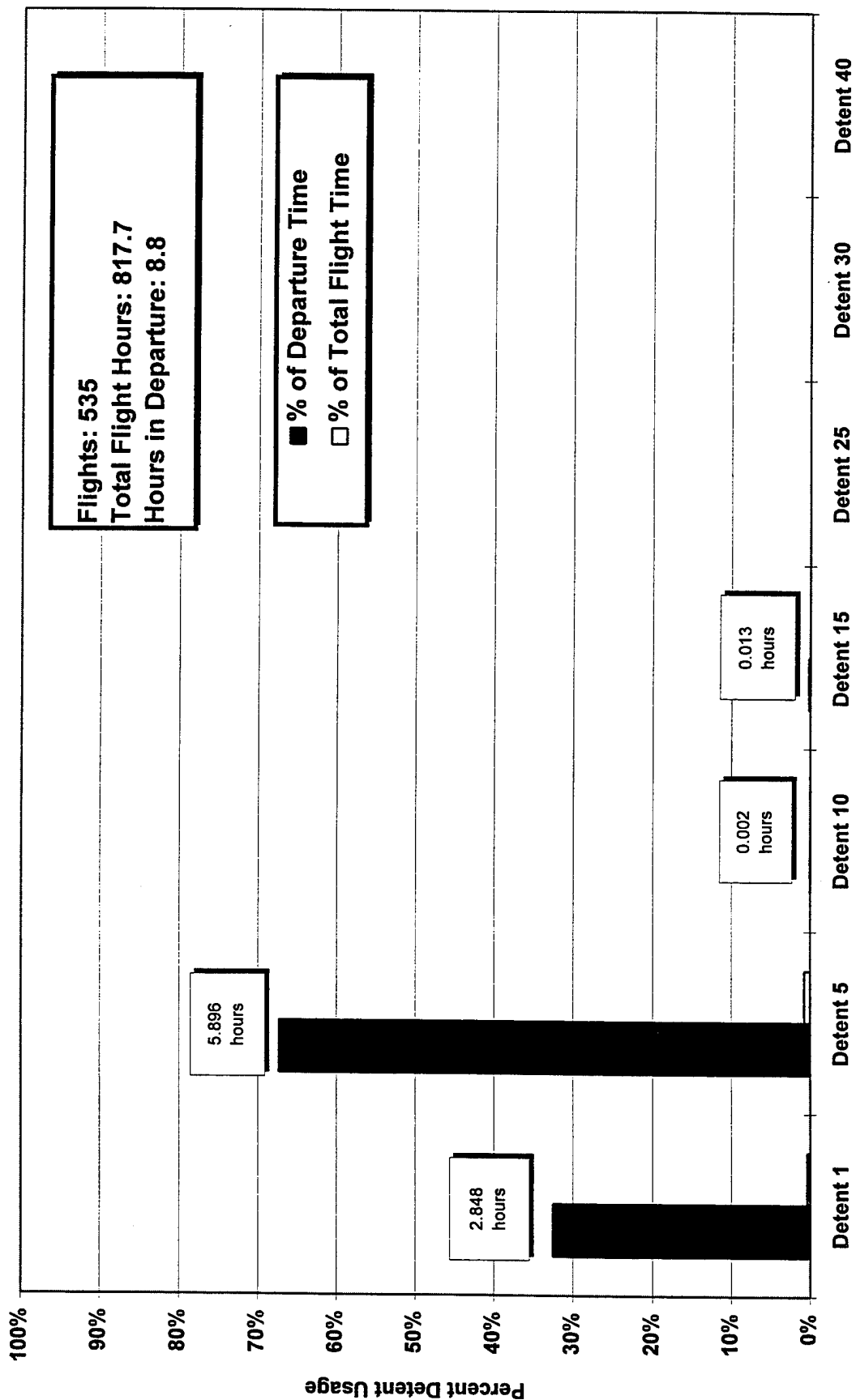
FIGURE 18. FLAPS USAGE BY FLAPS DETENT DURING DEPARTURE

31

Flap Detent Usage (Approach)
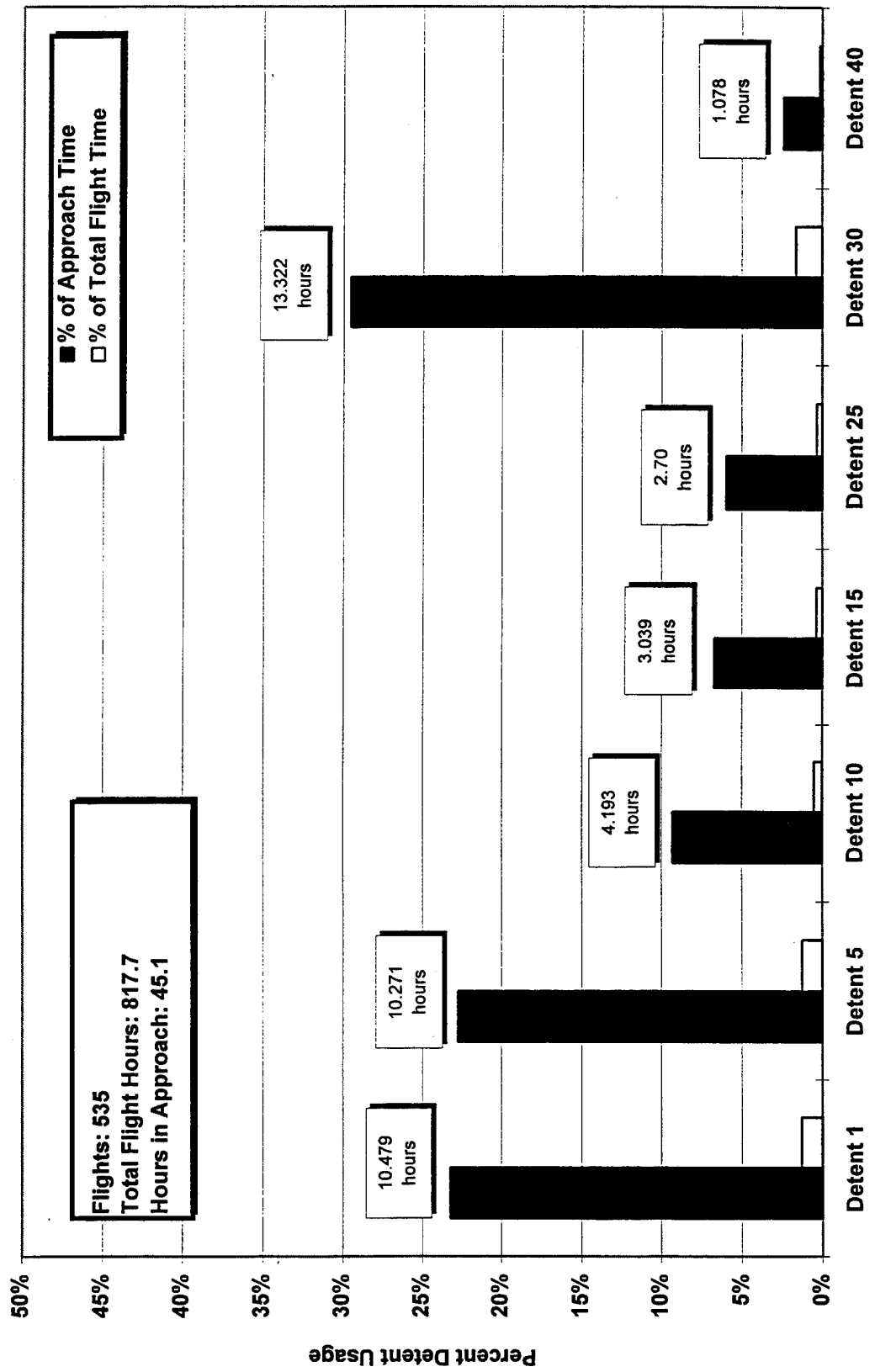
FIGURE 19. FLAPS USAGE BY FLAPS DETENT DURING APPROACH

32
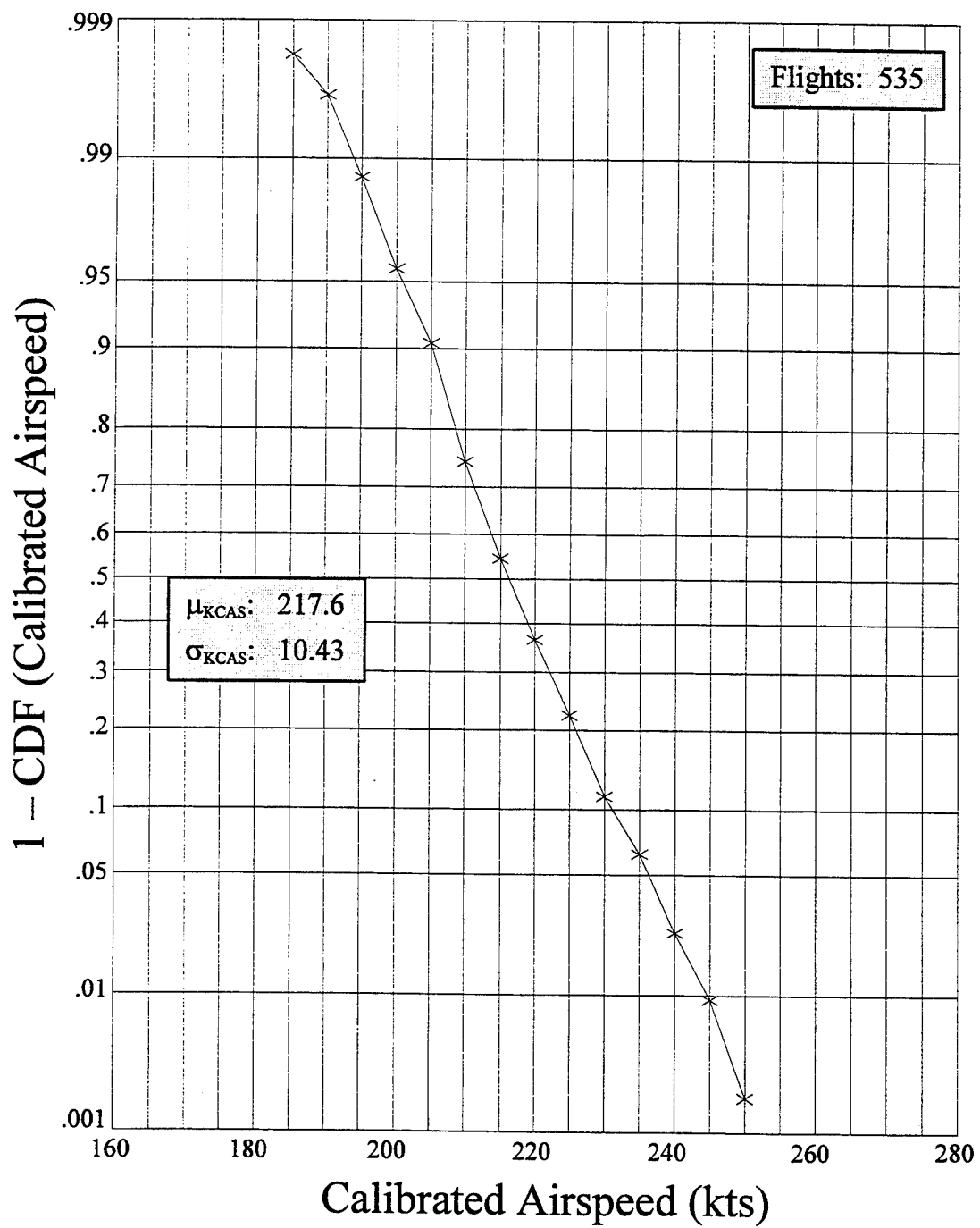
FIGURE 20.   CUMULATIVE DISTRIBUTION OF CALIBRATED AIRSPEED
AT FLAP DETENT 1
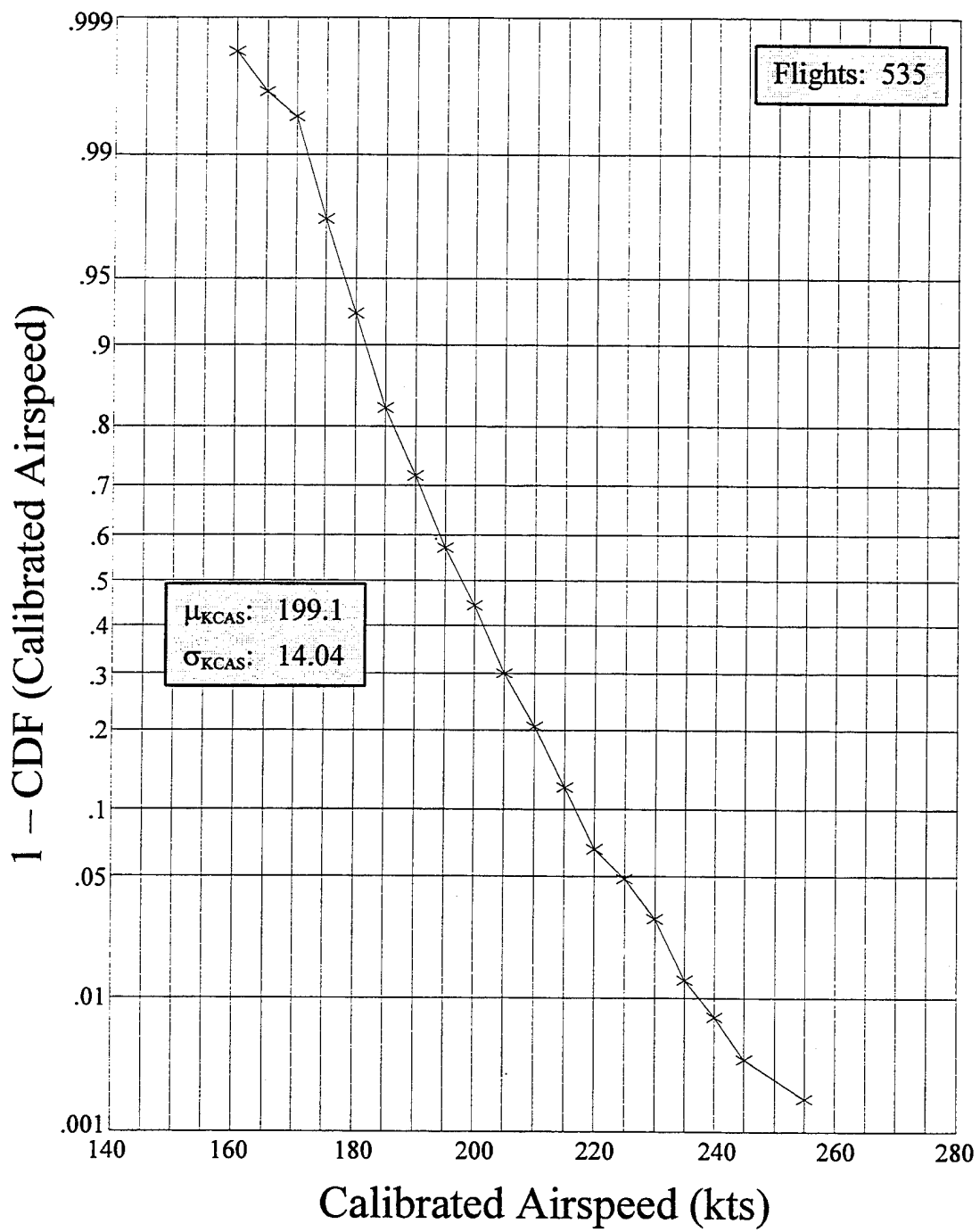
FIGURE 21. CUMULATIVE DISTRIBUTION OF CALIBRATED AIRSPEED
AT FLAP DETENT 5
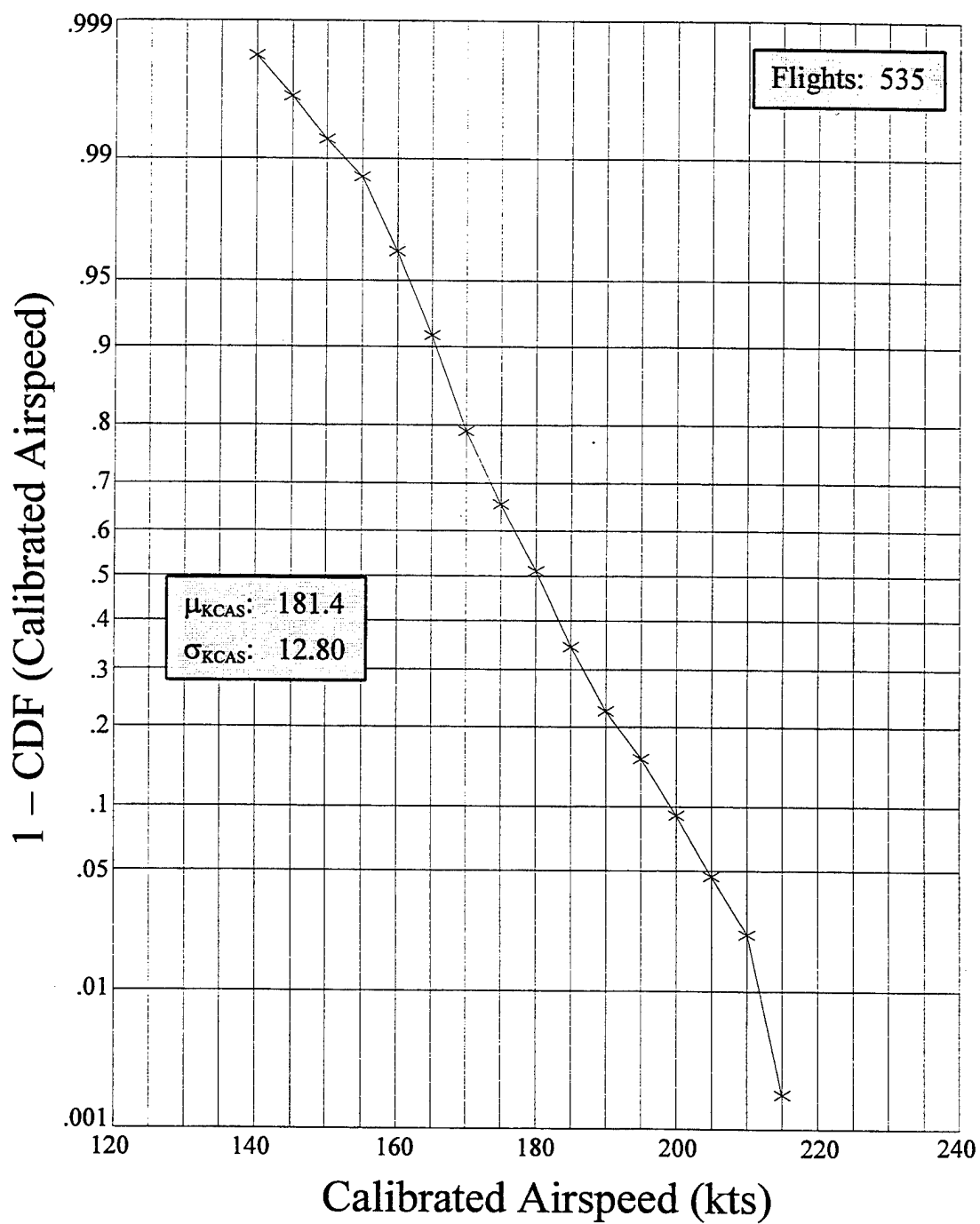
FIGURE 22.   CUMULATIVE DISTRIBUTION OF CALIBRATED AIRSPEED
AT FLAP DETENT 10
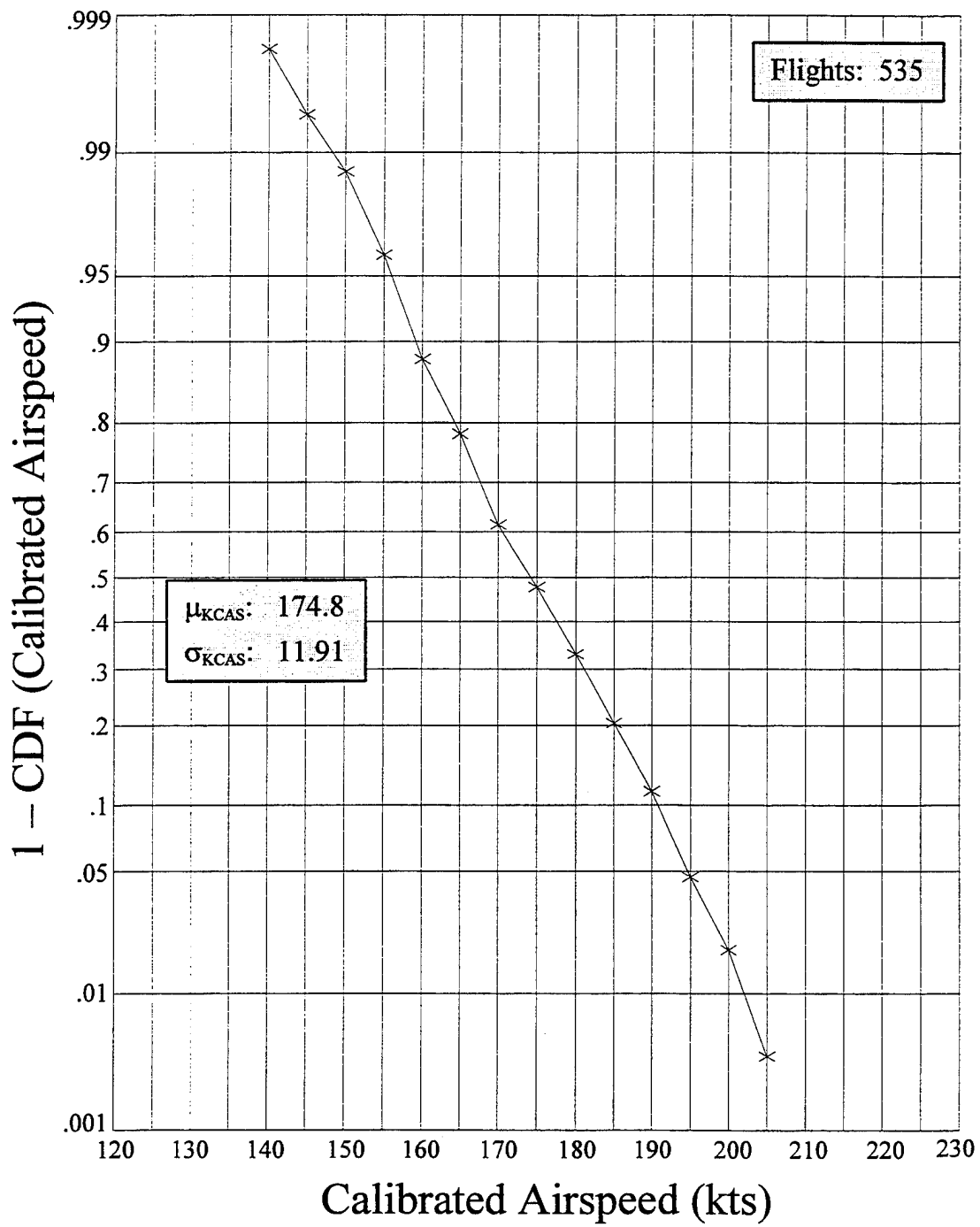
FIGURE 23. CUMULATIVE DISTRIBUTION OF CALIBRATED AIRSPEED
AT FLAP DETENT 15.
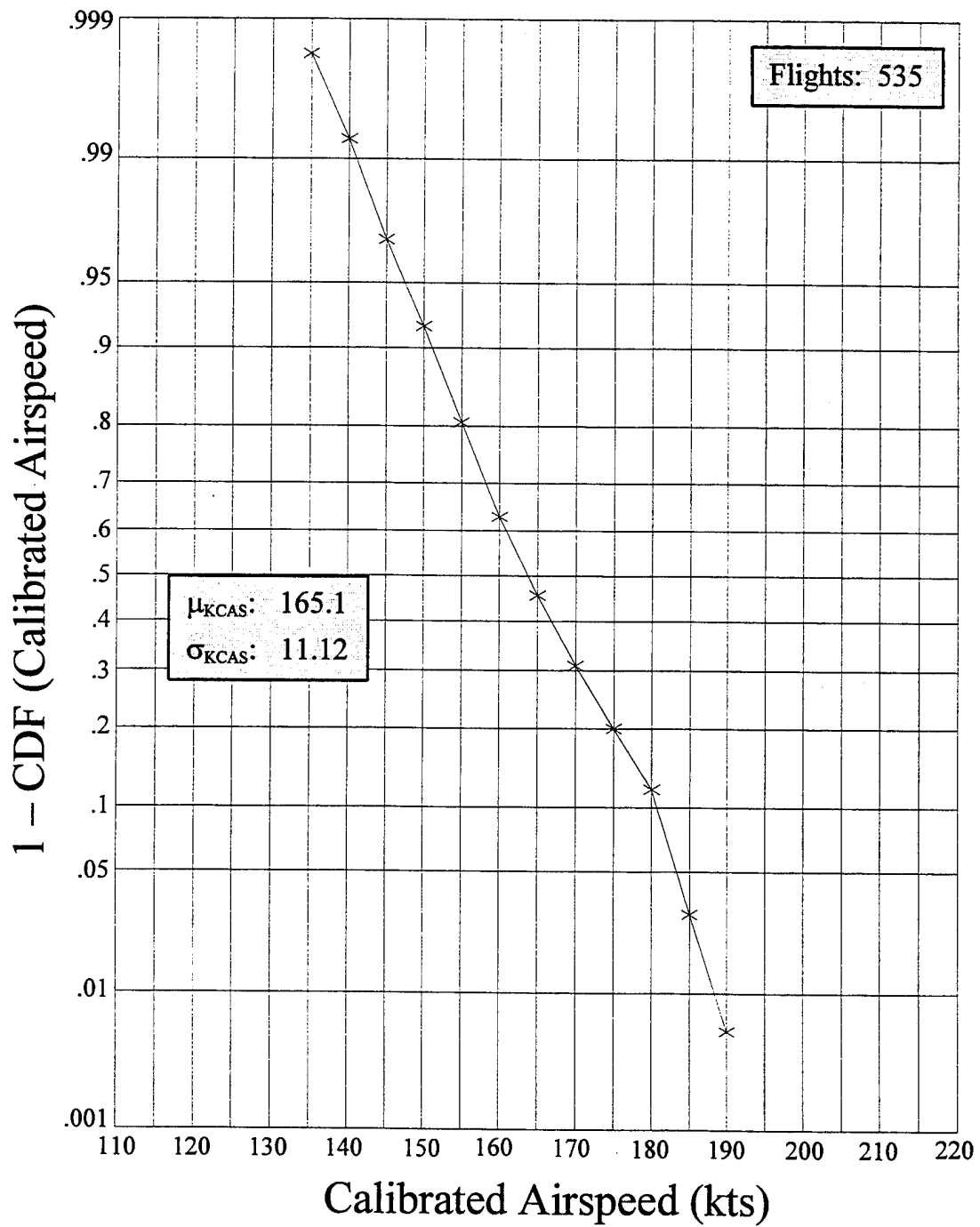
FIGURE 24.   CUMULATIVE DISTRIBUTION OF CALIBRATED AIRSPEED
             AT FLAP DETENT 25

37
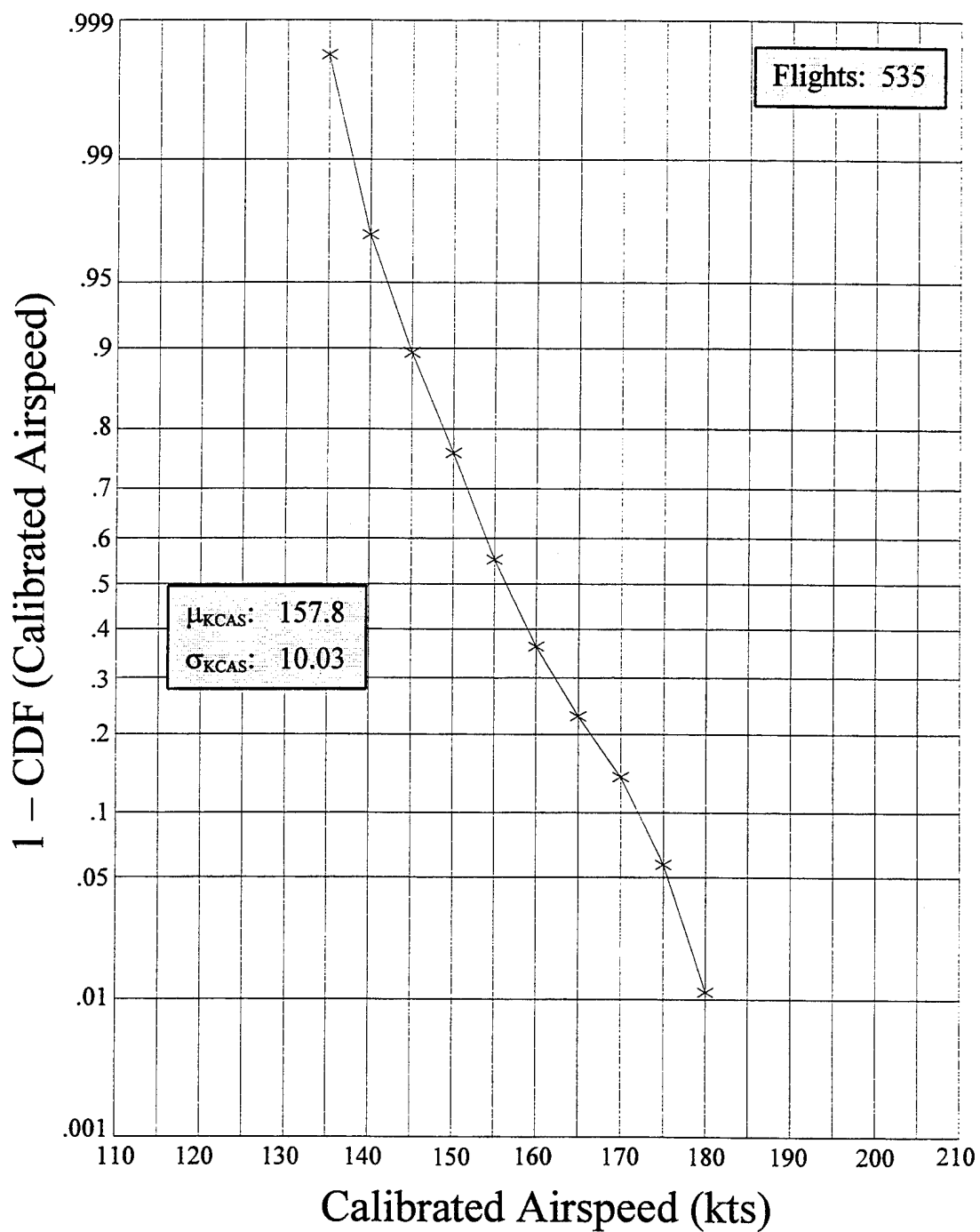
FIGURE 25. CUMULATIVE DISTRIBUTION OF CALIBRATED AIRSPEED
AT FLAP DETENT 30
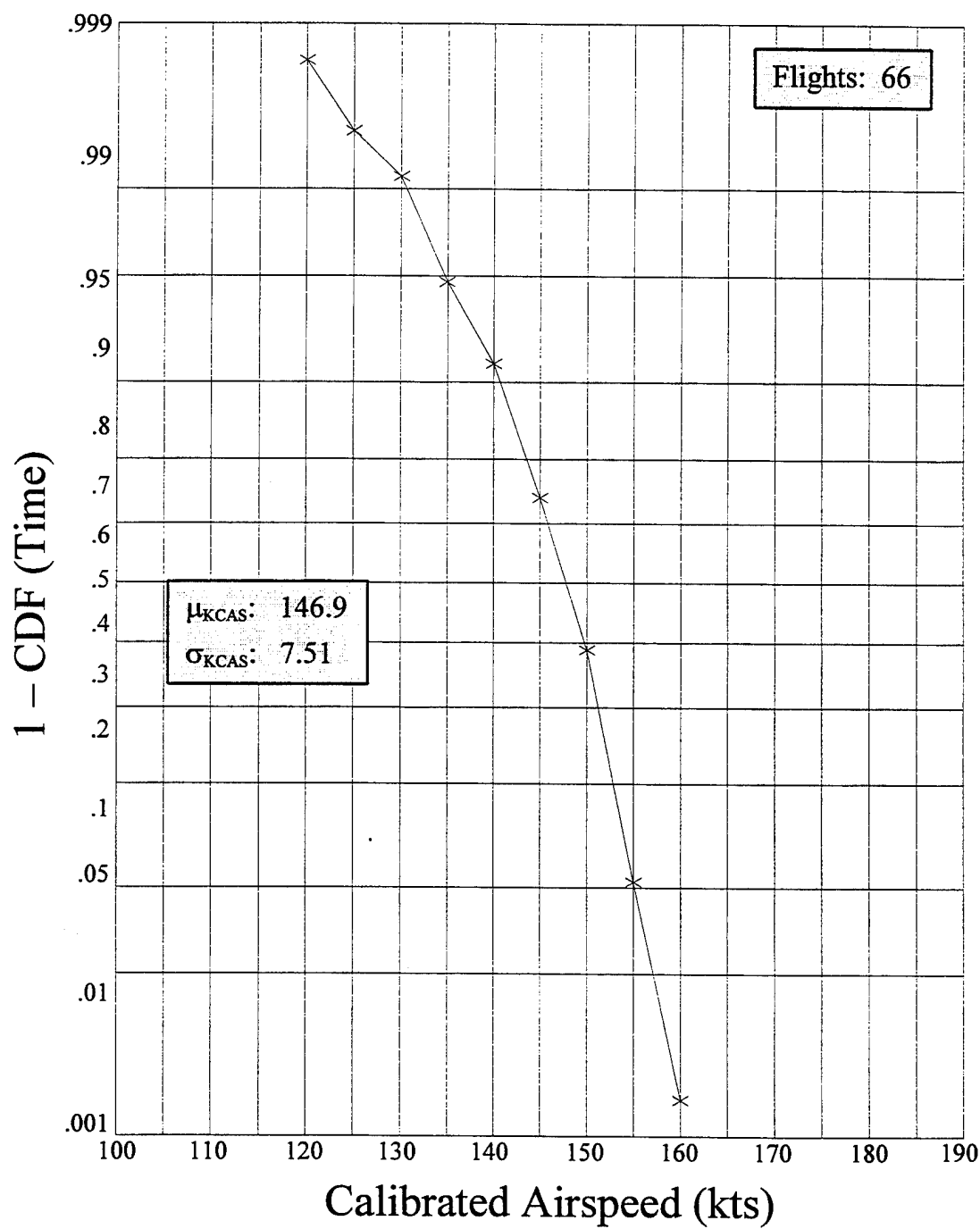
FIGURE 26. CUMULATIVE DISTRIBUTION OF CALIBRATED AIRSPEED
AT FLAP DETENT 40

4.5 PRESENTATION OF SPEED BRAKE DATA.

Speed brake usage was observed mostly in the descent and approach phases of flight; however, sporadic usage was also seen in the other airborne phases. The speed brake data are summarized in terms of speed brake deployment cycles. A deployment cycle is defined as the time from when the speed brake handle setting exceeds two degrees until the time when the speed brake handle setting drops back below two degrees. The maximum handle setting observed during the deployment cycle determines whether the cycle was classified as partial (2 to 20 degrees) or full (20 to 45 degrees).

Figure 27 presents the cumulative distribution of calibrated airspeed at the start of partial and full speed brake deployment cycles. The number of observed deployment cycles, mean calibrated airspeed, and standard deviation of calibrated airspeed are presented as tabular data on the plot.

4.6 PRESENTATION OF LANDING GEAR DATA.

The landing gear is lowered during final approach. Figures 28 and 29 present cumulative distributions of the length of time that the landing gear is in the lowered position and the maximum calibrated airspeed while the gear is in the lowered position, respectively. Both figures present mean and standard deviation of their respective parameters.

4.7 PRESENTATION OF ACCELERATION DATA.

Acceleration data were collected for the normal, lateral, and longitudinal directions. Normal and lateral acceleration are plotted in terms of cumulative occurrences per 1000 hours. The normal accelerations are also plotted as cumulative occurrences per nautical mile. A similar plot for longitudinal acceleration is not presented.

4.7.1 Normal Acceleration Data - Ground Phase.

The ground loads Δn_z data are presented in figures 30 through 33 as cumulative occurrences per 1000 hours. Figure 30 shows the data from takeoff and landing roll phases as one curve and the taxi-in and taxi-out phase data as a separate curve. In figure 31, the data are divided into before liftoff phases (taxi-out and takeoff roll) and after flight phases (landing roll and taxi-in). Figure 32 presents the Δn_z data per on-ground phase of flight, and figure 33 presents all the on-ground data as one curve.

4.7.2 Normal Acceleration Data.

Since the 1950s, it has been common practice to present flight loads data as a cumulative frequency of exceedance curve. Data that were previously recorded on the B737 are reported in references 5 and 6 as cumulative occurrences per 1000 hours.
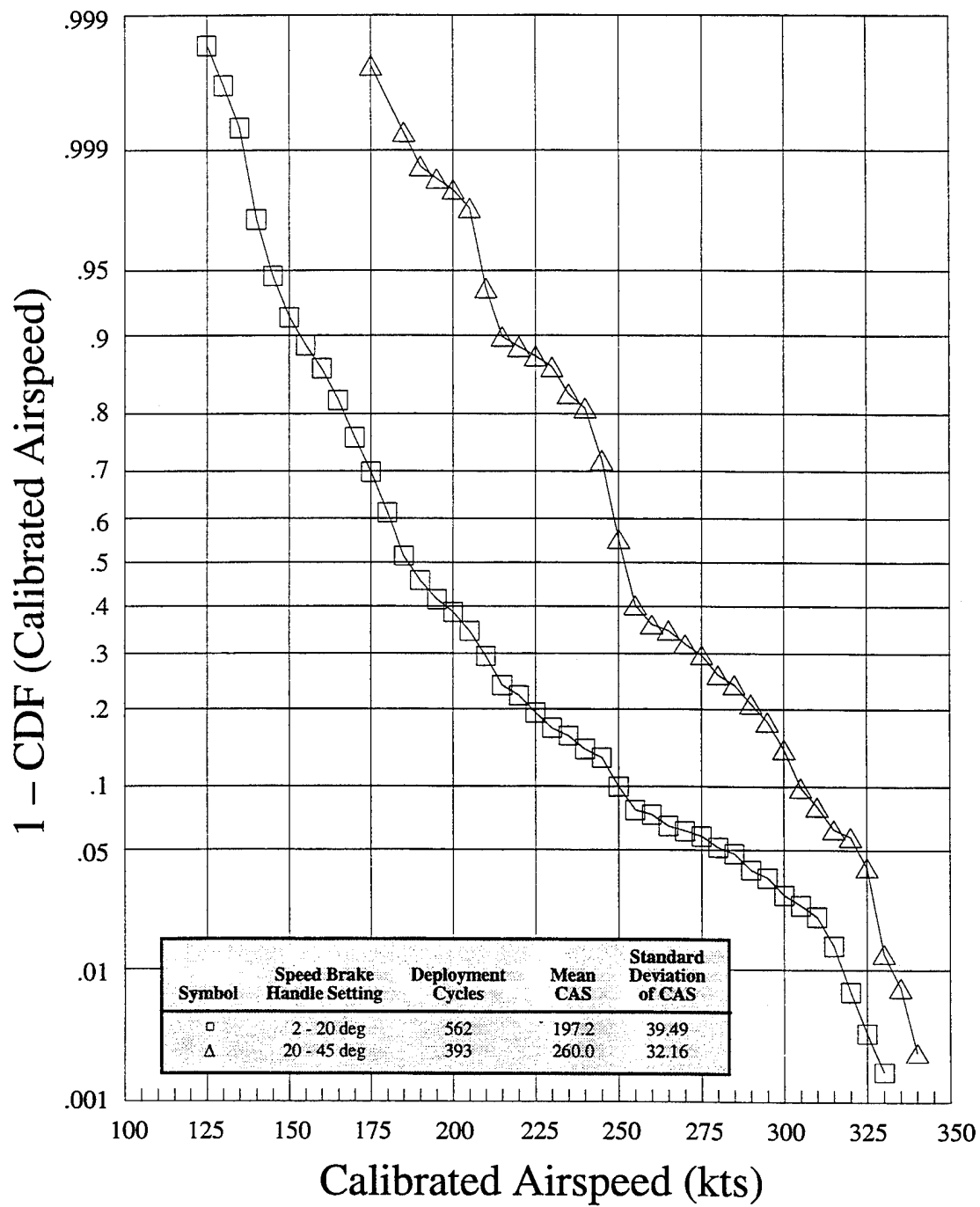
The y-axis is labeled "1 − CDF (Calibrated Airspeed)" with values: .999, .999, .95, .9, .8, .7, .6, .5, .4, .3, .2, .1, .05, .01, .001

The x-axis is labeled "Calibrated Airspeed (kts)" with values: 100, 125, 150, 175, 200, 225, 250, 275, 300, 325, 350

Symbol	Speed Brake Handle Setting	Deployment Cycles	Mean CAS	Standard Deviation of CAS
□	2 - 20 deg	562	197.2	39.49
Δ	20 - 45 deg	393	260.0	32.16

FIGURE 27. CUMULATIVE DISTRIBUTION OF CALIBRATED AIRSPEED
AT SPEED BRAKE DEPLOYMENT IN FLIGHT

41
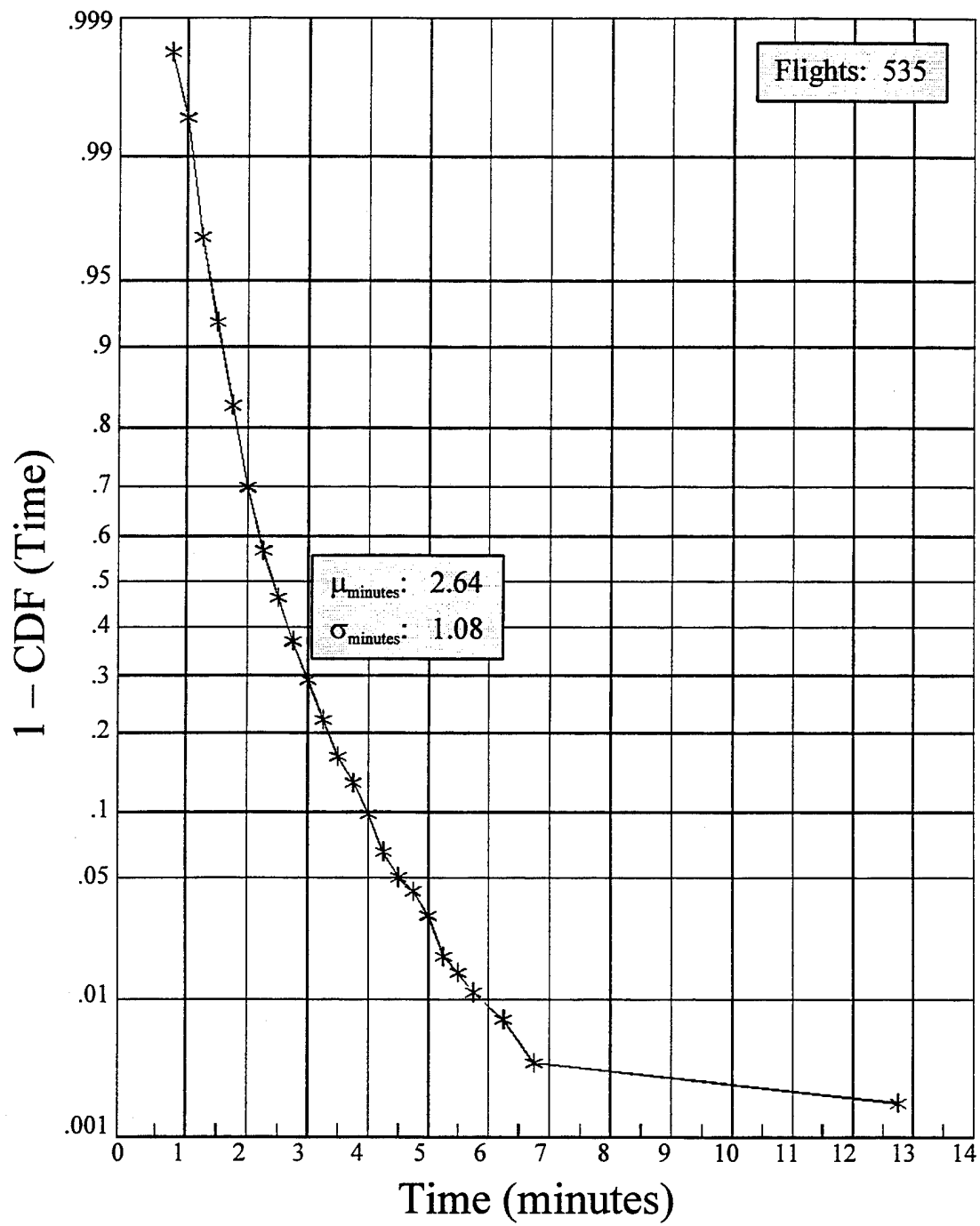
FIGURE 28. CUMULATIVE DISTRIBUTION OF NUMBER OF MINUTES
WITH GEAR DOWN IN APPROACH
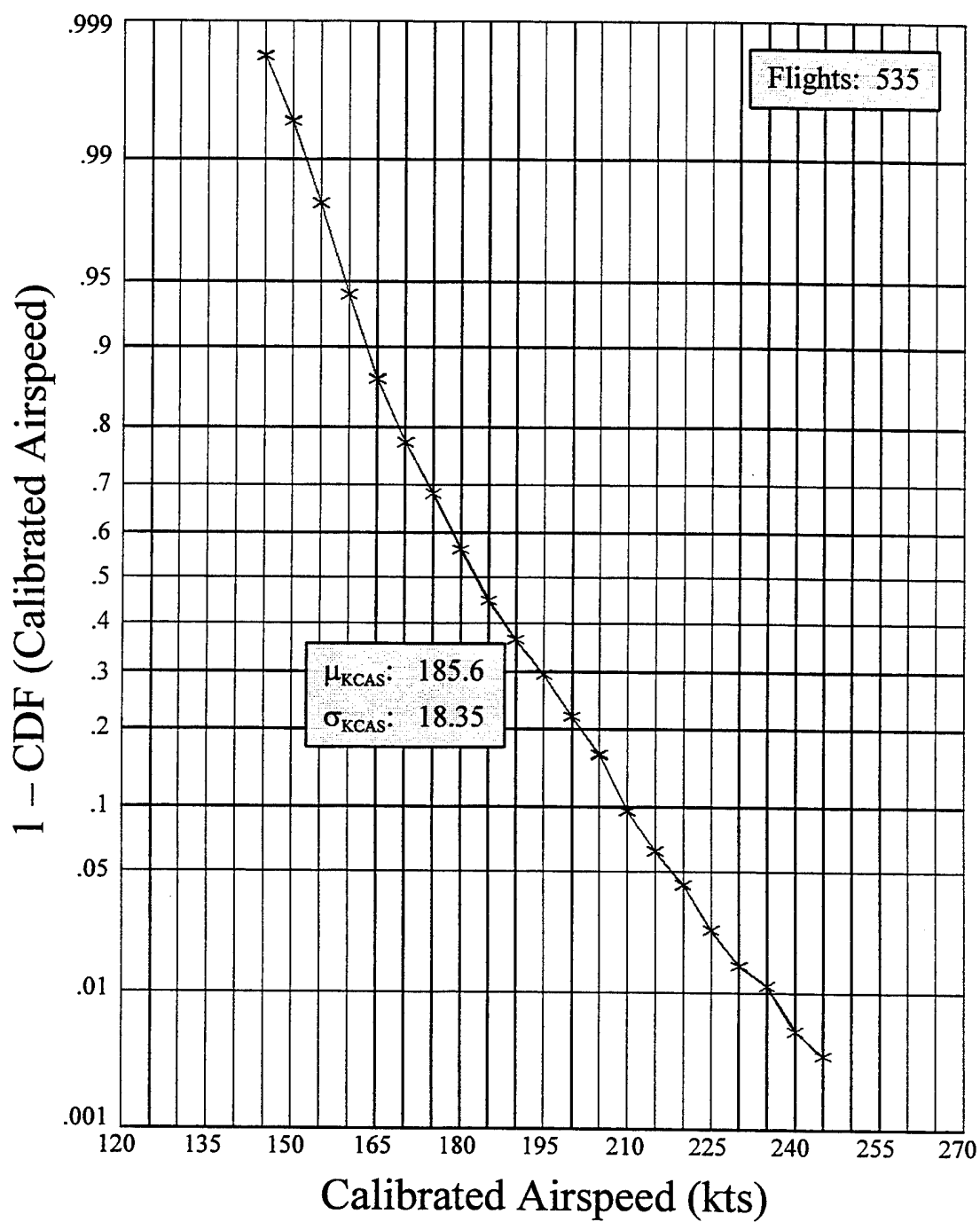
FIGURE 29. CUMULATIVE DISTRIBUTION OF CALIBRATED AIRSPEED
AT TIME OF GEAR EXTENSION

FIGURE 31. INCREMENTAL LOAD FACTOR CUMULATIVE OCCURRENCES PER 1000 HOURS BEFORE AND AFTER FLIGHT

FIGURE 30. INCREMENTAL LOAD FACTOR CUMULATIVE OCCURRENCES PER 1000 HOURS BY TAXI AND ROLL

44

FIGURE 33. ON-GROUND INCREMENTAL LOAD
FACTOR CUMULATIVE OCCURRENCES
PER 1000 HOURS

FIGURE 32. INCREMENTAL LOAD FACTOR
CUMULATIVE OCCURRENCES PER
1000 HOURS BY GROUND PHASE

45

To compare data from different references, the normal acceleration data are plotted two ways. In figures 34 through 39, the data are plotted as cumulative occurrences per 1000 hours, and in figures 40 through 45, the same data are plotted as cumulative occurrences per nautical mile. Figures 34 and 40 present Δn_z cumulative occurrences by airborne phases of flight. Figures 35 and 41 present Δn_z cumulative occurrences for all phases combined. Figures 36 and 42 present $\Delta n_{z_{gust}}$ cumulative occurrences by airborne phases of flight. Figures 37 and 43 present $\Delta n_{z_{gust}}$ cumulative occurrences for all phases combined. Figures 38 and 44 present $\Delta n_{z_{man}}$ cumulative occurrences by airborne phases of flight. Figures 39 and 45 present $\Delta n_{z_{man}}$ cumulative occurrences for all phases combined.

4.7.3 Lateral Acceleration Data.

The lateral acceleration data for airborne phases are presented in figure 46. The plot shows cumulative occurrences per 1000 hours for both positive and negative peak accelerations. The number of hours shown on the plot represents all phases. The deadband is 0.01 g with a mean value of zero and a threshold zone of ±0.005 g.

4.8 PRESENTATION OF GUST VELOCITY U_{de} AND U_σ.

In figures 47 through 51, the derived gust velocity U_{de} is plotted as cumulative counts per nautical mile by altitude range and is contrasted with the standard gust spectrum for these altitude ranges found in reference 7. Figures 52 and 53 present the derived gust (U_{de}) peak per nautical mile for flaps extended and retracted. Figures 54 and 55 present the continuous gust intensity (U_σ) peaks per nautical mile for flaps extended and retracted. The U_{de} and U_σ gust calculations are described above in sections 3.5 and 3.6.

FAR 25.341 establishes positive (up) and negative (down) rough air gust design requirements for three different aircraft design speeds: for maximum gust intensity (V_B); cruising speed (V_C) and dive speed (V_D). The requirements, shown in table 9, depend on altitude. Between sea level and 20,000 feet, the gust requirement is constant, then it varies linearly to the value given for 50,000 feet. FAR 25.345 sets a requirement of positive, negative head on 25-fps gusts when flaps are extended. Figures 52 and 53 show the requirements for U_{de} outlined in the FAR. The FAR limit for V_B is shown for the flaps retracted condition.

TABLE 9. FAR REQUIREMENTS FOR DERIVED
DISCRETE GUST VELOCITIES

Aircraft Design Speed	Gust Velocity	
	0- to 20,000-Feet Altitude	50,000-Feet Altitude
V_B	66 fps	38 fps
V_C	50 fps	25 fps
V_D	25 fps	12.5 fps
Flaps Extended	25 fps	—

FIGURE 35. AIRBORNE INCREMENTAL LOAD FACTOR CUMULATIVE OCCURRENCES PER 1000 HOURS
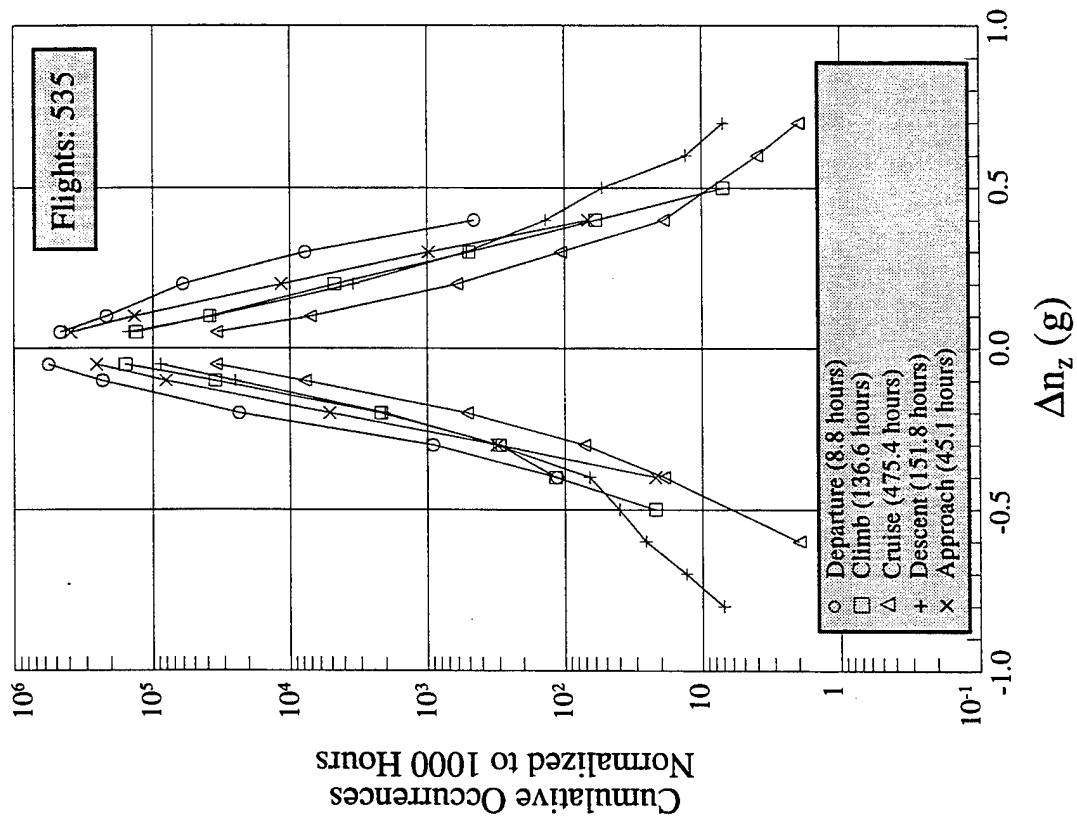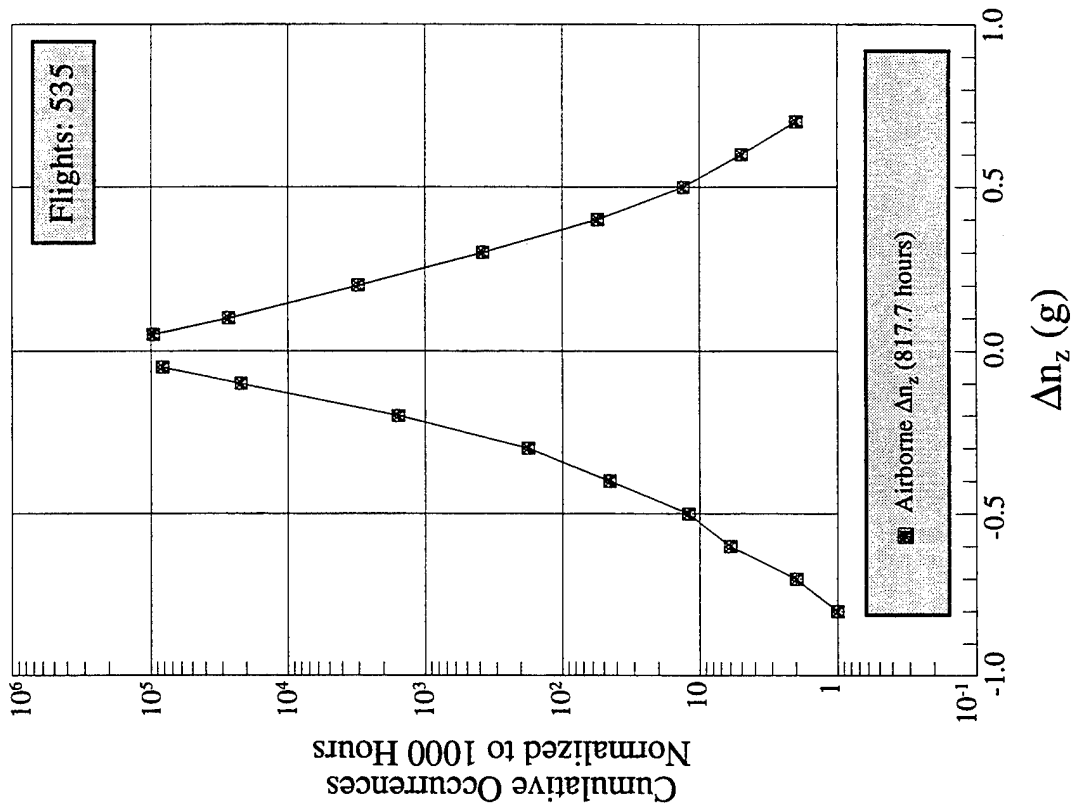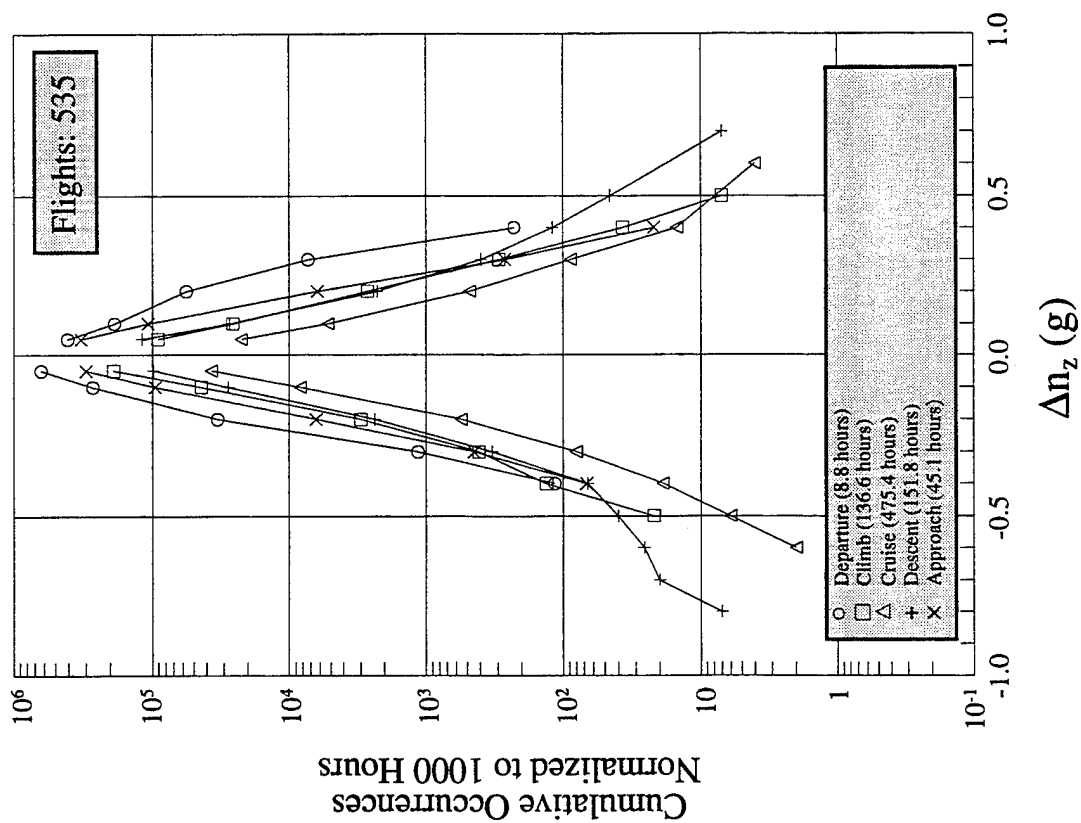

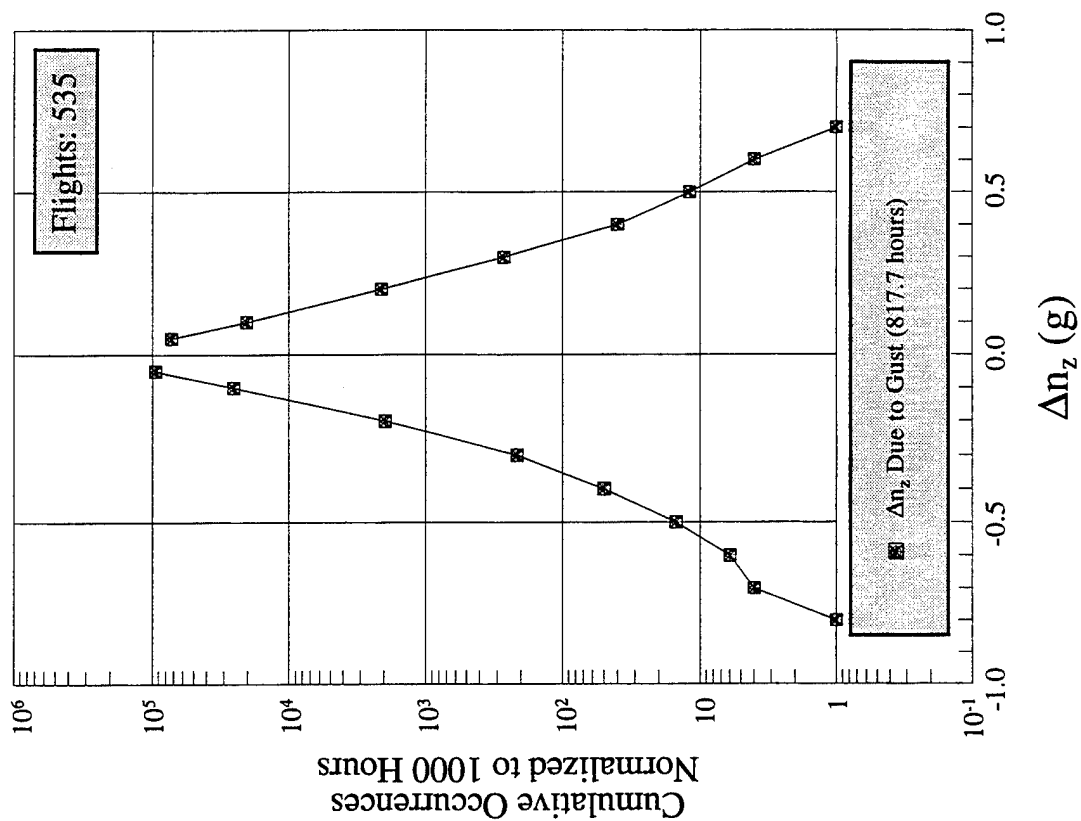FIGURE 34. INCREMENTAL LOAD FACTOR CUMULATIVE OCCURRENCES PER 1000 HOURS BY AIRBORNE PHASE OF FLIGHT

47

FIGURE 37. AIRBORNE INCREMENTAL
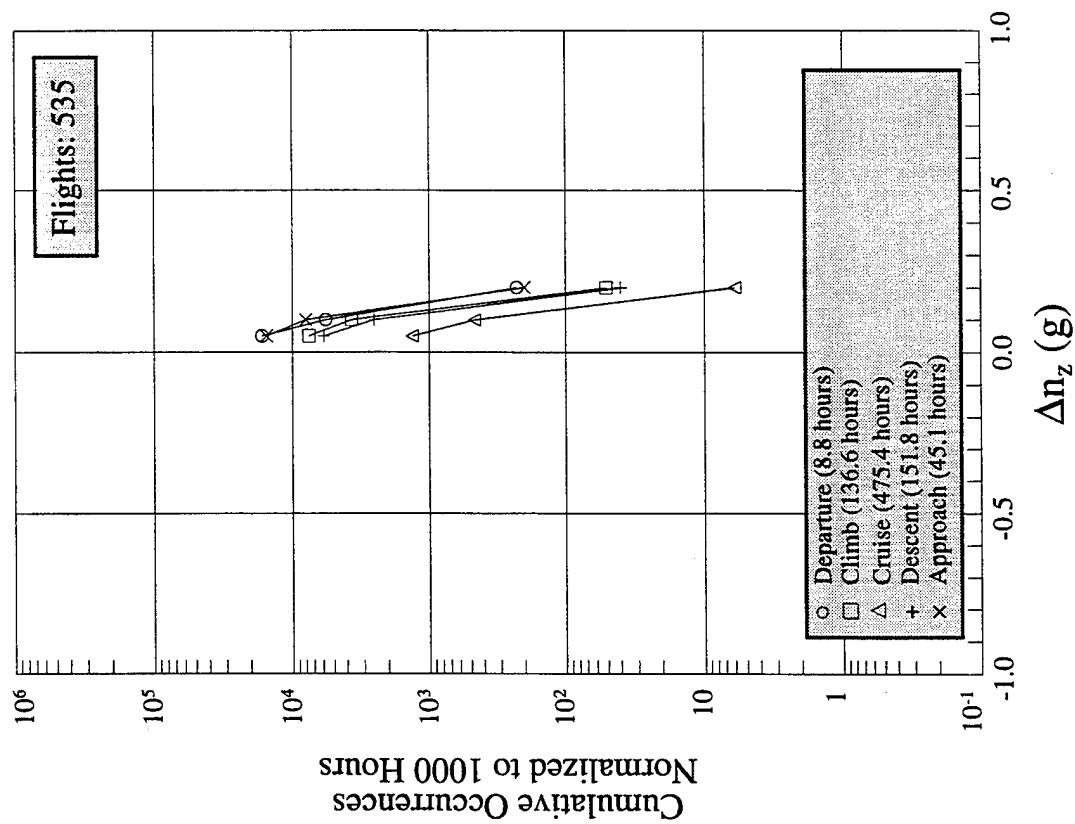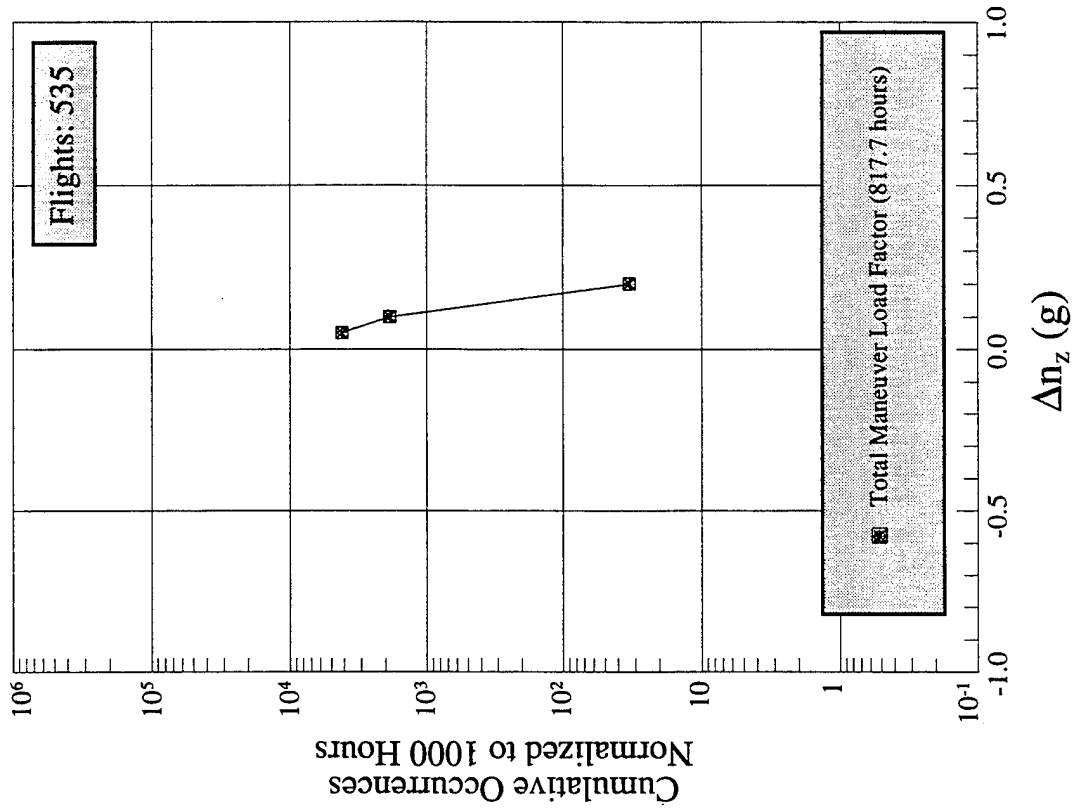GUST LOAD FACTOR CUMULATIVE CUMULATIVE
OCCURRENCES PER 1000 HOURS

FIGURE 36. INCREMENTAL GUST LOAD FACTOR
CUMULATIVE OCCURRENCES PER
1000 HOURS BY AIRBORNE PHASE
OF FLIGHT

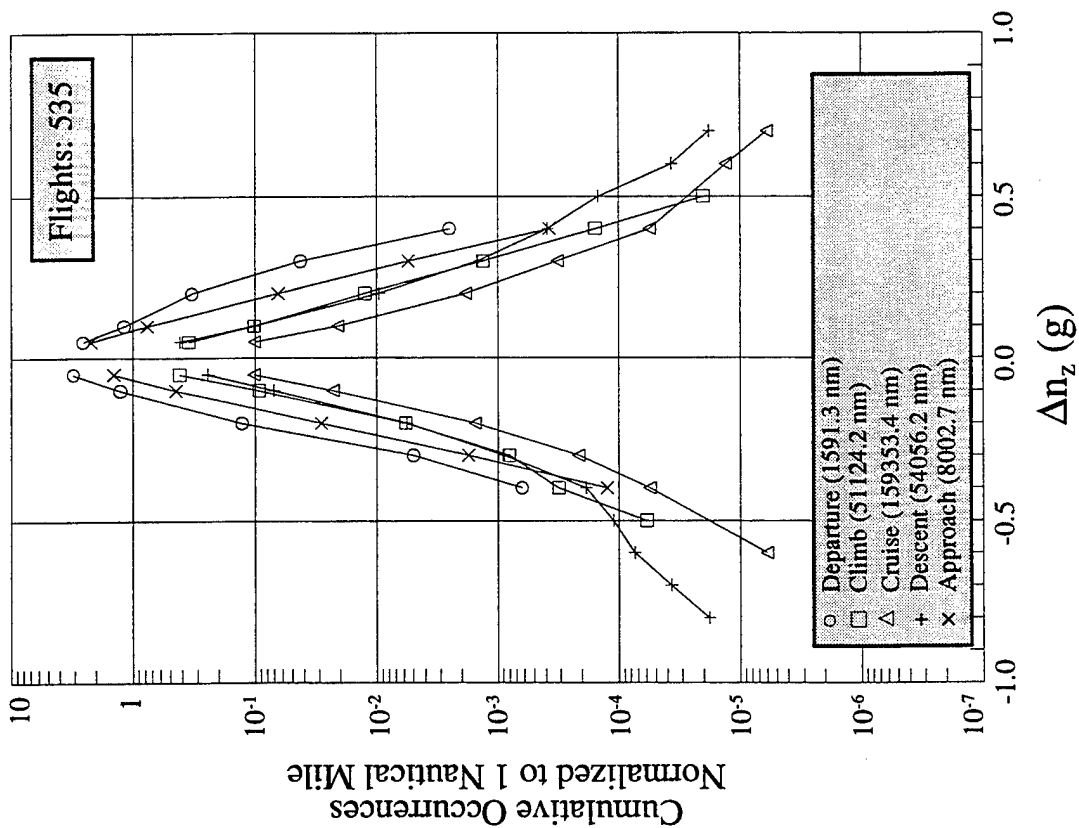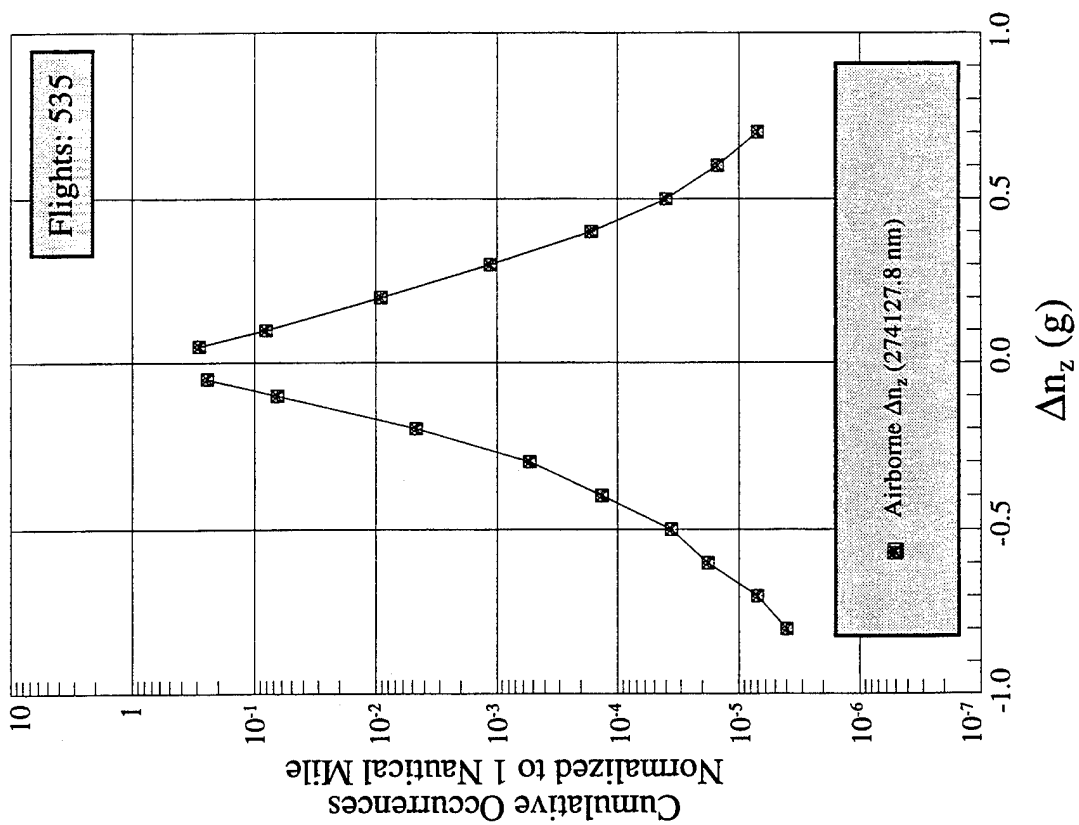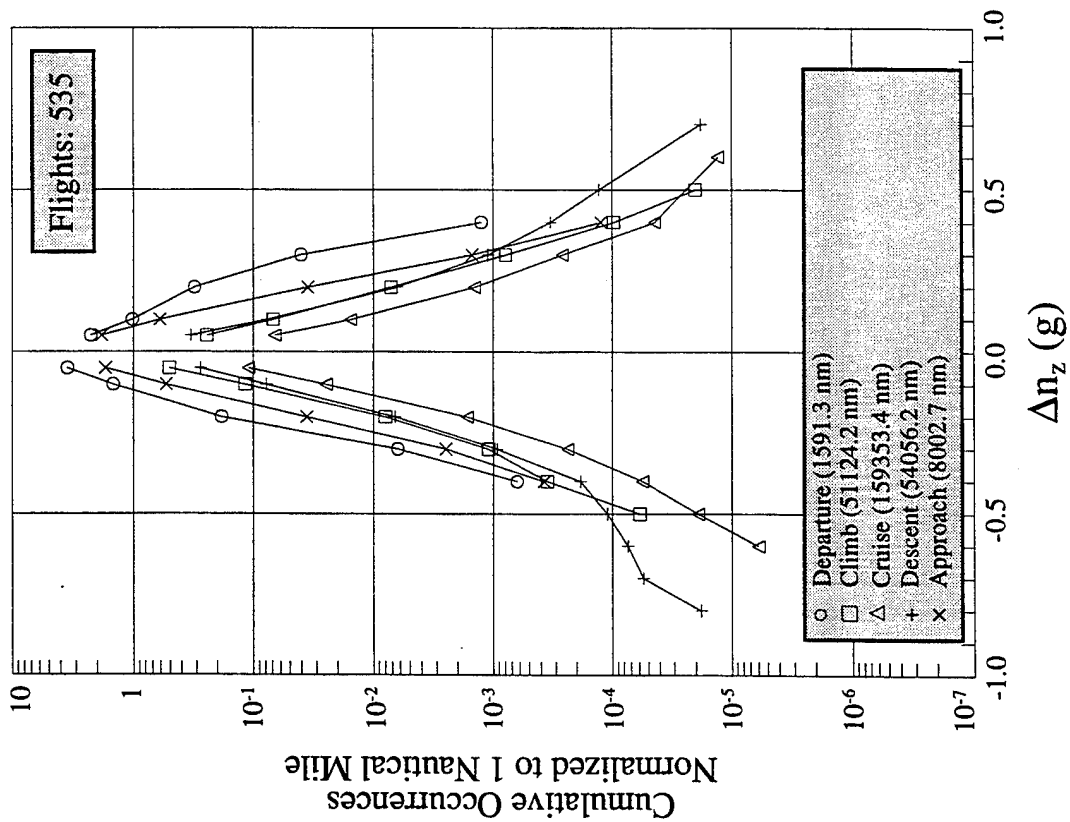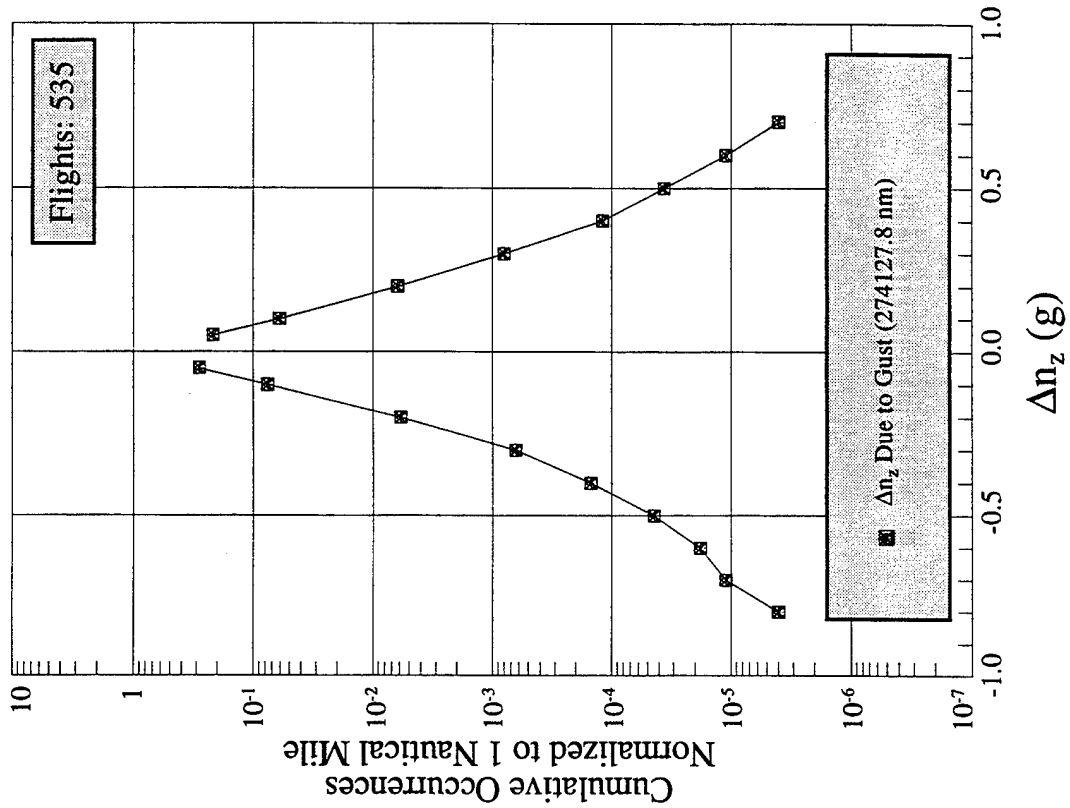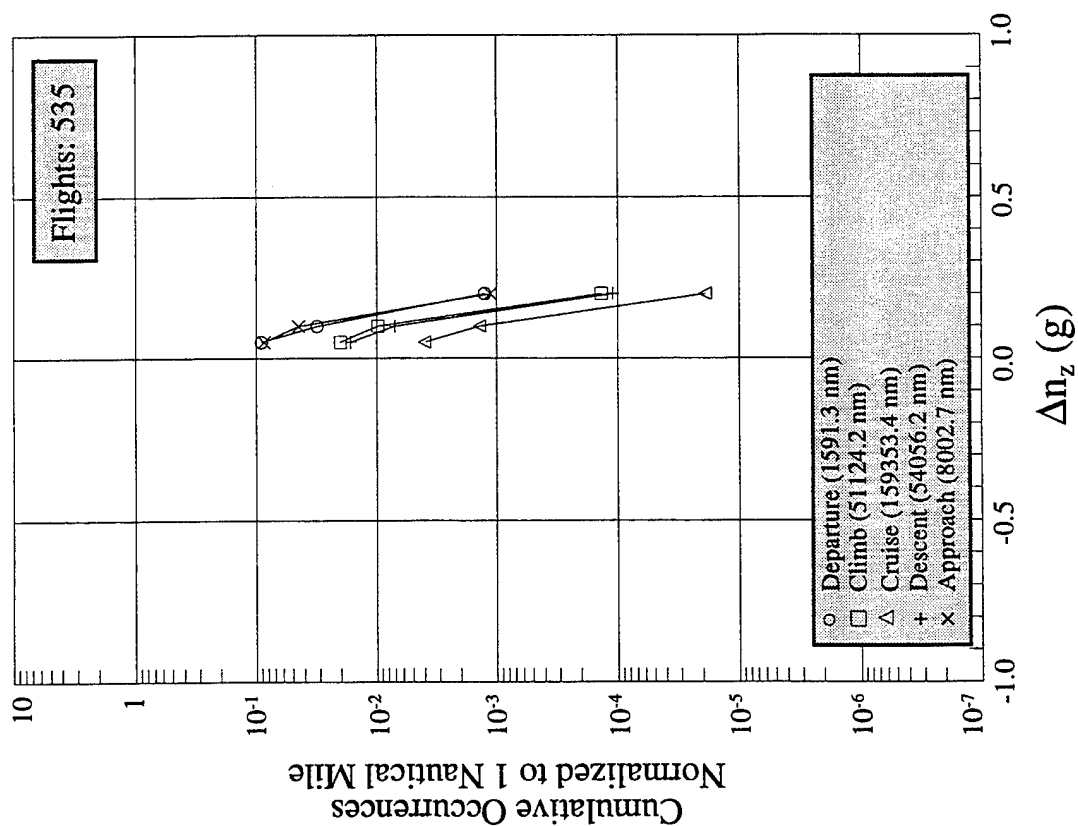FIGURE 39.   INCREMENTAL MANEUVER LOAD
FACTOR CUMULATIVE OCCURRENCES
PER 1000 HOURS

FIGURE 38.   INCREMENTAL MANEUVER LOAD
FACTOR CUMULATIVE OCCURRENCES
PER 1000 HOURS BY AIRBORNE
PHASE OF FLIGHT

49

FIGURE 41. AIRBORNE INCREMENTAL LOAD FACTOR CUMULATIVE OCCURRENCES PER NAUTICAL MILE

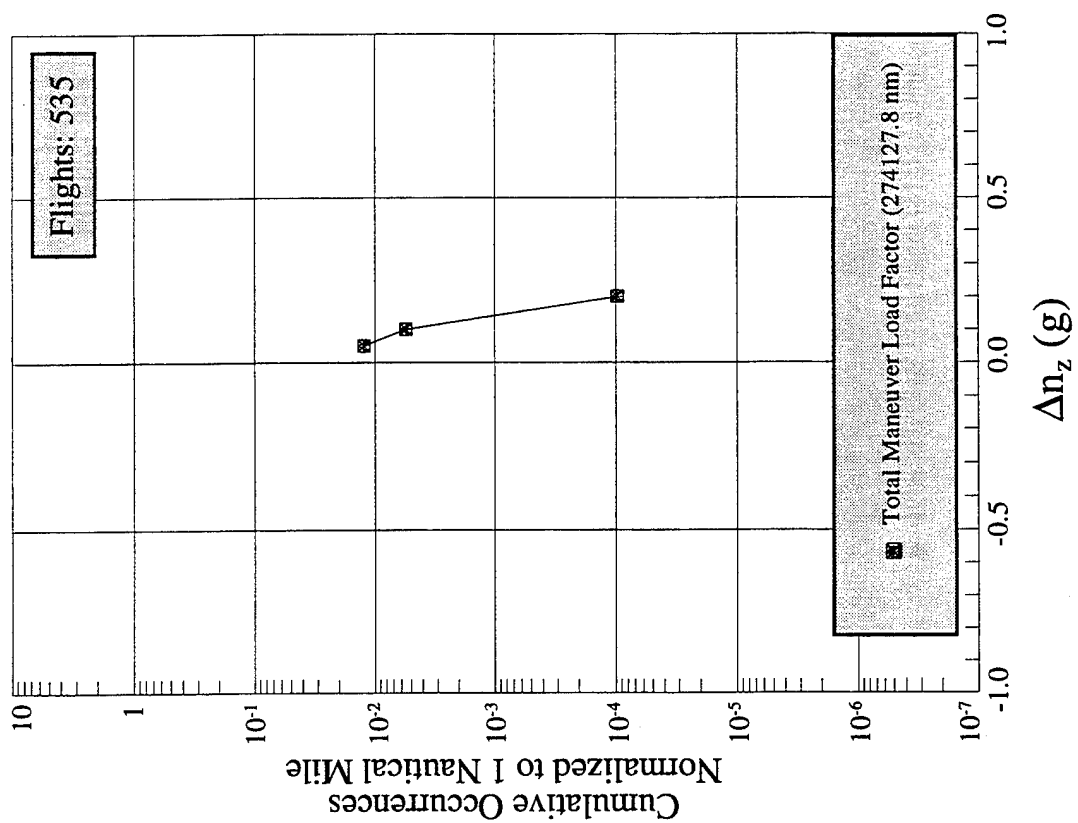FIGURE 40. INCREMENTAL LOAD FACTOR CUMULATIVE OCCURRENCES PER NAUTICAL MILE BY AIRBORNE PHASE OF FLIGHT

50

FIGURE 43. AIRBORNE INCREMENTAL GUST LOAD FACTOR CUMULATIVE OCCURRENCES PER NAUTICAL MILE

FIGURE 42. INCREMENTAL GUST LOAD FACTOR CUMULATIVE OCCURRENCES PER NAUTICAL MILE BY AIRBORNE PHASE OF FLIGHT

51

FIGURE 45.   INCREMENTAL MANEUVER LOAD
FACTOR CUMULATIVE OCCURRENCES
PER NAUTICAL MILE

FIGURE 44.   INCREMENTAL MANEUVER LOAD
FACTOR CUMULATIVE OCCURRENCES
PER NAUTICAL MILE BY AIRBORN
PHASE OF FLIGHT

52
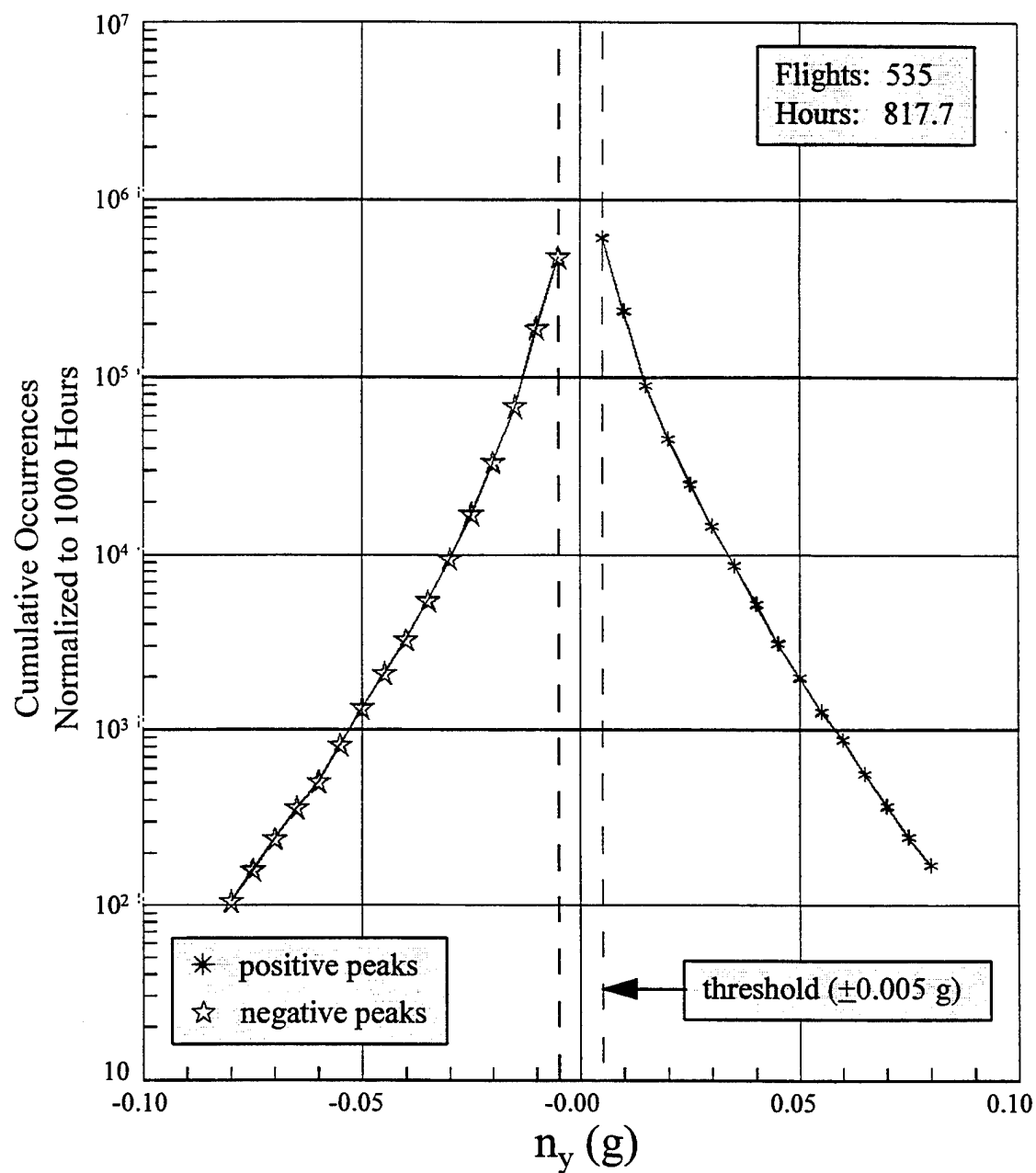
FIGURE 46. LATERAL ACCELERATION PEAK CUMULATIVE OCCURRENCES
FOR AIRBORNE PHASES OF FLIGHT
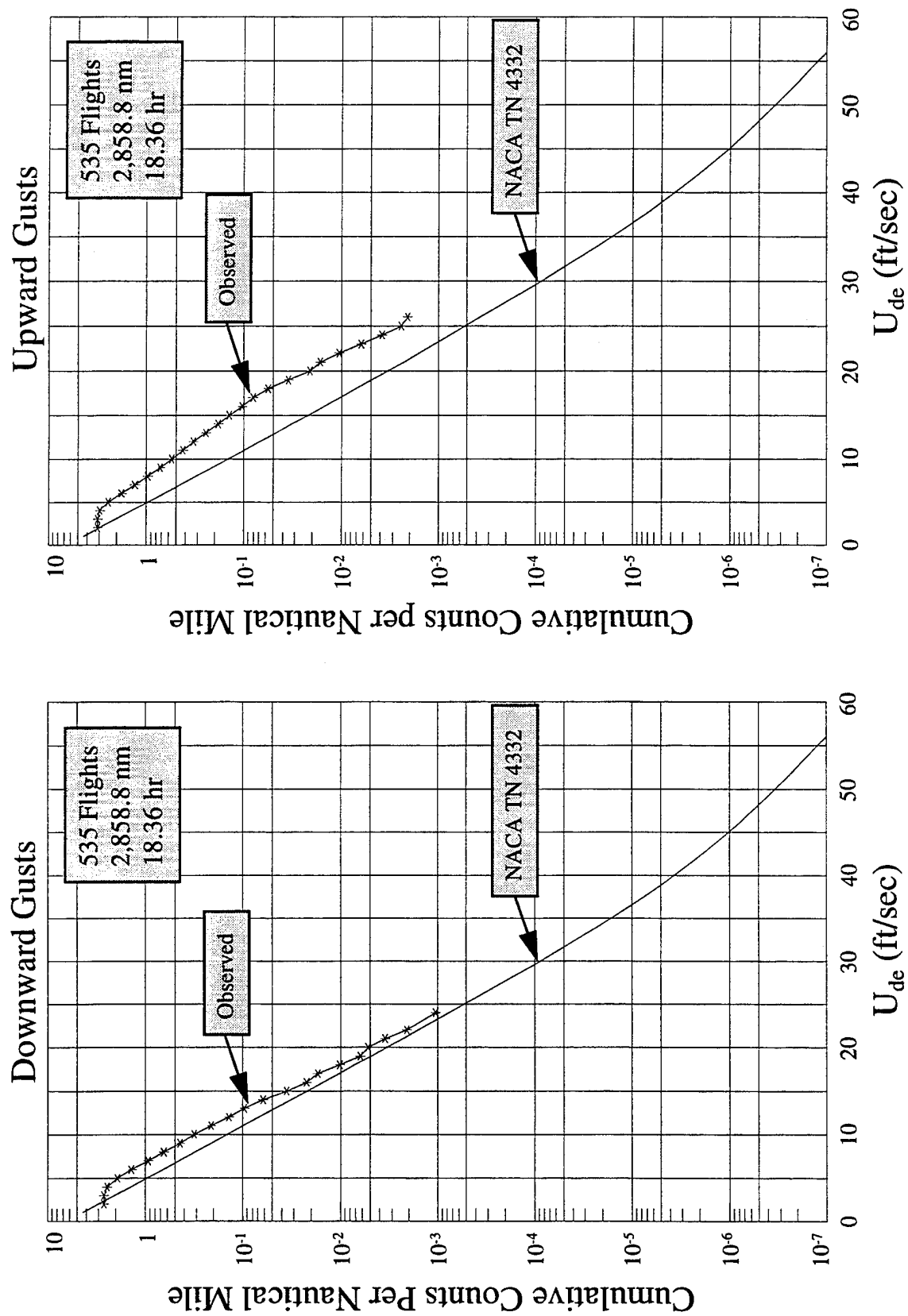
FIGURE 47. DERIVED GUST VELOCITY CUMULATIVE PEAK COUNTS PER NAUTICAL MILE (0-2000 FT.)
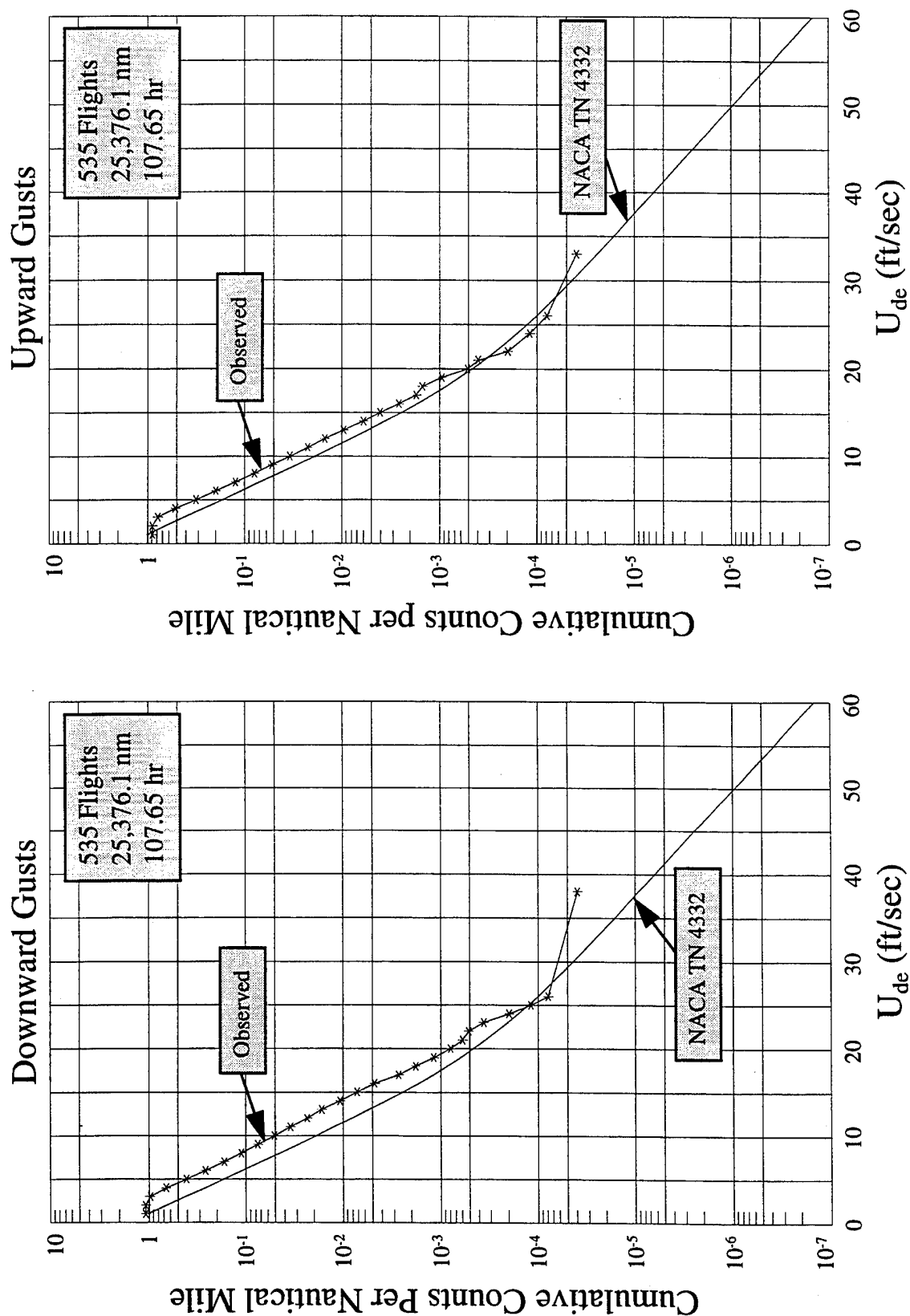
54

FIGURE 48. DERIVED GUST VELOCITY CUMULATIVE PEAK COUNTS PER NAUTICAL MILE (2000-10,000 FT.)
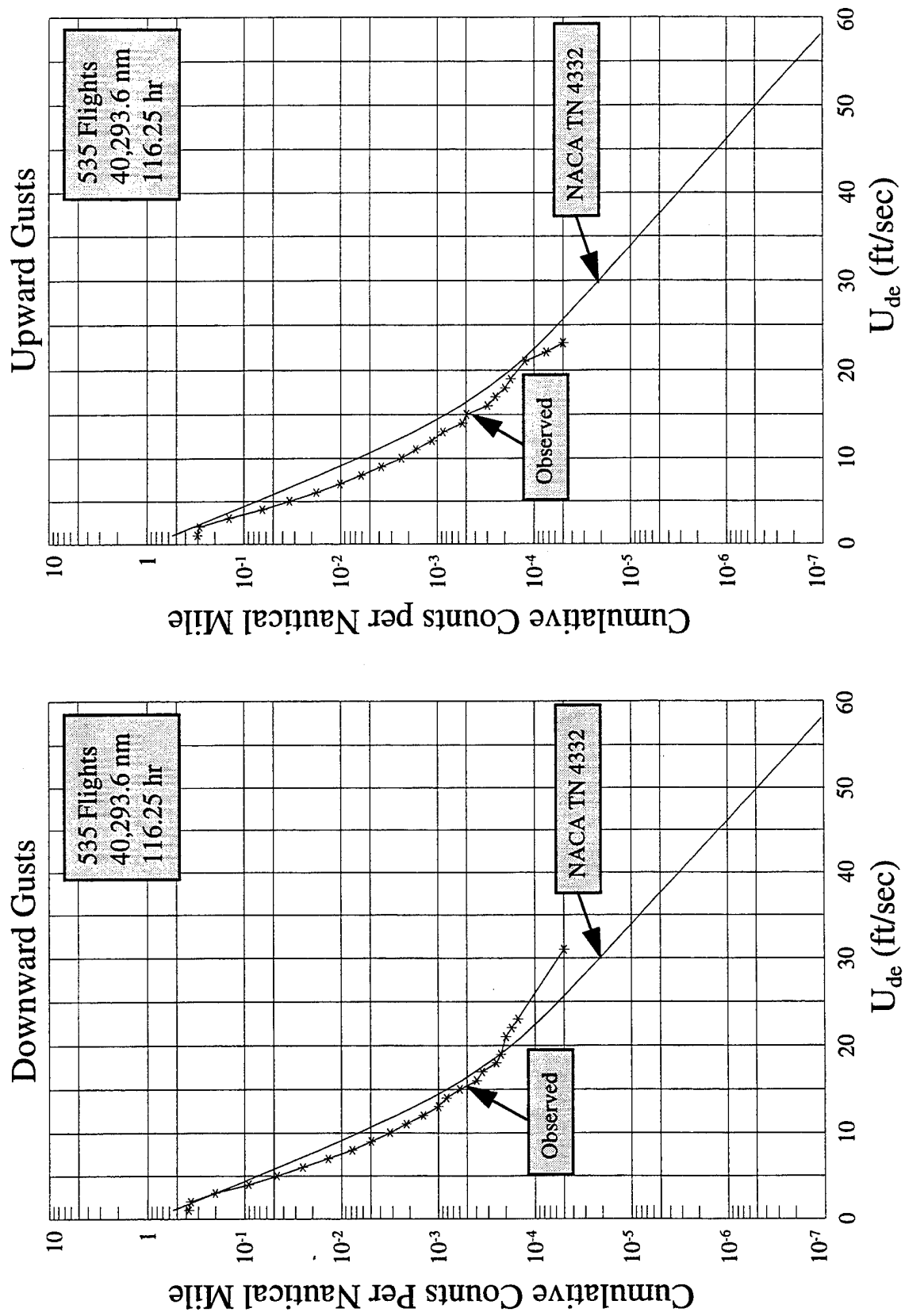
55

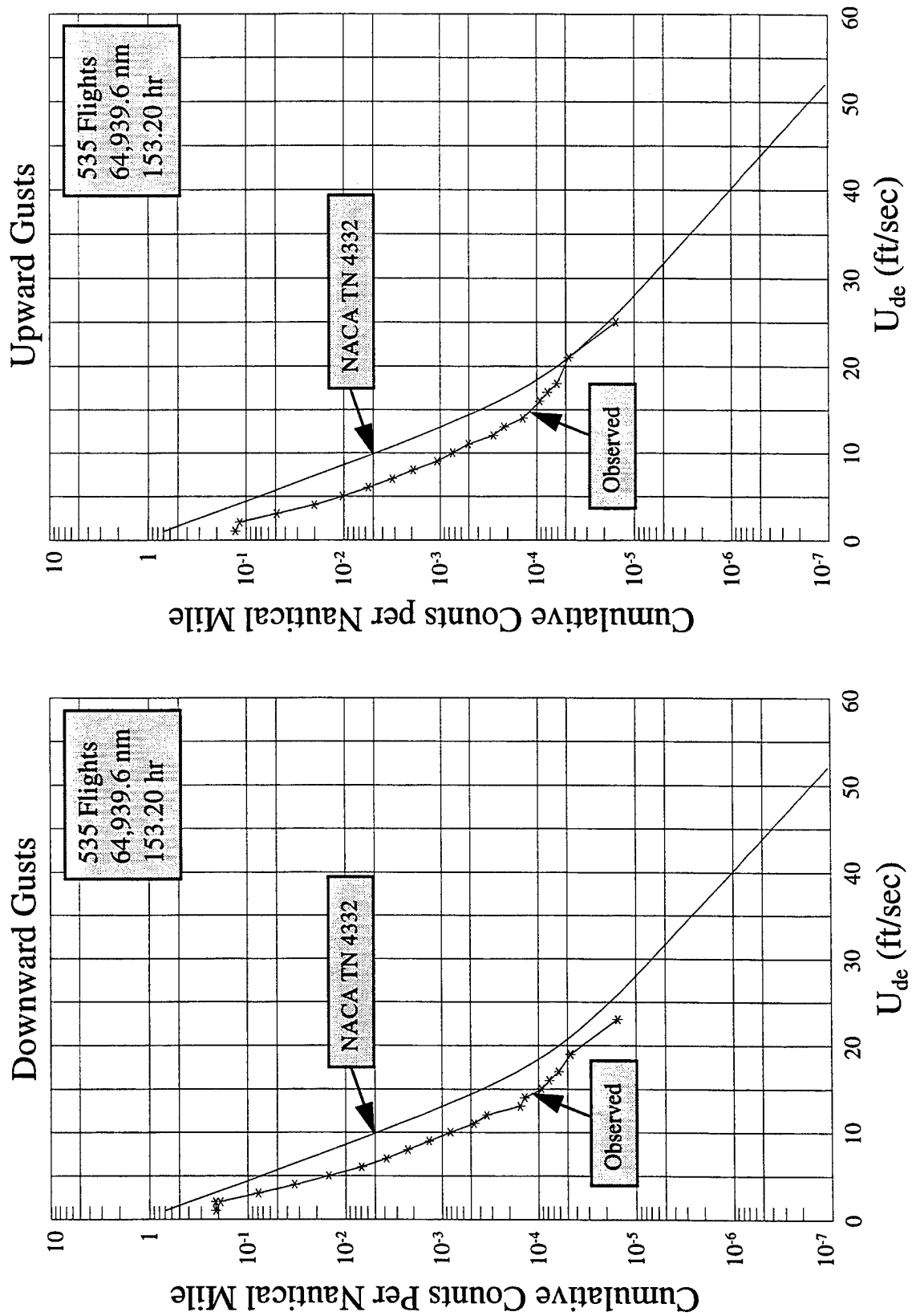FIGURE 49. DERIVED GUST VELOCITY CUMULATIVE PEAK COUNTS PER NAUTICAL MILE (10,000-20,000 FT.)

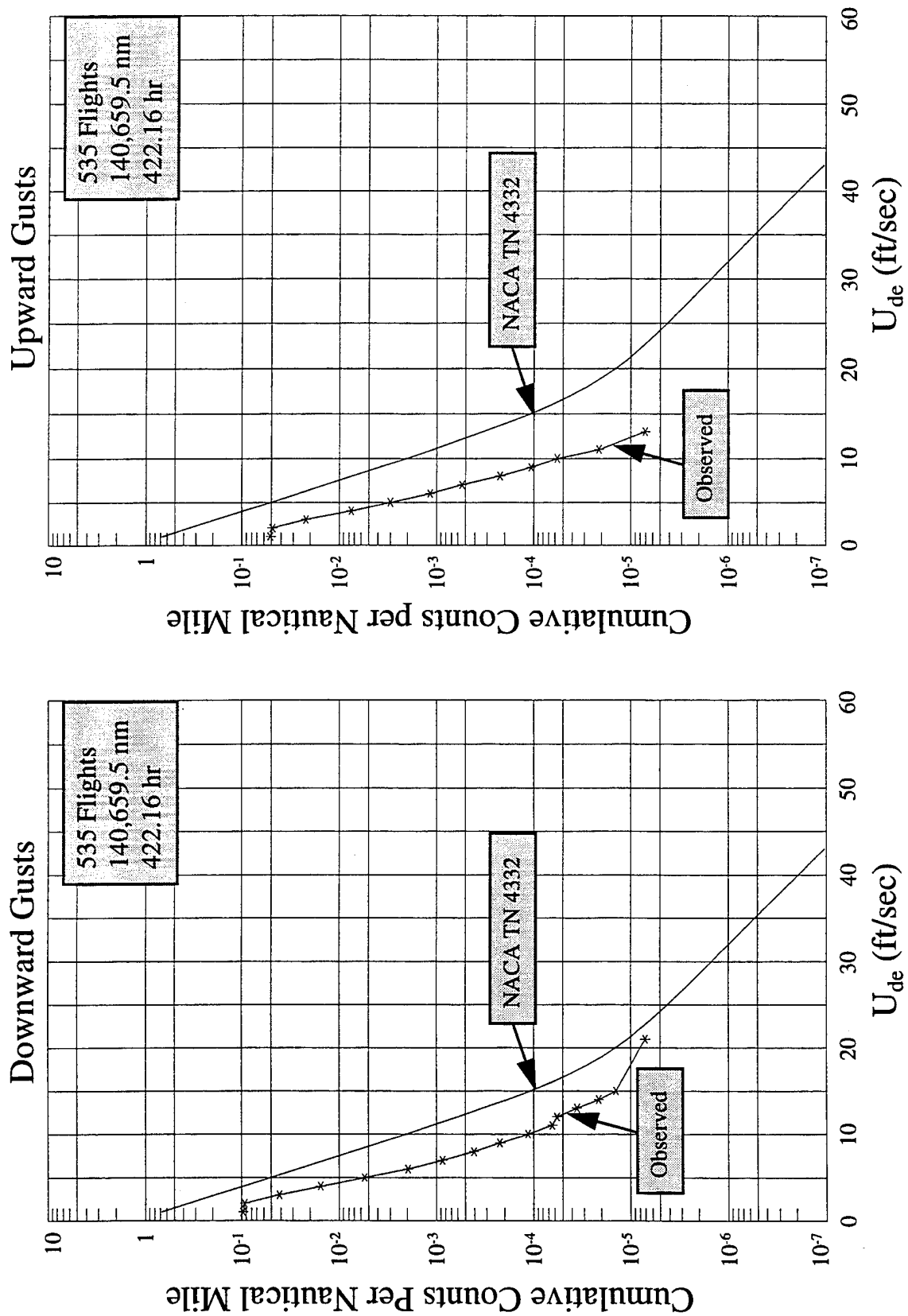FIGURE 50. DERIVED GUST VELOCITY CUMULATIVE PEAK COUNTS PER NAUTICAL MILE (20,000-30,000 FT.)

57

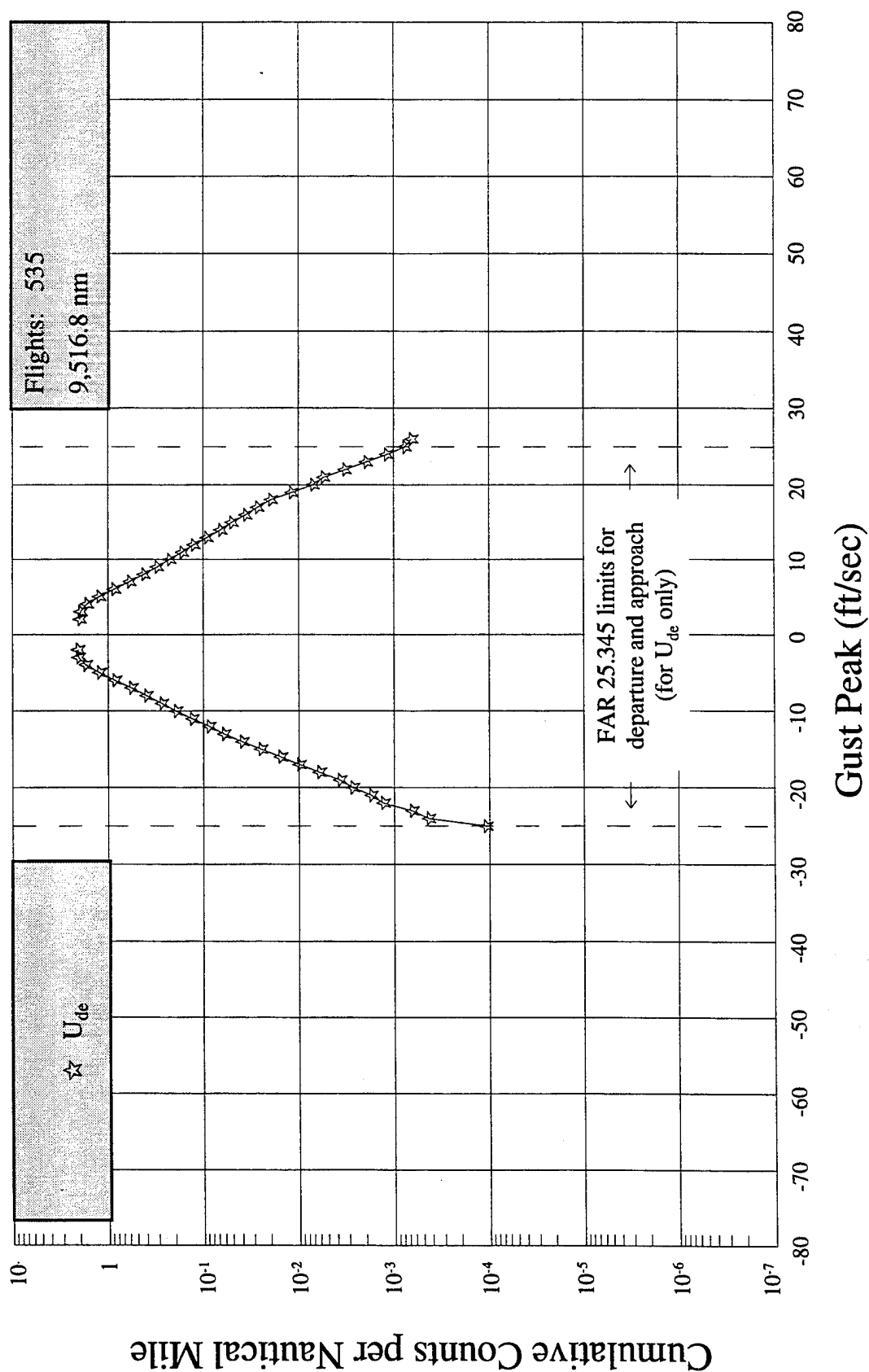FIGURE 51. DERIVED GUST VELOCITY CUMULATIVE COUNTS PER NAUTICAL MILE (30,000-40,000 FT.)

58

FIGURE 52. DISCRETE GUST CUMULATIVE PEAK COUNTS PER NAUTICAL MILE WITH FLAPS EXTENDED
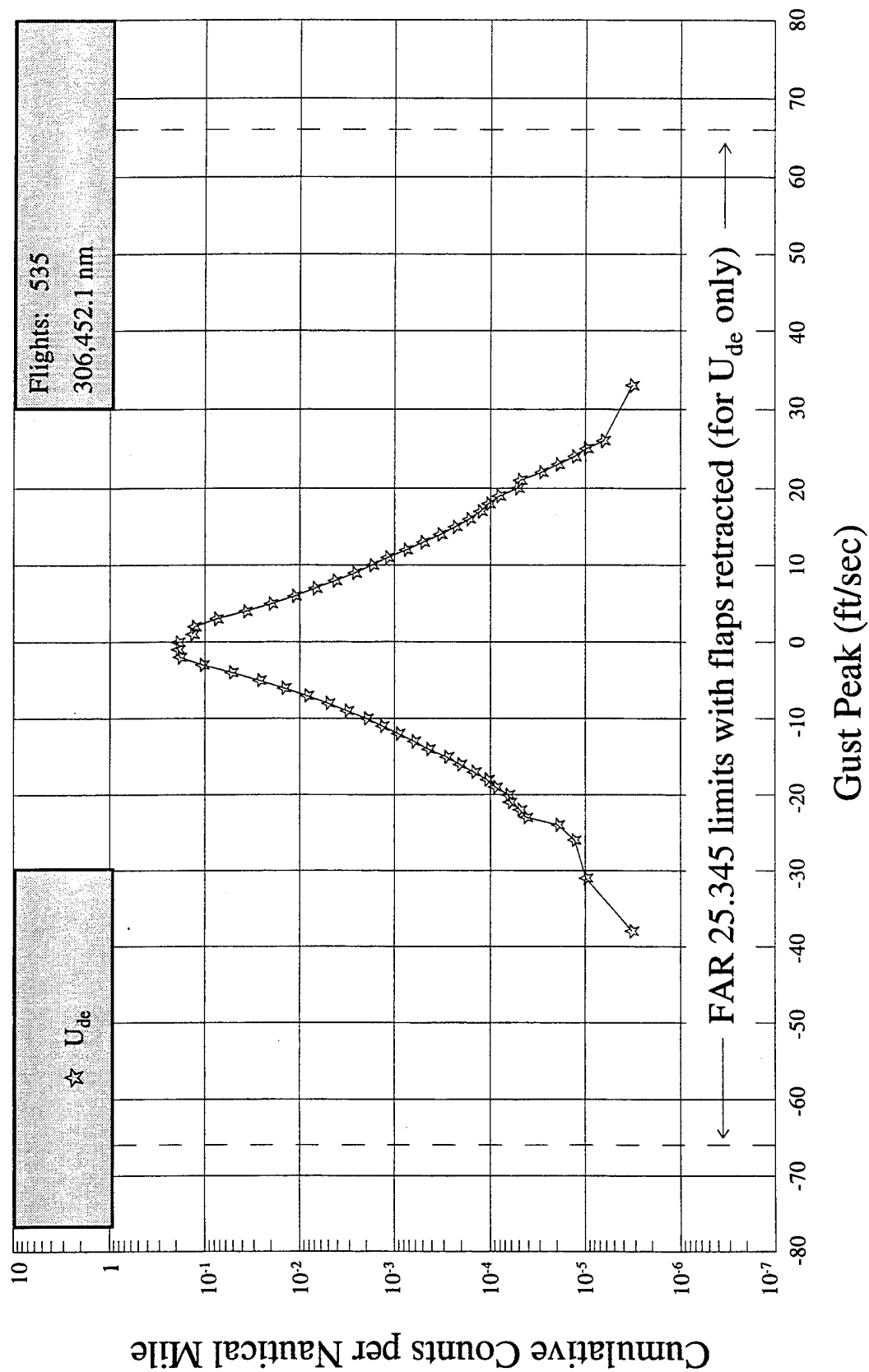
59

FIGURE 53. DISCRETE GUST CUMULATIVE PEAK COUNTS PER NAUTICAL MILE WITH FLAPS RETRACTED
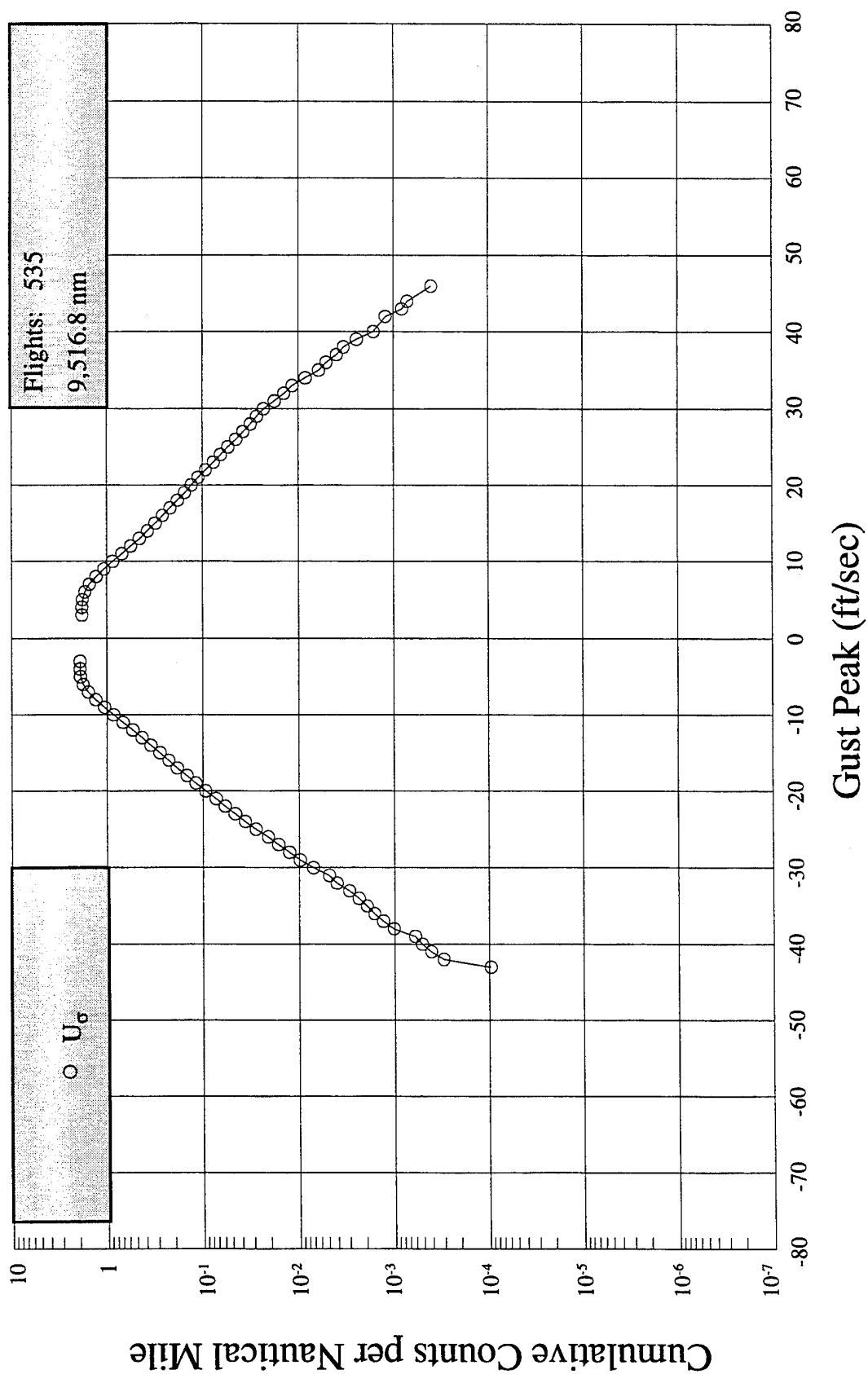
FIGURE 54. CONTINUOUS GUST CUMULATIVE PEAK COUNTS PER NAUTICAL MILE WITH FLAPS EXTENDED
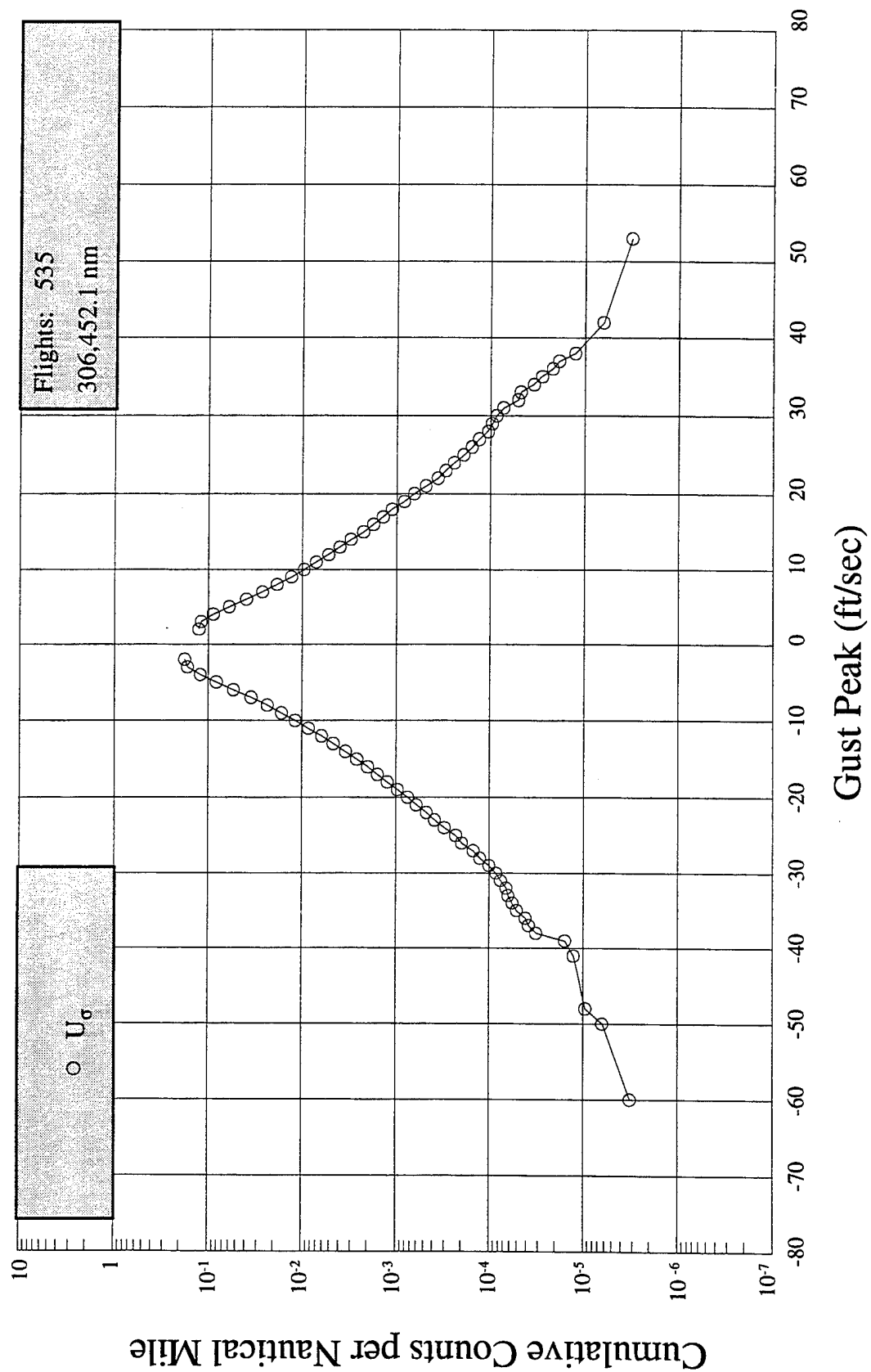
61

FIGURE 55. CONTINUOUS GUST CUMULATIVE PEAK COUNTS PER NAUTICAL MILE WITH FLAPS RETRACTED

The FAR, part 25 Appendix-G Continuous Gust Design Criteria, establishes a U_σ value of 85-fps true gust velocity for design cruising speed (V_C) for 0- to 30,000-ft altitude, linearly decreasing to 30-fps true gust velocity at 80,000-feet altitude. For the design speed for maximum gust intensity (V_B), the gust velocity is equal to 1.32 times the (V_C) value, and for the design diving speed (V_D), the value is equal to 1/2 the V_C value. These requirements are summarized in table 10.

TABLE 10. FAR REQUIREMENTS FOR CONTINUOUS
GUST DESIGN CRITERIA, BASIC

Aircraft Design Speed	True Gust Velocity	
	0- to 30,000-Feet Altitude	80,000-Feet Altitude
V_B	112.2 fps	39.6 fps
V_C	85 fps	30 fps
V_D	42.5 fps	15 fps

For an airplane model which is comparable to a similar design with extensive satisfactory service experience, the design gust intensities may be reduced. The Boeing 737-400 and similar twin jet transports are designed to the requirements summarized in table 11.

TABLE 11. FAR REQUIREMENTS FOR CONTINUOUS
GUST DESIGN CRITERIA, REDUCED

Aircraft Design Speed	True Gust Velocity	
	0- to 20,000-Feet Altitude	80,000-Feet Altitude
V_B	99 fps	39.6 fps
V_C	75 fps	30 fps
V_D	37.5 fps	15 fps

4.9 DEVELOPMENT OF FLIGHT ENVELOPE (V-n DIAGRAM).

FAR 25.333 requires that airplane structural operating limitations be established at each combination of airspeed and load factor on and within the boundaries of maneuvering and gust load envelopes (V-n diagrams). For purposes of displaying the measured normal maneuver and gust load factors, four representative V-n diagrams were developed from the FAR requirements. Figures 56 through 59 present these V-n diagrams.

The required limit load factor for maneuvers is specified in FAR 25.337. This states that the positive limit maneuvering load factor (n) may not be less than 2.5 and that the negative limit maneuvering load factor may not be less than -1.0 at speeds up to V_C, varying linearly with speed to zero at V_D. FAR 25.345 specifies that the positive limit maneuver load factor is 2.0 g when the flaps are extended. These limits are shown in figures 56 and 57. The stall curve on the left side of
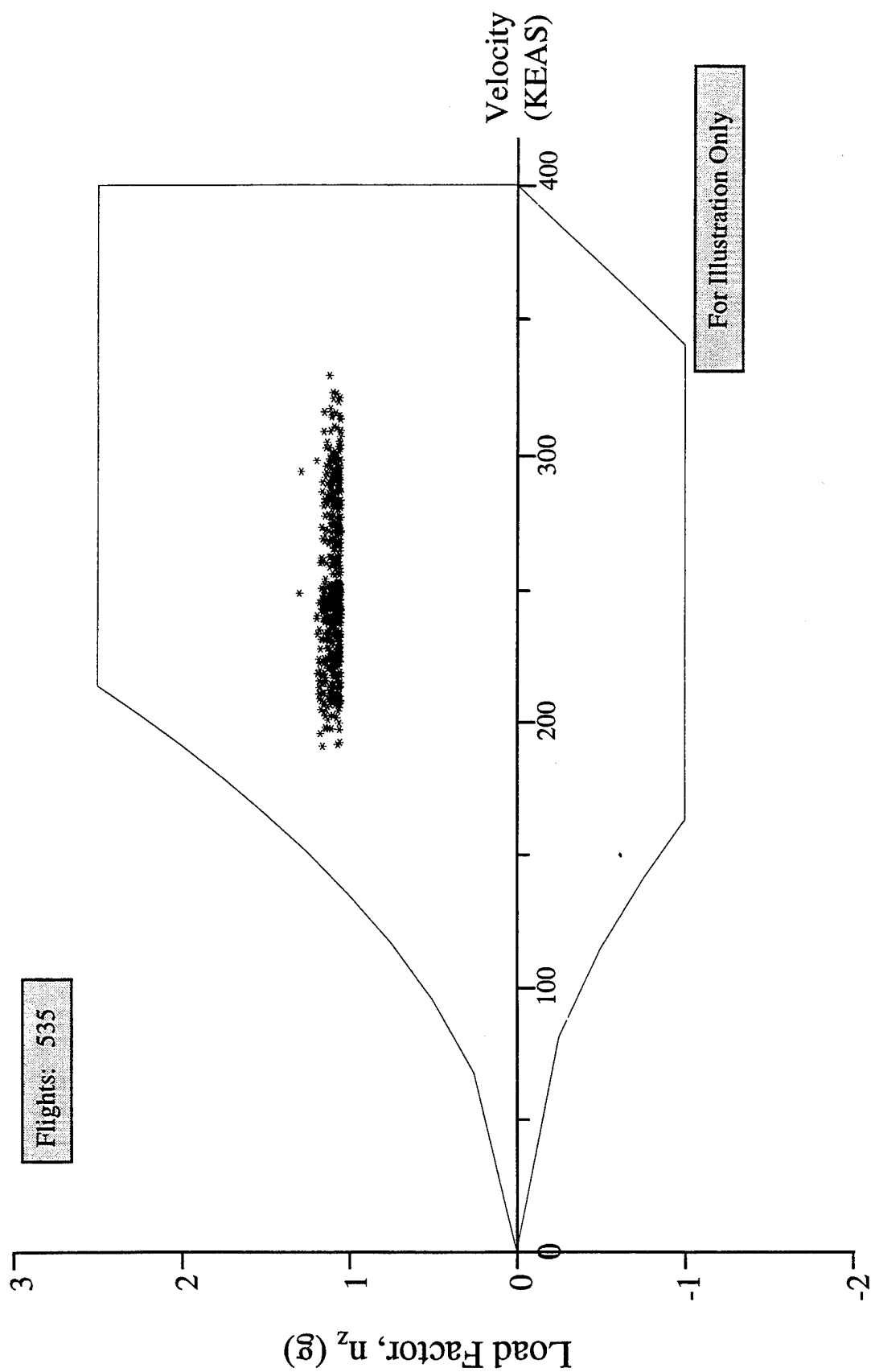
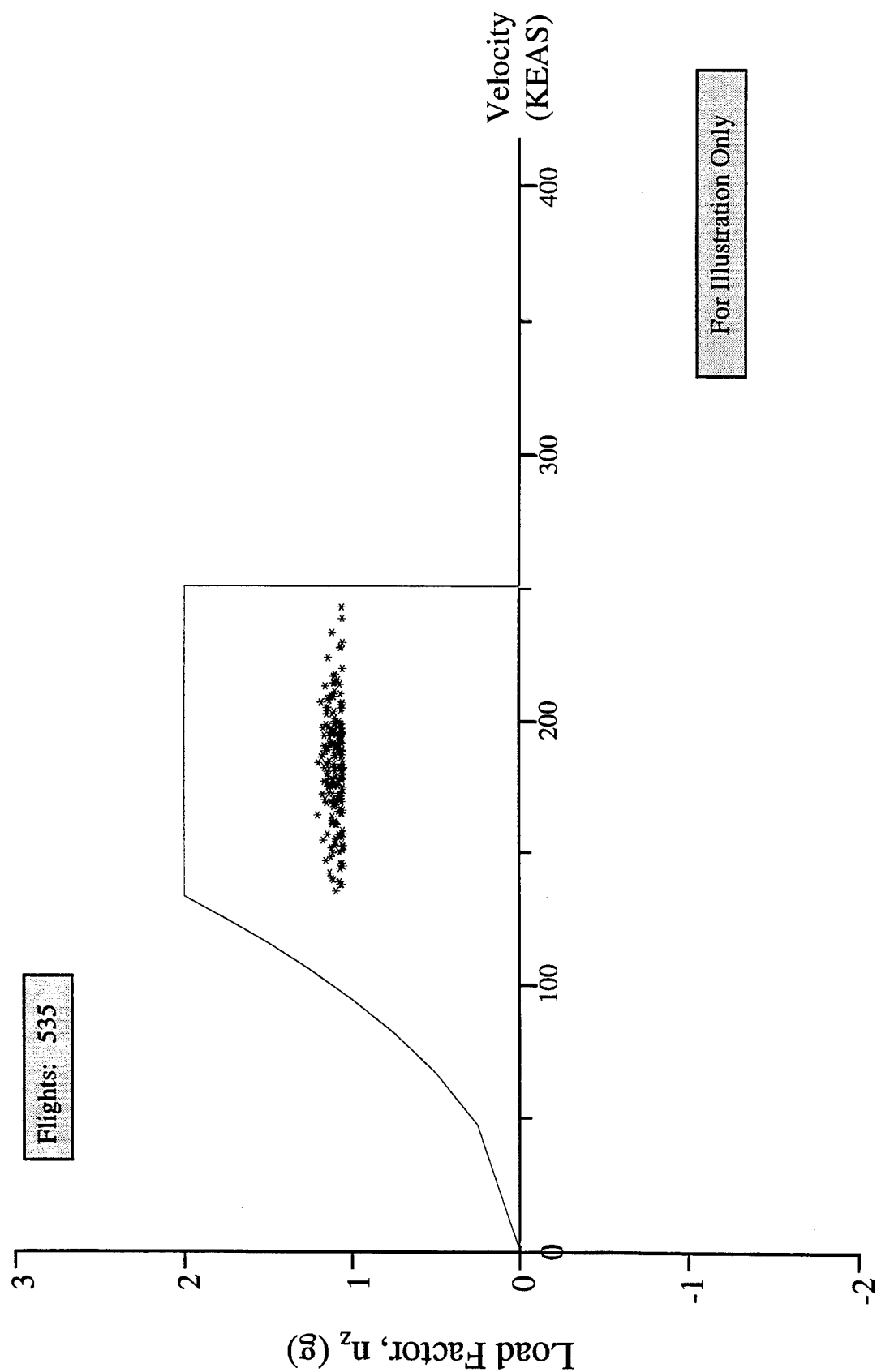FIGURE 56. V-n DIAGRAM FOR MANEUVERS WITH FLAPS RETRACTED, PER FAR 25.333B

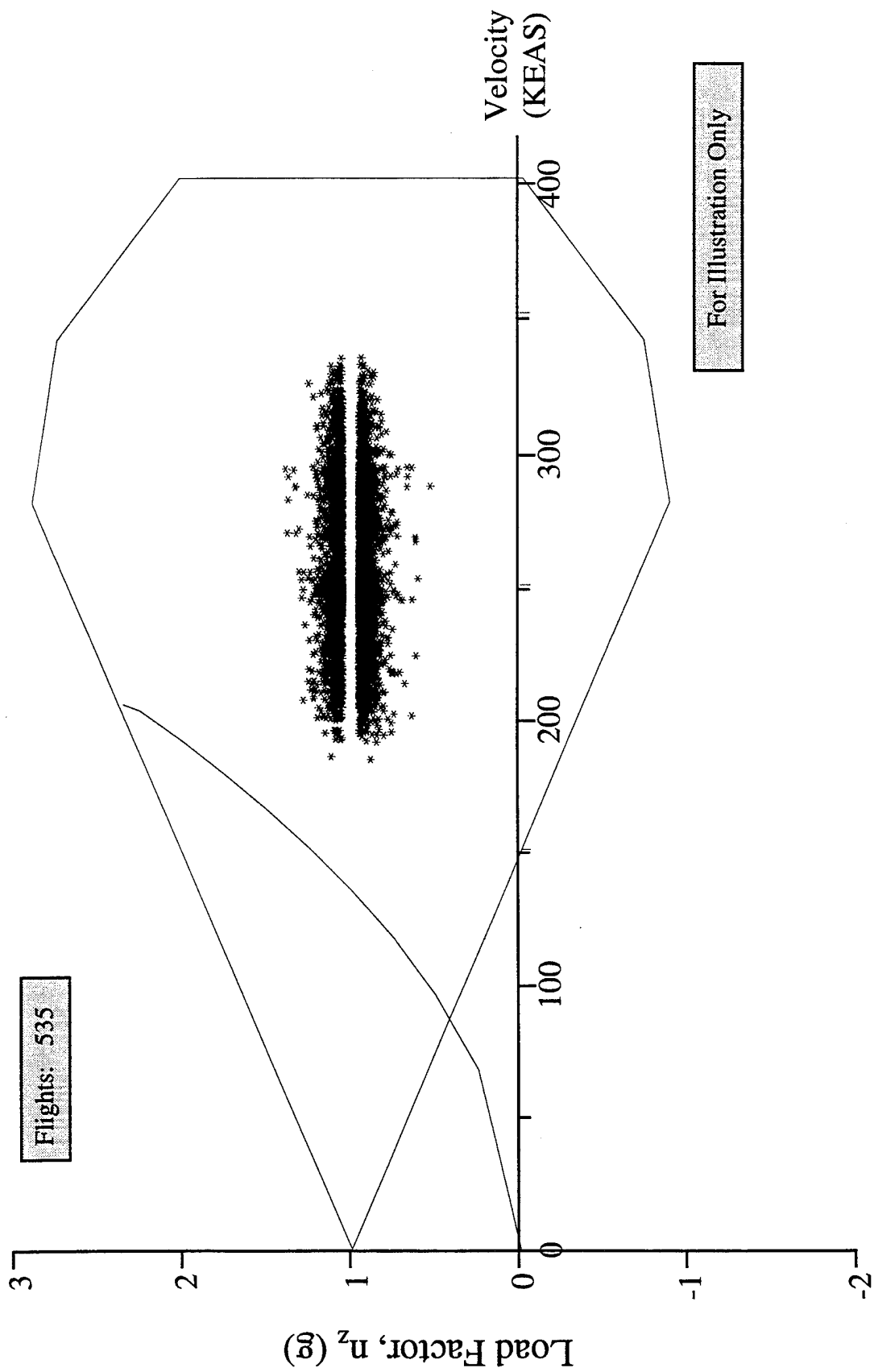FIGURE 57. V-n DIAGRAM FOR MANEUVERS WITH FLAPS EXTENDED AT ALL DETENTS, PER FAR 25.333B

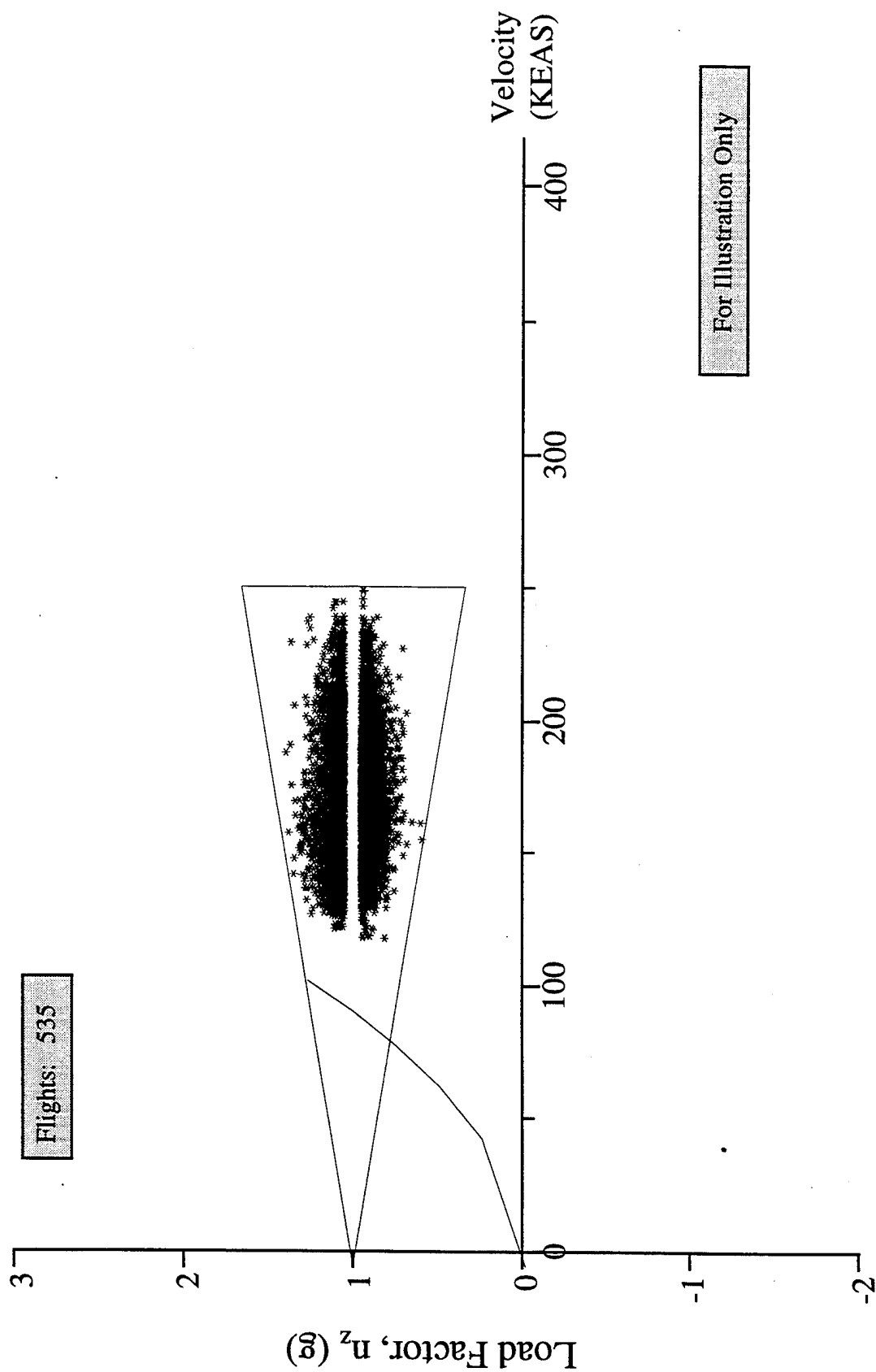FIGURE 58. V-n DIAGRAM FOR GUSTS WITH FLAPS RETRACTED, PER FAR 25.333C

FIGURE 59. V-n DIAGRAM FOR GUSTS WITH FLAPS EXTENDED AT ALL DETENTS, PER FAR 25.333C

the envelopes is determined by the maximum lift coefficient. The curve was estimated by using the 1 g stall speed to estimate $C_{L_{max}}$.

The limit load factors due to gusts correspond to the conditions defined in table 9. These limit load factors for V_B, V_C and V_D are plotted in figures 58 and 59. The stall curve is also shown. In figures 57 and 59, the placard speed when flaps are extended 5° is shown as the maximum velocity.

Sufficient data to generate V-n diagrams for all weight and altitude conditions are not available at this time. Therefore, sea level data were used to develop the representative diagrams, and all of the recorded maneuvers and gusts were plotted on these. A weight of 90,000 lbs., the lowest recorded weight, was used for the calculations required in developing these diagrams.

4.10 ADDITIONAL DATA.

Figure 60 shows the coincident pressure altitude for maximum Mach number per flight. The design limit is shown in the plot. Figure 61 shows the coincident pressure altitude for maximum equivalent airspeed, per flight, with the design limit. It should be noted that maximum Mach and maximum airspeed do not necessarily occur at the same time during a flight.

Figure 62 shows the range of n_z values recorded for gross weight ranges. The positive and negative limit maneuvering load factors are also shown per FAR requirements.
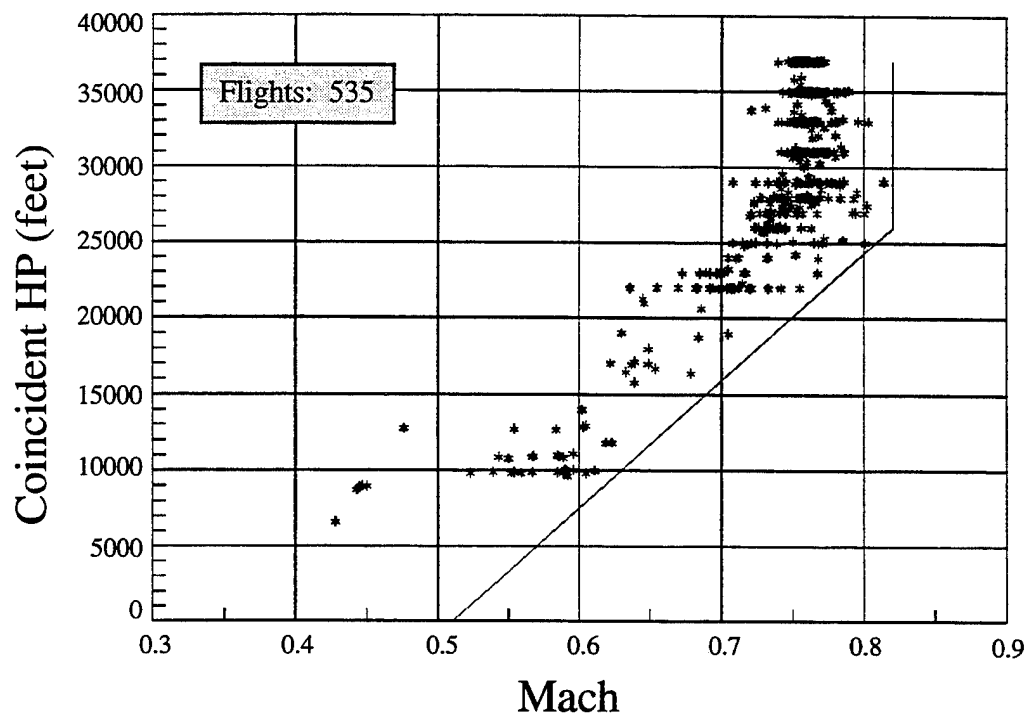
FIGURE 60. COINCIDENT PRESSURE ALTITUDE FOR MAXIMUM MACH NUMBER PER FLIGHT
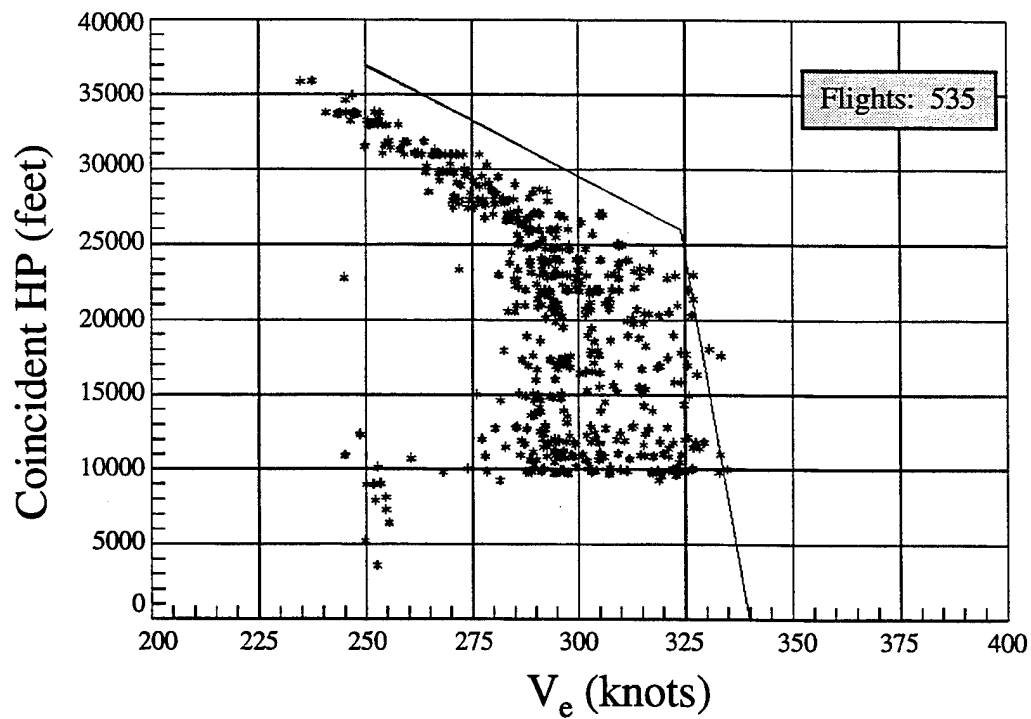

FIGURE 61. COINCIDENT PRESSURE ALTITUDE FOR MAXIMUM
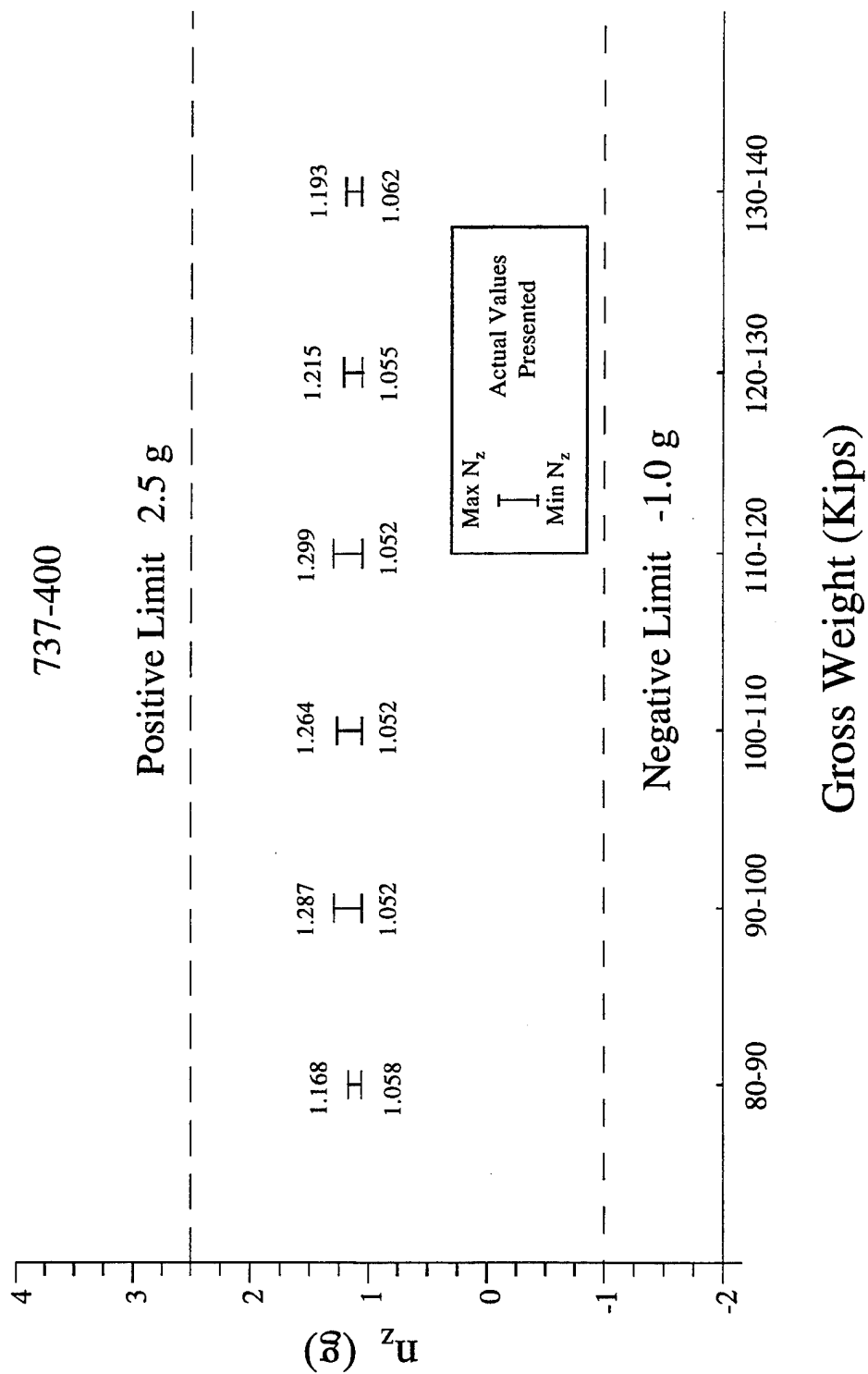EQUIVALENT AIRSPEED PER FLIGHT.

FIGURE 62. LIMIT MANEUVERING LOAD FACTOR PER GROSS WEIGHT BAND

5. REFERENCES.

1.   Crabill, Norman L., "FAA/NASA Prototype Flight Loads Program Systems Requirements, B737-400 Aircraft," Eagle Aerospace Inc., Contract NAS1-19659, report draft dated November 1994.

2.   Carrelli, David J., "FAA/NASA Prototype Flight Loads Program System Description (Preliminary)," AIB-92-0023, Lockheed Engineering and Sciences Company, September 1992.

3.   de Jonge, B., "Reduction of Incremental Load Factor Acceleration Data to Gust Statistics," DOT/FAA/CT-94/57, August 1994.

4.   Crabill, Norman L., "The NASA Digital VGH Program - Exploration of Methods and Final Results," DOT/FAA/CT-89/36 Volumes I-V, December 1989.

5.   "Data from Unusual Events Recording System in a Commercial 737 Aircraft," Technology Incorporated Instruments and Controls Division, Dayton OH, Report No. FAA-RD-72-113, November 1972.

6.   Clay, Larry E., DeLong, Robert C., and Rockafellow, Ronald I., "Airline Operational Data From Unusual Events Recording Systems in 707, 727, and 737 Aircraft," Report No. FAA-RD-71-69, September 1971.

7.   Press, Harry and Steiner, Roy, "An Approach to the Problem of Estimating Severe and Repeated Gust Loads for Missile Operations," National Advisory Committee for Aeronautics Technical Note 4332, September 1958, Langley Aeronautical Laboratory, Langley Field, Va.

APPENDIX A - SUPPLEMENTAL INFORMATION REQUIRED FOR REDUCTION OF FLIGHT DATA

GREAT CIRCLE DISTANCE CALCULATION
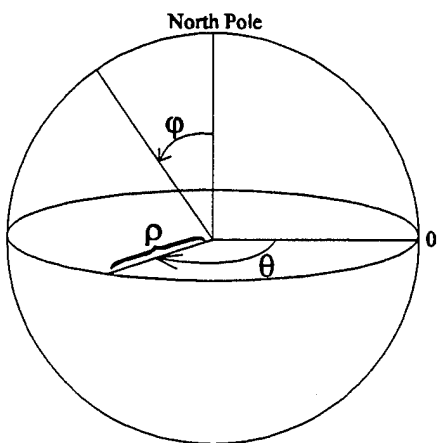
Given:

Latitude and Longitude of Departure and Destination Airports	ρ = distance from center φ = angle from North Pole θ = angle E/W of Prime Meridian

Procedure: (see sketch above)

The standard mathematical system for spherical coordinates is shown, in which three variables specify location: ρ, φ, and θ.

Let a = Great Circle Distance in angular measure.

Latitude is measured away from the Equator (0°) to the North Pole (+90°) and the South Pole (-90°); whereas in the standard spherical coordinate system, the North Pole, Equator, and South Pole lie at 0°, 90°, and 180°, respectively. Therefore,

$$\varphi = 90° - \text{latitude}$$

transforms latitude readings into equivalent angles (φ) in the standard spherical coordinate system.

Then

$$b = 90° - \text{Latitude}_{Dep}$$
$$c = 90° - \text{Latitude}_{Des}$$

where b and c are values of φ for the Departure and Destination locations, respectively.

Longitude is measured away from the Prime Meridian (0°). Longitudes are positive to the East and negative to the West. However, the standard spherical coordinate system measures its angles in the opposite direction. Therefore,

$$\theta = - \text{longitude}$$

transforms longitude readings into equivalent angles (θ) in the standard spherical coordinate system.

Then

$$A = (- \text{Longitude}_{Des}) - (- \text{Longitude}_{Dep})$$
$$= \text{Longitude}_{Dep} - \text{Longitude}_{Des}$$

where A is the value of θ between the Departure and Destination locations.

The following equation, based on the spherical coordinate system, allows the computation of the Great Circle Distance, a. (Law of cosines for oblique spherical triangles)

$$\cos a = \cos b \cos c + \sin b \sin c \cos A$$

Substituting for b, c, and A from the above equalities,

$$\cos a = \cos (90° - \text{Lat}_{Dep}) \cos (90° - \text{Lat}_{Des})$$
$$+ \sin (90° - \text{Lat}_{Dep}) \sin (90° - \text{Lat}_{Des}) \cos (\text{Lon}_{Dep} - \text{Lon}_{Des})$$

Since
$$\cos (90° - \text{Lat}_{Dep}) = \sin \text{Lat}_{Dep}$$
$$\cos (90° - \text{Lat}_{Des}) = \sin \text{Lat}_{Des}$$
$$\sin (90° - \text{Lat}_{Dep}) = \cos \text{Lat}_{Dep}$$
$$\sin (90° - \text{Lat}_{Des}) = \cos \text{Lat}_{Des}$$

by replacement one obtains

$$\cos a = \sin (\text{Lat}_{Dep}) \sin (\text{Lat}_{Des}) + \cos (\text{Lat}_{Dep}) \cos (\text{Lat}_{Des}) \cos (\text{Lon}_{Des} - \text{Lon}_{Dep})$$

Thus a, the angular measure of the great circle arc connecting the departure and destination locations, is obtained as

$$a = \cos^{-1} [\sin (\text{Lat}_{Dep}) \sin (\text{Lat}_{Des}) + \cos (\text{Lat}_{Dep}) \cos (\text{Lat}_{Des}) \cos (\text{Lon}_{Des} - \text{Lon}_{Dep})]$$

So, for a expressed in radians

$$GCD = a \text{ radians} \left(\frac{180 \text{ deg.}}{\pi \text{ radians}} \right) \left(\frac{60 \text{ min.}}{1 \text{ deg.}} \right) \left(\frac{1 \text{ Nm}}{1 \text{ min.}} \right) = \left(\frac{10800a}{\pi} \right) \text{Nm}$$

and for a expressed in degrees,

$$GCD = a \text{ degrees} \left(\frac{60 \text{ min.}}{1 \text{ deg.}} \right) \left(\frac{1 \text{ Nm}}{1 \text{ min.}} \right) = 60a \text{ Nm}$$